Pan African University
Institute of Water and Energy Sciences

جامعة أبو بكر بلقايد
UNIVERSITY OF TLEMCEN

PAN AFRICAN UNIVERSITY

INSTITUTE OF WATER AND ENERGY SCIENCES

(Including CLIMATE CHANGE)

Master Dissertation

Submitted in partial fulfillment of the requirements for the master's degree in

ENERGY ENGINEERING

Presented by

NYAGONG SANTINO DAVID LADU

Optimal Sizing of a Microgrid System using HOMER Software: A Case Study for a University Campus

Chair: Prof. Chewki Ziani-Cherif (PAUWES, Algeria)

Supervisor: Prof. Ravi Samikannu (Botswana International University of Science and Technology, Botswana)

External Examiner: Dr. Daniel YAMEGUEU NGUEWO (2IE, Burkina Faso)

Internal Examiner: Dr. Mohamed Choukri Benhabib (Tlemcen University, Algeria)

Draft Submitted on 10 October 2021

DECLARATION

I, **Nyagong Santino David Ladu,** hereby declare that this thesis is my work, and has not been submitted to another institution for the award of a degree, diploma, or certificate. I further declare that all information, materials, and results from other works in this thesis have been properly cited and referenced according to academic standards and ethics.

Nyagong Santino David Ladu

Signed: 17th October 2020.

CERTIFICATION

This is to certify that the thesis entitled "Optimal Sizing of a Microgrid System using HOMER Software: A Case Study for a University Campus" that is being submitted by Nyagong Santino David Ladu, Masters student, Registration number PAUWES/2019/MEE04, in partial fulfillment for the award of Masters in Energy Engineering to the Pan African University Institute of Water and Energy Sciences (Including Climate Change) is a record of bona fide work carried out by him. This thesis has been submitted with my approval as the supervisor.

Professor Ravi Samikannu

.....

Signed: 17th October 2020.

DEDICATION

This work is dedicated to God Almighty for his unwavering and unconditional love.

To my late mother Rose Kiden Nyagong, late grandmother Roda Jokudu, and late uncle Loku Joseph Ladu Roba.

To my parents and siblings, who are always there for me, you are my beams of hope, and I would not be here if it weren't for your support.

ACKNOWLEDGMENT

First and foremost, I am thankful to God for his unconditional love, mercy, protection, and the gift of life.

My sincere gratitude goes to the Pan African University and the African Union Commission, which funded my study at PAUWES and also provided funds for this research.

Special thanks to my supervisor, Professor Ravi Samikannu, for his continuous availability, guidance, insightful suggestions, revisions, and corrections of this thesis, and understanding, patience, and acceptance of any limitations during this work.

I am equally grateful to Prof. Dr. Abdellatif Zerga, PAUWES Director, and the PAUWES staff for their generosity in providing the necessary assistance and conducive learning space. It is also my pleasure to express my gratitude to all of my PAUWES professors, undergraduate lecturers, and all my teachers who assisted me during my studies and passed on their knowledge to mold me into the person I am today.

I'm also grateful to the administrations of Rumbek University of Science and Technology in South Sudan and the University of Bahr El Ghazal in South Sudan and everyone else who helped me finish this project in any manner. Your support was tremendously helpful to me during my studies.

Last but not least, my special thanks also go to my family for their love, support, prayers, and tenacity throughout my studies.

List of Symbols, Acronyms, Abbreviations

%:	Percentage
A/C:	Air Conditioning
AC:	Alternating Current
CDER:	Renewable Energy Development Centre
CFL:	Compact Fluorescent Lamps
CIR:	Cast Iron Radiator
CMC:	Central Management Control
CO_2:	Carbon dioxide
DC:	Direct Current
DERs:	Distributed Energy Resources
DG or DGs:	Distributed Generation or Distributed Generations Generations
ESS:	Energy Storage Systems
FL:	Fluorescent Lamps
HBMG:	Hybrid Microgrid
HOMER:	Hybrid Optimization Model for Electric Renewables
IMF:	International Monetary Fund
km:	Kilometer
kW:	Kilowatt
kWh:	Kilowatt-hour
LCOE:	Levelized Cost of Energy or Cost of Electricity
LED:	Led Emitting Diodes
m/s:	Meters per Second
NPC:	Net Present Cost
O&M:	Operation and Maintenance costs
PC:	Personal Computer
PV:	Photovoltaic
ROI:	Return on Investment

WHO:	World Health Organization
Yr:	Year

List of Tables

Table 1. Algeria's plans to generate electricity from renewable energy [12] 12

Table 2. Hydropower plants and their generation capacities in Algeria [44] 15

Table 3. Possible benefits of microgrids 22

Table 4. Typical Characteristics of Microgrid DG Sources [63] 24

Table 5. Types of PV cell generations [68][69][70] 25

Table 6. Time series load profile of the case study 60

Table 7. Monthly average global horizontal irradiance data of Chetouane 63

Table 8. Monthly Average Wind Speed 64

Table 9. Monthly average temperature data 66

Table 10. Sensitivity analysis inputs under consideration 72

Table 11. Categorized optimization Result of standalone HBMG 73

Table 12. Categorized optimization Result of grid-connected without batteries HBMG 76

Table 13. Categorized optimization Result of grid connected with batteries HBMG 78

Table 14. Compared cases with allocated points 82

Table 15. Economic metrics for the optimal System 83

Table 16. Selected optimal system simulation results for PV and wind turbine setups 84

Table 17. Inverter and rectifier optimization results of the optimal system 86

Table 18. Monthly grid purchases, sales, peak load, and energy charge 87

Table 19. Emissions from the selected optimal system 88

Table 20. Emissions from only the grid 88

List of Figures

Figure 1. Global electricity generating sources in 2017 [2]..... 2

Figure 2. Map of Algeria [32]..... 10

Figure 3. Algeria's energy capacity installed in 2019 vs. predicted capacity in 2028 [34]..... 12

Figure 4. Solar potential of Algeria per region [39] 13

Figure 5. a) Global horizontal irradiation of Algeria; b) Solar PV potential in Algeria [40] 13

Figure 6. Wind speed (m/s) potential of Algeria [43]..... 14

Figure 7. Installed hydropower plants locations in Algeria [44] 15

Figure 8. Algeria's geothermic chart [44] 16

Figure 9. stakeholders involved in Microgrids [50]..... 18

Figure 10. A Potential microgrid Distribution Architecture in the Future [55]..... 20

Figure 11. A simple microgrid architecture [58]. 21

Figure 12. Total global microgrid capacity market share by region [60] 23

Figure 13. PV cell, module, panel, and array structures [67] 25

Figure 14. a) PV cells efficiency b) cost comparisons [73]..... 26

Figure 15. A simplified block diagram of a Stand-alone PV system [74]..... 27

Figure 16. A block diagram of a grid-tied PV system using a single central inverter [74] 27

Figure 17. A block diagram of a grid-tied PV system using multiple micro-inverters [74]..... 28

Figure 18. Solar PV cell equivalent circuit [77] 29

Figure 19. Remodeling of the I-V Curve with changing FF [79] 31

Figure 20. I-V and P-V characteristics curves of a PV cell [81] 32

Figure 21. a) VAWTs b) HAWTs..... 34

Figure 22. Typical wind turbine power characteristics curve [88] 39

Figure 23. Comparison of Electrical Energy Storage (EES) systems used in Microgrids [92].... 41

Figure 24. Energy storage benefits [93]..... 41

Figure 25. Microgrid PE interfaces [97]..... 45

Figure 26. Energy management system in a microgrid [108]..... 47

Figure 27. Benefits of smart grid schemes, broken down per value segment [110]..... 48

Figure 28. Smart grid components [112]..... 49

Figure 29. A simplified simple microgrid structure[113]..... 50

Figure 30. A typical configuration of multi-DG microgrids [114]..... 50

Figure 31. A typical utility microgrid's structure [115]..... 51

Figure 32. A feeder based microgrid example [116]..... 52

Figure 33. Independent microgrid consisting of biomass-based independent microgrid, PV-based independent microgrid and wind-based independent microgrid [117]..... 53

Figure 34. AC microgrid architecture [121]. 54

Figure 35. DC microgrid architecture [121] 55

Figure 36. AC/DC microgrid architecture [123]..... 56

Figure 37. HOMER as a communication tool that brings together various stakeholders [127]... 58

Figure 38. Load profile of the faculty under consideration 61

Figure 39. Schematic diagrams of the proposed HBMG systems with the figure on the top left showing a stand-alone system. The figure on the top right shows a configured grid connected system without batteries. The figure on the bottom is a grid connected-configured with batteries. 62

Figure 40. Chetouane monthly daily solar radiation and Clearness index 63

Figure 41. Individual daily changes of global horizontal solar radiation source throughout 12 months..... 64

Figure 42. Average wind speed data for Chetouane 65

Figure 43. Individual daily changes of wind speed source throughout 12 months..... 65

Figure 44. Average monthly mean temperatures data for Chetouane 66

Figure 45. Simulated PV system considered for optimization 67

Figure 46. Simulated wind system considered for optimization 68

Figure 47. Simulated battery system considered for optimization 69

Figure 48. Simulated converter system considered for optimization 69

Figure 49. Cost summary of standalone HBMG 74

Figure 50. Cash flow of standalone HBMG 75

Figure 51. Cost summary of grid connected without batteries HBMG 76

Figure 52. Cash flow of grid connected without batteries HBMG 77

Figure 53. Cost summary of grid connected with batteries HBMG 78

Figure 54. Cash flow of grid connected with batteries HBMG 79

Figure 55. Comparison of Scenarios based on NPC, initial costs, operating costs, and LCOE ... 80

Figure 56. Comparison of scenarios based on excess electricity, capacity shortage, return on investment, unmet electrical load, and renewable energy fraction 81

Figure 57. A Pie chart showing total points and percentage share for each scenario 83

Figure 58. Monthly share of Electricity Generation from the Optimum System (scenario 2) with a 77.5% renewable fraction 84

Figure 59. Annual share of electricity generation and consumption from the optimum system a 77.5% RF 85

Figure 60. Time series plot of electrical generation and consumption 86

Figure 61. Inverter output (top) and rectifier output (bottom)..... 87

Figure 62. Energy purchased from the grid (top) and energy sold to the grid (bottom)..... 88

Figure 63. Optimal system types and configurations for different levels of solar radiation and wind speed 89

Figure 64. Optimization surface plot for different levels of solar radiation and wind speed with NPC..... 90

Table of Contents

CHAPTER ONE 1

1 Introduction 1

1.1 Background of the Study 3

1.2 Problem Statement 4

1.3 Research questions 4

1.4 Research Objectives 5

1.5 Thesis contribution 5

1.6 Scope and limitation of the Study 6

1.7 Possible obstacles 6

1.8 Relevance of the study 6

CHAPTER TWO 7

2 Literature review 7

2.1 Previous works related to this topic 7

2.2 Geographical and Climatic Overview of Algeria 9

2.3 The Economic Situation in Algeria 10

2.4 The renewable energy potential of Algeria 10

2.4.1 Algeria's potential in solar energy 12

2.4.2 Algeria's potential in wind energy 14

2.4.3 Algeria’s hydropower potential 14

2.4.4 Algeria’s biomass energy potential 16

2.4.5 Algeria’s geothermal energy potential 16

2.5 Background of Microgrids 16

2.5.1 Overview of Microgrids 17

2.5.2 Current situation of Microgrids 18

2.5.3 Microgrid Prospects 18
2.6 Concept of Microgrids 20
2.6.1 Microgrid Structure 21
2.6.2 Possible benefits and applications of Microgrids 21
2.6.3 Microgrid Components 23
2.6.4 Power electronics (PE) in microgrids 45
2.6.5 Mechanisms for Microgrid optimization 47
2.6.6 What is a smart grid? 48
2.6.7 Classification of microgrids 49
CHAPTER THREE 57
3 Methodology of the proposed system 57
3.1 HOMER as a Tool for HBMG 57
3.2 Case study – Faculty of Technology of University of Tlemcen 58
3.3 Estimation of Electric Load 59
3.3.1 Electrical load Simulation in HOMER 60
3.4 System Configurations of the Proposed HBMG System for the Faculty 61
3.5 Resources of the Location 62
3.5.1 Solar resource 62
3.5.2 Wind resource 64
3.5.3 Temperature 66
3.6 Properties of Components 67
3.6.1 Solar PV properties 67
3.6.2 Wind Turbine properties 68
3.6.3 Battery Storage properties 68
3.6.4 Converter 69

3.6.5 Main grid connection 70
3.7 Economics Analysis 70
3.7.1 Net Present Cost 70
3.7.2 Levelized Cost of Energy 71
3.8 Sensitivity Analysis Inputs 71
CHAPTER FOUR 73
4 Result Analysis and Discussion 73
4.1 The Scenarios 73
4.1.1 Standalone system (scenario one (1)) 73
4.1.2 Grid-connected system without batteries (scenario two (2)) 75
4.1.3 Grid connected system with batteries (scenario (3)) 77
4.2 The First Approach (Techno-economic) to Scenario Comparison to Choose the Most Viable HBMG System 79
4.3 The Second Approach (awarding/allocation of points) to Scenario Comparison to Choose the Most Viable HBMG System 82
4.4 Further Analysis of the Selected System, Scenario 2 83
4.4.1 More economical results of Scenario 2 83
4.4.2 Energy generation and consumption 84
4.4.3 Converter optimization results of the optimal system 86
4.4.4 Grid 87
4.4.5 Sensitivity Analysis 89
CHAPTER FIVE 91
5 Conclusion and Recommendations and Future Suggestions 91
5.1 Conclusions and Recommendations 91
5.2 Future suggestions 92
6 References 93

7 Appendix 107
7.1 Appendix A 107
7.2 Appendix B 114

ABSTRACT

The rapid depletion of fossil fuels and the drive to reduce carbon emissions have resulted in a greater emphasis on renewable energy resources. The use of renewable energy resources benefits both the community and the economic growth of the country. Many African countries rely on fossil fuels, hence renewable energy resources must be implemented.

This research focuses on the optimal sizing of a microgrid based on renewable energy sources, with simulation results considering various backup solutions such as battery systems and the grid, with both standalone and grid-connected modes of operation being studied. The most optimal solution was found to be a grid-connected hybrid microgrid (HBMG) system without batteries. Solar radiation and wind speed values were also varied in the sensitivity analysis. The sensitivity analysis revealed that as solar radiation and wind speed values approach maximum values, NPC declines, and vice versa.

The Hybrid Optimization Model for Electric Renewables (HOMER) software created all of the configurations, simulations, and component selections. The average demand on the faculty scale is projected to be 165.29 kWh/day, with a peak load of 81.48 kW.

The study was conducted to increase power system reliability, lowering emissions, and ensure economic sustainability through the integration of renewable energy technologies. Various technologies, such as solar PV, wind turbines, converters, batteries, and the grid, were investigated for system configuration with the lowest net present cost (NPC) and Levelized Cost of Energy (LCOE).

The average solar radiation and wind speed simulation results from the stand-alone with batteries, grid-connected with batteries, and grid-connected without batteries scenarios were analyzed.

The only system with a 100% renewable fraction was the stand-alone with batteries as backup scenario, while the grid-connected with batteries scenario has the lowest renewable fraction capacity, with 77.2% renewable fraction for the grid connected without batteries scenario and 77.5% renewable penetration for the grid-connected with batteries. However, the results also showed that the grid-connected system without batteries scenario has the lowest NPC and LCOE, whereas the standalone system with batteries scenario has the highest NPC and LCOE. The results indicate that the grid-connected scenarios' LCOE and NPC are reduced by more than 80% and 70% for grid-connected without batteries scenario and grid-connected with batteries

scenario respectively when compared to the standalone scenario's LCOE and NPC. The selected scenario's renewable penetration was found to be 87.3 %.

The study is also in line with Algeria's efforts to promote the implementation of renewable energy technologies in its power sector.

CHAPTER ONE

1 Introduction

Global population growth, the need to address the effects of climate change, and promote sustainable energy resources have all contributed to the urgent need to accelerate the development of renewable energy technologies. As a result, access to clean energy generation to address energy security, technology advancement, and sustainable development creates greater interest worldwide.

Due to the global spread of the coronavirus, most renewable energy projects in Africa scheduled for 2020 and 2021 have been delayed. The pandemic's specific impact on renewable energy has yet to be determined. Some studies believe that the pandemic period had a positive effect on the clean energy transition. Others disagree, claiming that the pandemic may have slowed or delayed the development of renewable energy installations [1]. Funds that may have been allocated or planned for the development and growth of renewable energy technologies may have been utilized, aiding in the fight and combat of the pandemic.

And despite issues such as environmental degradation, global warming, and gradual depletion, fossil fuels (such as coal, gas, and oil) account for 65% of global energy generation. In comparison, nuclear accounts for 10%, and renewable energy sources account for only 25% [2]. According to the International Renewable Energy Agency, nuclear energy is classified as a nonrenewable energy resource due to its complicated processes. Thus, in 2017, electricity generation from nonrenewable energy sources stands at a total of 75% [3]. Figure 1 Shows the percentages of electricity-generating sources in 2017.

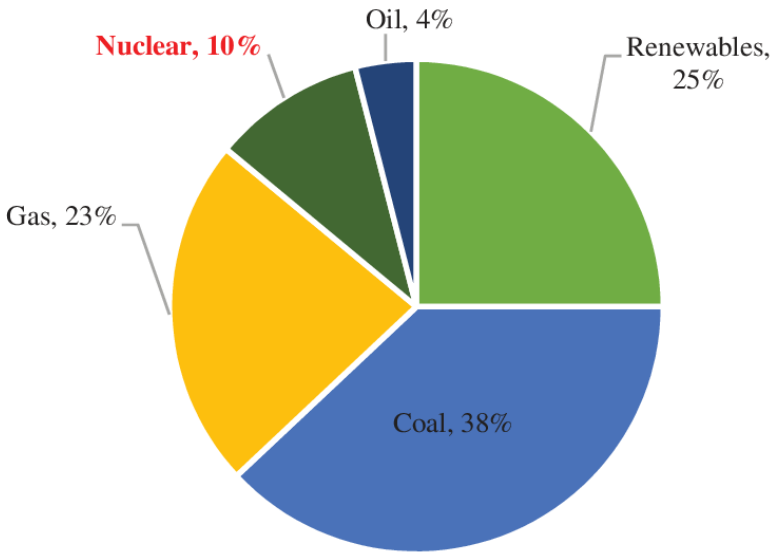

Figure 1. Global electricity generating sources in 2017 [2]

Solar photovoltaic (PV), wind, micro-hydro, and biomass are environmentally friendly, secure, efficient, and have reduced total costs. As a result, they have recently stimulated interest in microgrid applications and power generation. For example, the 2015 Paris Agreement set a target of rapidly shifting to renewable energy to keep global temperatures below 2°C. This goal can only be met with the global use of renewable energy sources [4].

Microgrids can run on their own or as part of a larger utility grid. To size and build a hybrid system that efficiently uses both solar and wind energy, variables such as solar radiation data and wind speed data must be studied and available. [5].

Microgrids provide important loads with long-term stability in the event of power outages in grid-connected modes, and they are more resilient than utility grids [6].

To optimize performance, a renewable energy-based (HBMG) architecture combines two or more renewable energy sources with a storage system or connected to the grid [7]. Microgrids can integrate different renewable energy sources with backup storage systems due to intermittency difficulties. The fact that the costs of renewable energy sources are decreasing makes it a more viable option than a power system that relies on a single renewable energy source [8].
The objectives of the microgrid optimization challenges are to maximize power while lowering expenses, extending the life of the ESS, and reducing environmental costs [8].

1.1 Background of the Study

Algeria has massive natural gas reserves, ranking third in the world for shale gas reserves. Algeria's electrical sector is heavily reliant on natural gas due to its abundance and low cost. In 2015, natural gas and oil accounted for 95% of Algeria's exports. Despite the low cost of gas in Algeria, natural gas is a fossil resource that could run out in the future, posing a risk to the country's economic development and future power plants [9]. In 2016, fossil fuels accounted for 98.75% of Algeria's power generation [10].

Despite government efforts to boost renewable energy in the energy industry, Algeria has had little success in promoting renewable energy. This slow transition may be influenced by the country's low cost of fossil fuels [11].

Exploiting and promoting a country's renewable energy resources, on the other hand, provides a way to resolve energy-related and economic issues while also contributing to the country's long-term progress. In the Sahara region of the country, Algeria has enormous solar energy potential, and it may even be able to satisfy all of Europe's electricity needs [12].

Increasing costs, such as implementing significant taxes and eliminating subsidies for carbon-emitting sources, will encourage consumers and businesses to lower their demand for fossil fuels in favor of sustainable energy [13].

Algeria's energy-related companies include Sonelgaz, the Renewable Energy Development Center (CDER), Sonatrach, NAFTEC, and NAFTAL.

Sonelgaz is Algeria's largest provider of power and natural gas utilities. **CDER** (Renewable Energies Development Center) is in charge of scientific research on renewable energy, and **Sonatrach** exploits the country’s hydrocarbons in the country. National Petroleum Refining Company (**NAFTEC)**, a supporting company within Sonatrach, is in charge of oil refineries' operation, management, and market development. **NAFTAL**, another supporting company within Sonatrach, is in charge of the selling of petroleum [14].

Microgrids based on renewable energy improve productivity in a range of applications. The Hybrid Optimization Model for Electric Renewables (HOMER) software will be used to simulate and optimize the cost of electricity production, renewable energy fraction (solar and wind), and carbon dioxide emissions from hybrid systems used in campus electrification, as well as to determine

which hybrid mode of operation is most appropriate and the HOMER software will also be used to examine the data.

1.2 Problem Statement

The World Health Organization (WHO) estimated in 2018 that ambient air pollution causes 4.5 million deaths annually. Furthermore, the World Bank predicted in 2020 that the number of people at risk of poverty as a result of climate change effects would rise from 68 million to 138 million by 2030. According to International Monetary Fund (IMF), the cost of fossil fuel-related consequences such as climate change, air pollution, traffic accidents, and vehicle congestion costs world governments approximately $5 trillion per year [15]. As the electricity demand grows, reliance on fossil fuel plants increases the rate of emissions.

Algeria is a major Carbon dioxide (CO_2) emitter, ranking third in Africa with 147 metric tons of CO_2 emissions in 2014, primarily from natural gas, and ranking 34th globally in gas flaring emissions. Over the last decade, Algeria's yearly rainfall has plummeted by 30%. Its carbon capture capacities are limited due to land characteristics (such as vegetation, water bodies, and so on) [10].

Utility grids sometimes experience high peak loads and power outages that can lead to failure. They also incur high operation costs. Power grids are sometimes far from consumers, causing transmission losses. Other challenges and potential challenges encountered on utility grids include potential cyber-attacks, which can generate incorrect data and block error messages, resulting in grid failure; old and aging infrastructures, which reduce system efficiency; the issue of reliability, which natural forces could cause utilities present; degradation of transmission lines, corrosion, mechanical and electrical stresses [16].

1.3 Research questions

The following questions will lead this research to address the issues raised in this study:

1. Can an optimally sized campus microgrid powered by renewable energy sources provide reliable clean energy while incurring lower operational costs?
2. Which is the least cost-effective between stand-alone and grid-connected microgrid modes?
3. What environmental benefits will microgrids bring?

4. How far has the development of microgrids progressed in Algeria?
5. What are the setbacks for renewable energy (wind and PV) based hybrid microgrids deployment in Tlemcen?
6. Can developing countries like Algeria achieve industrialization without relying too heavily on fossil fuels?

1.4 Research Objectives

General Objective

Optimal Sizing of a Microgrid is the main objective of this study.

Specific objectives

- ✓ To reduce carbon emissions by minimizing the generation of electricity from fossil fuel sources.
- ✓ To minimize reliance on conventional energy sources and on a grid that may face power outages.
- ✓ To improve energy efficiency and reliability, microgrids are smart grid systems.
- ✓ To minimize life cycle costs.
- ✓ To determine the most optimum renewable energy-based hybrid system between stand-alone and grid-connected systems by determining optimal Hybrid Microgrid (HBMG) component sizes, including energy storage, analyzing technical and economic performance, and considering environmental impacts for the Chetouane campus.

1.5 Thesis contribution

The thesis' contribution is a comparison of the three scenarios using HOMER pro software simulation, optimization, and sensitivity analysis, with standalone and grid-connected types of operational modes investigated and incorporating both completely renewable power and grid-backed renewable microgrids. These simulations were run to meet a campus load requirement.

1.6 Scope and limitation of the Study

A series of studies are required to investigate all of the topics and characteristics of HBMG, and this master's thesis focuses on a single case study. The HOMER software will design, simulate, optimize, and perform a sensitivity analysis of an HBMG employing renewable energy sources for a particular university faculty in Chetouane, Tlemcen, Algeria.

In Algeria, little research has been conducted on microgrids, with some studies focusing on stand-alone hybrid systems' economic and technical feasibility. This study will analyze stand-alone and grid-connected HBMG modes for a university campus in Tlemcen and determine which mode of operation is the best option to consider after different analyses.

Solar PV is chosen for this study because its potential is abundant at the study site. It is supplemented by wind energy, despite studies showing that wind potential is not promising in most parts of Tlemcen. The Tlemcen highlands are suitable sites for wind energy generation. Since batteries are the most expensive portion of the system, adding an ESS makes it difficult for the generated power to be cost-competitive with grid power. As such, a grid-tied HBMG will also be considered in the analysis of this study.

1.7 Possible obstacles

One of the potential barriers at the study site could be obtaining primary data, as there may be numerous bureaucracies in place to access the necessary data. The primary data source is the Chetouane campus administration of the University of Tlemcen, Faculty of Technology.

Another obstacle during primary data collection could be indigenous language barriers. Algeria’s official and commonly used languages are Arabic and French.

1.8 Relevance of the study

This study is relevant for the following reasons:

The study will seek how institutions in Algeria can apply clean, reliable, and cost-effective distributed energy resources (DERs) to minimize emissions and seek a future cost-effective means of generating power and finding a solution to minimize occurring or possible power outages and support critical loads.

CHAPTER TWO

2 Literature review

The goal of this literature review is to provide a quick overview of previous work on this topic, microgrids concepts, power management of microgrids, Distributed Generations (DGs) and microgrids, microgrid power electronics, microgrid stability, and mathematical modeling of components. It will also outline the study country's renewable energy resources and the sector's development.

2.1 Previous works related to this topic

This research is linked to several scientific studies, including the following:

An analysis of a microgrid performed for both stand-alone and grid-tied using HOMER energy pro to design the parameters of an energy system based on local weather conditions in available databases comprising of the PV system, wind system, and a diesel plant in a study carried out in Columbia shows wind system having limited influence on the microgrid which unsuitable wind profiles may cause for the wind generator technologies in the software. Both modes show to be technically viable though not viable economically caused by higher implementation costs [17].

An optimal configuration study in India of a campus microgrid using HOMER software investigated and analyzed economic parameters and CO_2 emissions with solar and wind data obtained from NASA and enviro engineer's site respectively and after some simulations and modeling on various microgrid modes. A grid-connected microgrid based on solar, wind, and batteries was likewise discovered to be the optimal solution [18].

Another study using HOMER to evaluate the viability of a microgrid and performing sensitivity analysis based on wind speed data, solar radiation of the area, and diesel generator was carried out to reduce costs and CO_2 emissions by 50% with the study goal achieved for an institution [19].

Building microgrids is inspired by the desire to eliminate typical power grid outages and reliance on fossil fuels by using locally accessible renewable energy sources. As such it is essential to carry out unit sizing in the design of microgrid architectures. The optimum system configuration regarding total system size and cost would benefit from the proper combination of distributed units. The type and number of microgrid units considered would have a major impact on total device sizing [20].

S. Salisu, M. W. Mustafa, L. Olatomiwa, and O. O. Mohammed used HOMER to perform a techno-economic and environmental assessment of a microgrid, taking cost analysis and sensitivity analysis into account. The optimal design was shown to be environmentally friendly and less costly after the results and sensitivity analysis [21].

A study in south Jordan seeks a smart grid method for distributed generations of PV and wind hybrid design using HOMER software to shift away from imported energy and transition into clean and less costly energy. Following the modeling by the software, the design was found to be economically feasible [22].

For a rural site in Algeria, a techno-economic optimization using MATLAB software to build a standalone hybrid system based on PV, wind turbine, diesel generator, and battery system revealed an optimized cost of using the design's generating sources [23].

A feasibility study by L. Uwineza, H. G. Kim, and C. K. Kim proposes integrating renewable energy sources into an already existing diesel generator at Popova Island by using Monte Carlo Model and HOMER. The conclusion of the study based on the scenarios indicated valuable inputs from stakeholders, increased renewable sources potential, the resulting configuration, and minimized electricity costs [24].

A. M. Abdilahi, A. H. Mohd Yatim, M. W. Mustafa, O. T. Khalaf, A. F. Shumran, and F. Mohamed Nor also used HOMER to conduct a feasibility analysis of a hybrid system supported by renewable energy in Hargeisa, Somalia. The results showed increased renewable energy sources use, reduced energy costs compared to electricity supply from a diesel generator that has been the sole source of electricity in Hargeisa [25].

Another related study by A. Hirsch, Y. Parag, and J. Guerrero investigated microgrid's background, challenges, prospects, and applications. The findings of the work showed microgrids are a resilient and reliable solutions to electricity supply [26].

The application of control mechanisms to operation modes of a hybrid system using solar and wind and battery under charge regulation yielded high-quality supply for the load from direct wind and PV supply in a study by [27].

In another study by N. Shirzadi, F. Nasiri, and U. Eicker, an optimal configuration of a renewable energy sources-based microgrid was conducted at Concordia University with the target of

minimizing net present cost. The findings showed that the cost of energy was minimized by 50% and vertical axis solar tracker usage was preferred [28].

Research on the optimal configuration of a renewable energy sources-based microgrid was undertaken at Concordia University in a study by (Shirzadi et al., 2020) to minimize net present cost. According to the results, the Levelized Cost of energy was reduced by 50%, and a vertical axis solar tracker was favored.

B. E. Türkay and A. Y. Telli used HOMER software to conduct an economic analysis of autonomous and grid-tied hybrid systems for a university campus in Istanbul, Turkey, intending to determine the best optimal hybrid renewable system based on the location's solar radiation and wind resource potential, as well as hydrogen as a storage system, and found that a grid-tied system is the most feasible [29].

Using solar and wind data from a site inNepal, a simulation of a solar PV and wind stand-alone hybrid system revealed the system as reliable and reduced transmission costs [30].

Using the HOMER tool, a feasibility and sensitivity analysis for standalone and grid-connected renewable energy-based systems in Bangladesh revealed an optimal system, with NPC being more sensitive to nominal discount and wind speeds [31].

2.2 Geographical and Climatic Overview of Algeria

Algeria, located at 28.03° N, 1.66° E, is Africa's largest country, with a total size of 2.38 million $km^{2,}$ with the Sahara Desert covering 80% of the territory. The Mediterranean Sea borders it on the north, Mali, Niger, and Mauritania on the South, Libya and Tunisia on the East, and Morocco and Western Sahara on the west. On the sea, Algeria is as well bordered by Italy and Spain. Summers are hot and dry, and winters are moderate and rainy in Algeria's coastal and northern regions, which have a Mediterranean climate.

Figure 2. Map of Algeria [32]

2.3 The Economic Situation in Algeria

Like most others globally, Algeria's economy saw a significant fall in 2020 due to the COVID 19 epidemic. The drop in Algeria's economy can also be ascribed to a decline in hydrocarbon demand and market hydrocarbon prices. The government has vowed to restore economic growth and stability through the private sector, but the pace of recovery is expected to be slow.

Algeria's population is estimated to be about 44 million people in 2020, with a Gross Domestic Product (GDP) of $ 147.6 billion and a life expectancy of about 77 years [33].

2.4 The renewable energy potential of Algeria

Algeria has abundant natural resources, and its economy relies mainly on fossil fuels, with natural gas and oil accounting for about all of its country's primary energy consumption. Natural gas alone accounts for 96% of installed capacity, with the remaining 4% coming from oil, solar, hydro, and wind. According to the Algerian Commission for Energy and Gas Regulation (CREG), total installed capacity will increase by 14,600 MW by 2028, with natural gas's share dropping to 84 percent and solar's share rising to 15% of total energy generation. Algeria's predicted rise in energy production is due to the country's growing population, which has increased at a rate of 2% per year on average between 2009 and 2019, with populations of 35 million and 43 million, respectively

[34]. Currently, the installed capacity of renewable energy sources is estimated at 450 MW, which is expected to rise to 22,000 MW by 2030 to meet the targets of Algeria's pursuit of a renewable energy transition by 40 percent [12], [34].

Algeria began adopting renewable energy policies and funds in 1998, and its solar, wind, hydropower, biomass, and geothermal resources have the substantial potential [35].

In a decree issued in 2014, the Algerian government-mandated feed-in tariffs for wind and solar PV projects with a capacity of 1MW or greater [36]. The power purchasing agreement contains two phases of implementation, with the first phase to be implemented over 5 years based on predicated production for solar projects between 1 MW and 5MW, allocating a fixed sell back price of about 0.18 USD/kWh that is expected to fluctuate between 0.12 $/kWh and 0.22 $/kWh in the second phase. For solar projects of 5MW or more, the fixed price was set at about 0.13 USD/kWh for the first phase, and it is expected to fluctuate in the second phase to an estimated price between 0.095 $/kWh and 0.18 $/kWh. For wind farm projects between 1 MW and 5MW, the allocated fixed sell back price is about 0.14 USD/kWh that is expected to fluctuate between 0.095 $/kWh and 0.18 $/kWh in the second phase. For projects of 5MW or more, the fixed price was set at about 0.11 USD/kWh for phase 1, which is expected to fluctuate in the second phase at an estimated price between 0.083 $/kWh and 0.14 $/kWh. The first phase was set to be implemented over 5 years based on forecasted production, while the second phase was set to be implemented over 15 years depending on the first phase's successful output [37]. Based on these prices, the sell-back rates decrease from the first phase to the second phase.

Algeria has also set an objective of achieving 40% of its electricity generation from renewables by 2030. Algeria's planned phases for implementing renewable energy technology are summarized in Table 1 shows Algeria's planned capacities of renewable energy technologies deployment and figure 3 shows its installed capacity as of 2019 and the projected growth in the capacity as of 2028.

Table 1. Algeria's plans to generate electricity from renewable energy [12]

Target date	1st phase 2010-2013 (MW)	2st phase 2015-2020 (MW)	2nd phase 2021-2030 (MW)	TOTAL (MW)
Photovoltaic	6	3000	13500	16581
Solar Thermal	25	1025	2000	3850
wind	10	1010	5010	6030
Biomass	-	360	100	460
Others	-	260	450	710
TOTAL	41	6455	21135	27631

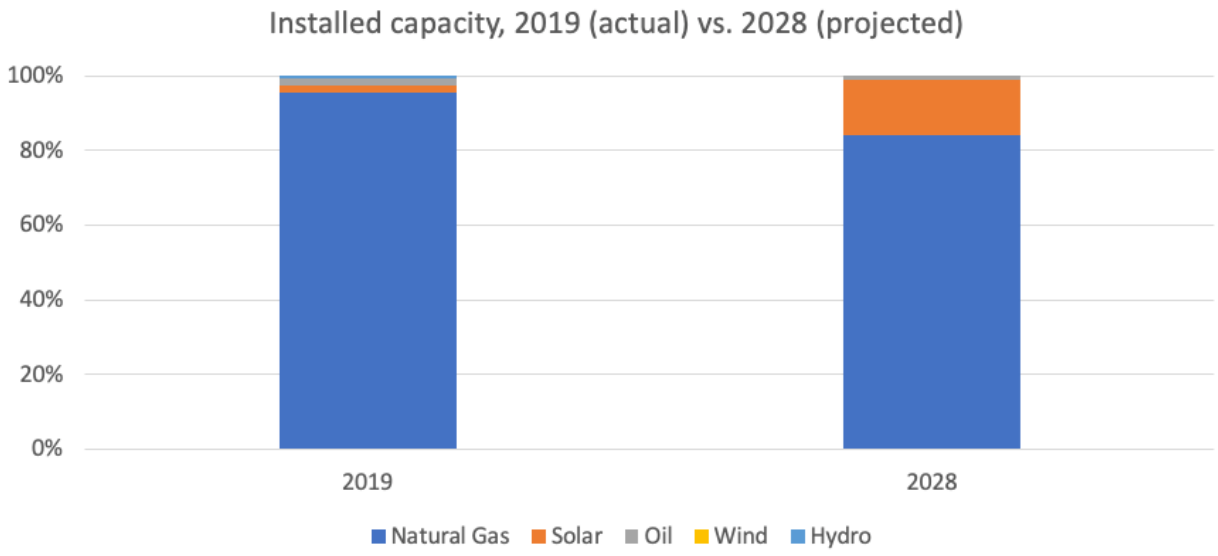

Figure 3. Algeria's energy capacity installed in 2019 vs. predicted capacity in 2028 [34].

2.4.1 Algeria's potential in solar energy

According to a German Space Centre study, Algeria has enormous solar potential, estimated at 169,440 TWh/year, with over 2000 hours of sunshine annually across the nation and up to 3900 hours in the highlands and Sahara [38]. In the north, the average horizontal surface radiation is around 1700 KWh/m^2/year, while in the south, it is roughly 2263 KWh/m^2/year. Figure 4 and Figure 5 summarize the solar potential in Algeria.

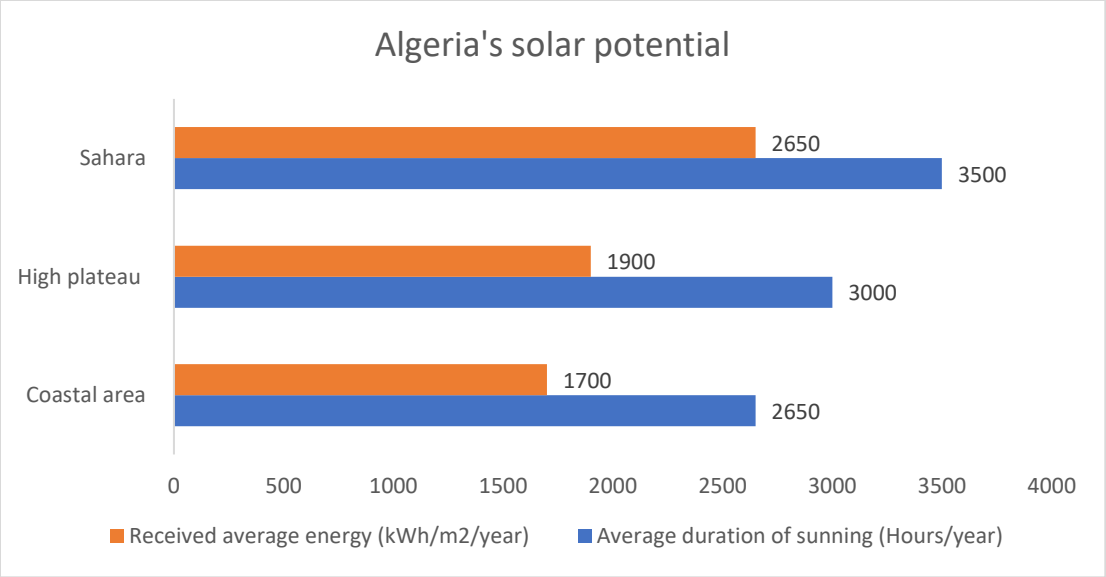

Figure 4. Solar potential of Algeria per region [39]

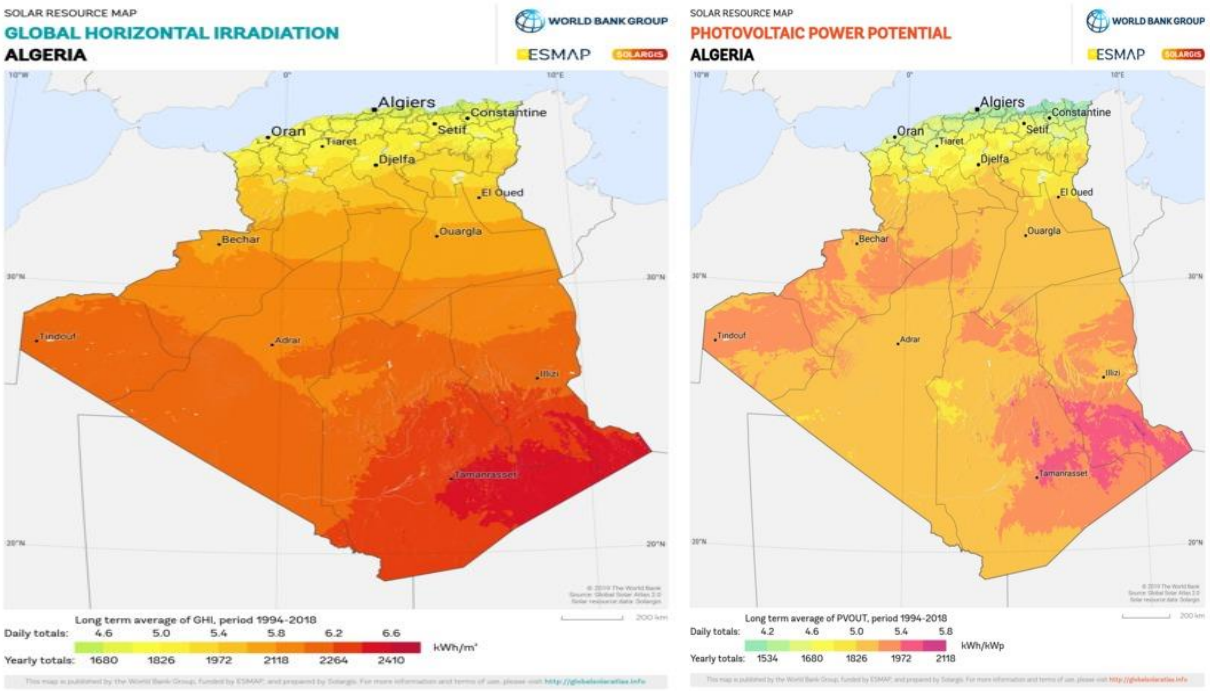

a) *b)*

Figure 5. a) Global horizontal irradiation of Algeria; b) Solar PV potential in Algeria [40]

For modest PV installations, around 4 kWh/m^2/day is sufficient, and for solar thermal installations, approximately 5 kWh/m^2/day is sufficient [41].

2.4.2 Algeria's potential in wind energy

A location's topography and climate influence wind power. The northern region of Algeria is regarded as an excellent wind-harried area due to its proximity to the Mediterranean Sea, the Atlas Mountains, and the highlands. Despite its low elevation, the southern part of Algeria has higher wind potential, with winds ranging from 4 to 6 m/s. According to studies, the province of Adrar has the best wind potential in the country. Strong winds surrounding high hills have the advantage of facilitating the installation of wind power plants [42]. The wind potential of Algeria is presented in figure 6.

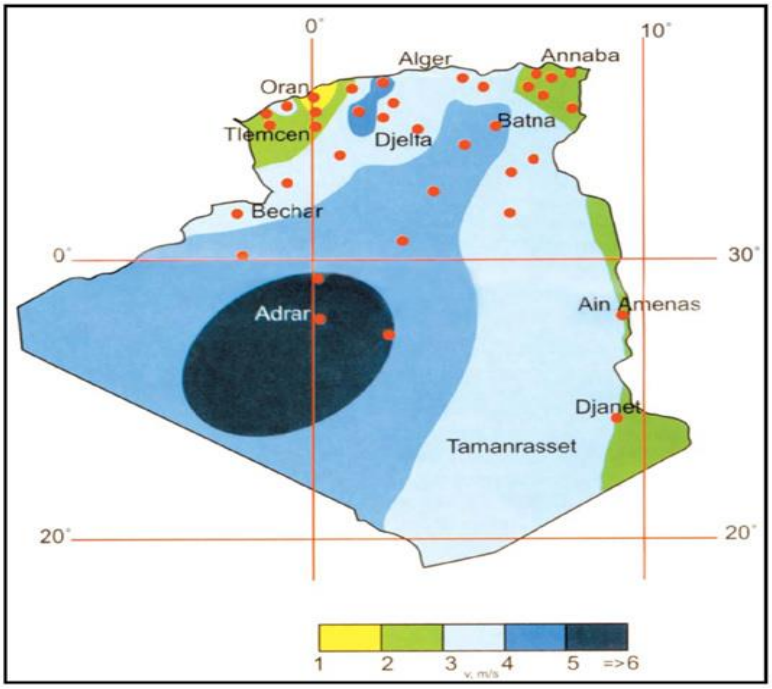

Figure 6. Wind speed (m/s) potential of Algeria [43]

2.4.3 Algeria’s hydropower potential

Algeria's hydropower potential is promising, with 103 prospective dam sites in the country. The yearly output of 13 installed hydropower facilities totals an estimated 389.4 GWh [44]. Figure 7 shows the 13 installed hydropower plants in Algeria, which are located in the north. Table 2 shows the hydropower plants' generation capacities of about 269 MW in Algeria between 2017 and 2019.

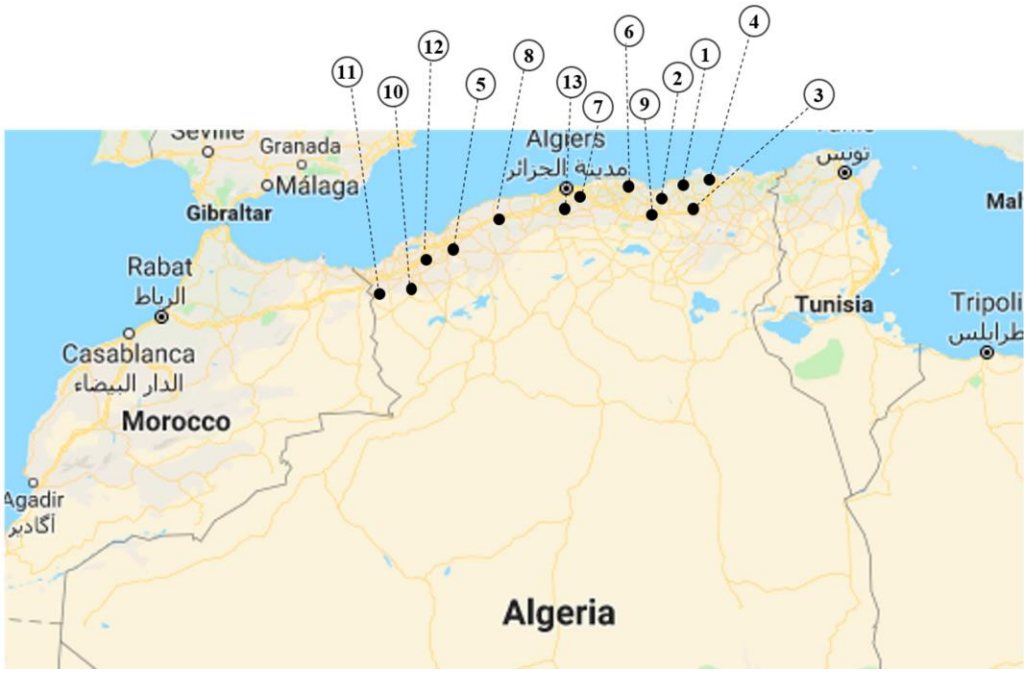

Figure 7. Installed hydropower plants locations in Algeria [44]

Table 2. Hydropower plants and their generation capacities in Algeria [44]

STATION	PROVINCE	CAPACITY (MW)
DRAGUINA	Bejaia	71.5
IGHIL EMDA	Bejaia	24
MANSORIA	Bejaia	100
ERRAGUENE	Jijel	16
SOUK EL DJEMAA	Relizane	8.085
TIZI MEDEN	Tizi ouzou	4.458
IGHZENCHEBEL	Algiers	2.712
GHRIB	Ain defla	7
GOURIET	Bejaia	6.425
BOUHANIFIA	Mascara	5.7
OUED FODDA	Chlef	15.6
BENI BEHDEL	Tlemcen	3.5
TESSALA	Algiers	4.228

2.4.4 Algeria's biomass energy potential

Municipal solid waste is the most important source of biomass in Algeria, with an estimated capacity of 10 million tons per year generated [42]. Although the target is to extract 1 GW of biomass by 2030, no installed biomass-producing facility [35].

2.4.5 Algeria's geothermal energy potential

Geothermal power projects in Algeria are used for various purposes, including heating, cooling, fish farming, and agriculture. There are over 240 springs in the country, with the highest temperature in the western part of the country being 68°C, the highest in the central part of the country being 80°C, the average temperature in the southern springs being 50°C, and the highest temperature in the eastern part of the country being 98°C [45]. Algeria has 41 geothermal spots, as shown in Figure 8.

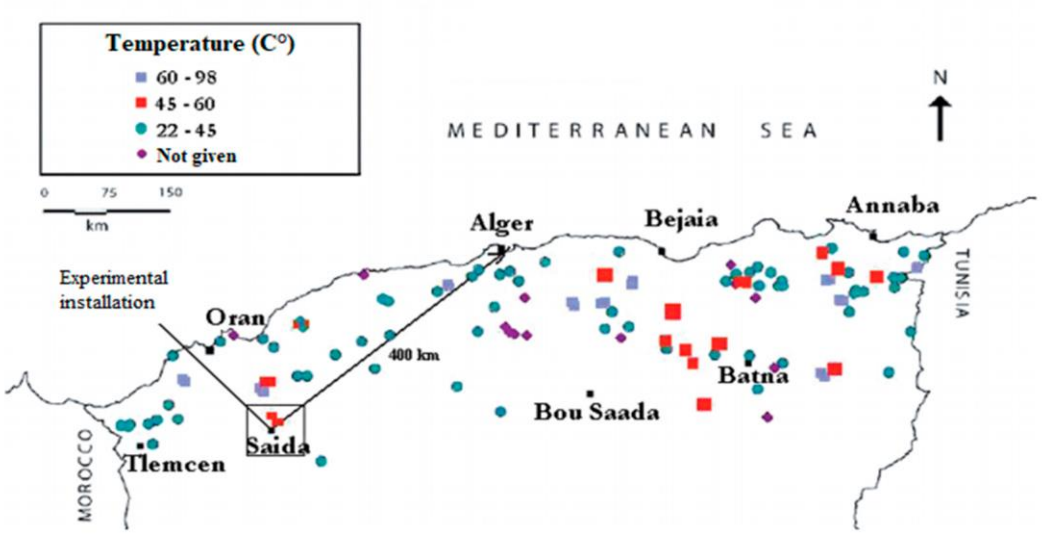

Figure 8. Algeria's geothermic chart [44]

2.5 Background of Microgrids

Due to the multiple blackouts that occurred in many countries around the world in the early 2000s, the idea of using distributed generation (DG) sources has gained a lot of popularity due to its unique characteristics, such as durability, decentralized generation, renewable energy usage, and increased local reliability. Despite these benefits, DG suffers from intermittency, sluggish response

times, and controllability, which is why international scholars first proposed the micro-network definition [46].

With the increasing decentralization, decarbonization, and democratization of electrical structures, greater enhancement of DGs coupled with the necessity for resilient and reliable electricity supply as well as the requirement for low electricity costs and the global fight against minimizing CO_2 emissions has led to an interest in the pursuit of microgrids to meet a variety of community needs. Microgrid generation capacities for developed countries should be measured in gigawatts. Decentralized technologies were first proposed in 1990 to handle distributed resources, increase power stability, resilience, and reliability on critical loads [26].

There are various definitions of a microgrid in literature, the definition adopted in this study is from the U.S Department of Energy (DOE), which defines a microgrid as a "characterized collection of interconnected loads and DERs functioning as a single controllable entity concerning the grid within clearly defined electrical limits". A microgrid can operate in grid-connected or island mode by connecting and disconnecting the grid [47]. Microgrids that are well-designed are more effective, resilient, reliable, environmentally friendly, versatile, and stable. Microgrids are suitable for changing electrical loads because they provide uninterrupted power, and with the right control system, microgrids can be easily controlled from cyber threats [48].

2.5.1 Overview of Microgrids

On the other hand, a microgrid is a small electrical entity that can generate, transmit, and distribute energy efficiently over a vast area. As such, Microgrids offer more flexibility than traditional electricity systems [49].

In situations of power interruption occurring on a traditional grid, a grid-tied microgrid with well-designed control mechanisms can be an island and still feed its load without affecting the integrity of the main grid.

Consumers, technology suppliers, power transmission and distribution providers, and policymakers are all involved in microgrid activities as stakeholders, as shown in Figure 9.

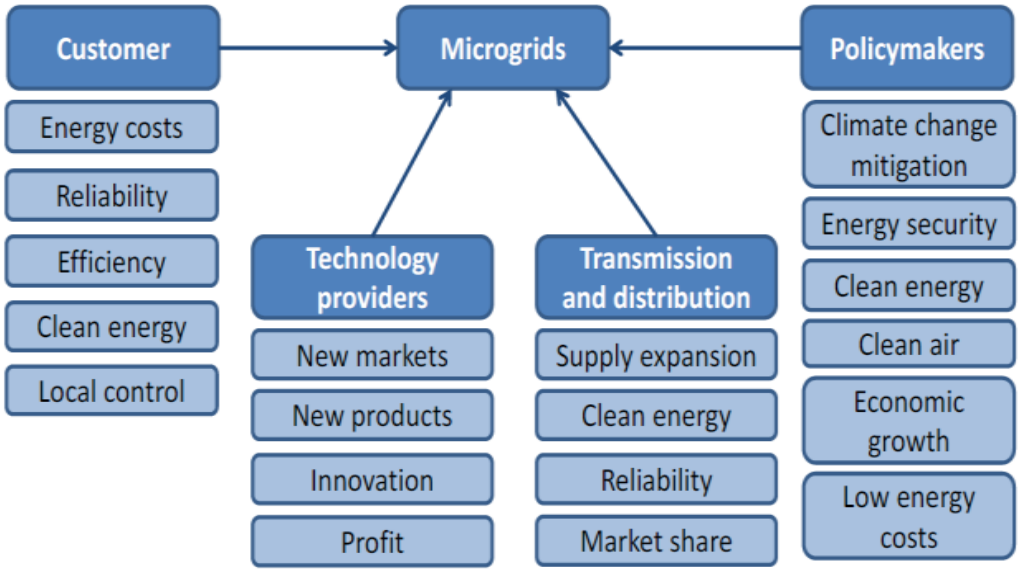

Figure 9. stakeholders involved in Microgrids [50]

2.5.2 Current situation of Microgrids

Many research activities and microgrid projects have been established in response to microgrids' numerous advantages, including one pilot 1-phase microgrid project and the Sendai Microgrid in Japan, a DERs test facility in Europe, and the United States a microgrid facility for controlling the energy sources and loads [51]. In another development using intentional islanding, the IEEE explored ways to link DERs to the grid. DER may be connected to an area in various ways to provide cogeneration or prime, peak-shaving (load reduction at peak times), emergency, backup, premium, or remote control (Del Carpio Huayllas et al., 2011).

Technical constraints, infrastructural impediments, economic limitations, and public awareness are among the developmental downsides of microgrids, according to [52].

Microgrids' high capital investment cost is the most significant impediment to widespread and rapid implementation [48].

2.5.3 Microgrid Prospects

Electric power grids have become smarter and more efficient as a result of technological advancements. The distribution network must migrate from passive to active in order to encourage the installation of the smart grid, which promotes DG and permits real-time participation of generation units and consumers in power systems optimization. Implementing DG and ESS in a microgrid encourages renewable energy and promotes sustainability [49].

The International Renewable Energy Agency report highlighted five innovative solutions to help renewable energy-based microgrids become “the energy of the future” [53]. They are as follows [53]:

- Availability of load data

When correct load data is presented, it can help in the development of microgrid efficiency. However, due to a lack of data, the development of microgrids has been hampered.

- Long-term Supervisory Control

According to the study, creating of control algorithms that balance economically-based decisions with renewable consumption will help with real-time decision-making.

- Storage Manufacturing

Falling ESS costs will help cut costs, promoting microgrid deployments throughout the globe. Increased storage manufacturing can stimulate market competition, resulting in lower ESS pricing, boosting microgrid installations. The paper further states that eliminating N-methyl pyrrolidone and reducing electrolyte wetting and solid electrolyte interface layer creation in the ESS manufacturing processes are crucial for potential advancement in microgrids.

- Inverter Performance

According to the paper, improvements to dual-mode inverter capabilities, such as droop control, will make it easier to transition from the grid to island mode with black start and seamless types.

- Power Output

According to the paper, one way to have that kind of dependable service is to use graphene in supercapacitors' electrodes, which will result in a power capability 10 to 100 times greater than current batteries.

Despite substantial research and development into various microgrid features, further work on interoperability, optimization, and incorporation within a microgrid is still needed, which causes utilities and developers to perceive risks [54].

Microgrid based on renewable energy has a bright technological and commercial future, fosters sustainability, and provides a solid foundation for consumers to influence their electricity quality and cost substantially. Their position determines microgrids' future, and microgrids heavily rely on state policy and funding [55].

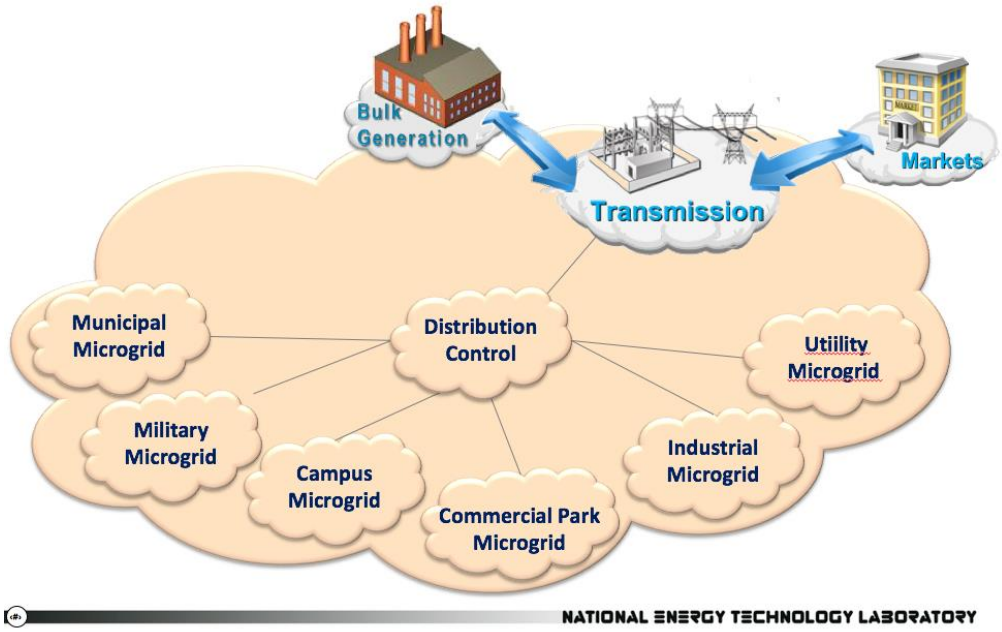

Figure 10. A Potential microgrid Distribution Architecture in the Future [55]

2.6 **Concept of Microgrids**

Currently, some regions have different ideas about what a microgrid is. For example, in the United States, a microgrid can provide both heat and electricity, while in the EU, it only provides electricity. Apart from these differences, all microgrids have islanded, and grid-connected functionalities establish electrical boundaries and a control body that can handle energy resources and loads. Since power grids are prone to outages, a grid-connected microgrid mode must have enough installed generation capacity to keep feeding its load even if the grid is disconnected [56].

Microgrids can store, transform, and recycle their energy, and in the presence of plentiful and cheap energy, they can buy and thus supply loads in energy-short situations. The microgrid's current emphasis is on ensuring that it has enough energy at all times. Smaller operating margins combined with more volatile supply are smart grids' core issues designed to address. The excess electrical power over the amount used at any time is referred to as the operating margin. More

sources, such as wind and solar, are being used, and their production cannot be precisely calculated or regulated, resulting in a volatile supply. These modifications, taken together, result in an oversupply or undersupply at any given point in time [57].

2.6.1 Microgrid Structure

A microgrid system's core system comprises energy sources, ESS, distribution networks, communication networks and control mechanisms.

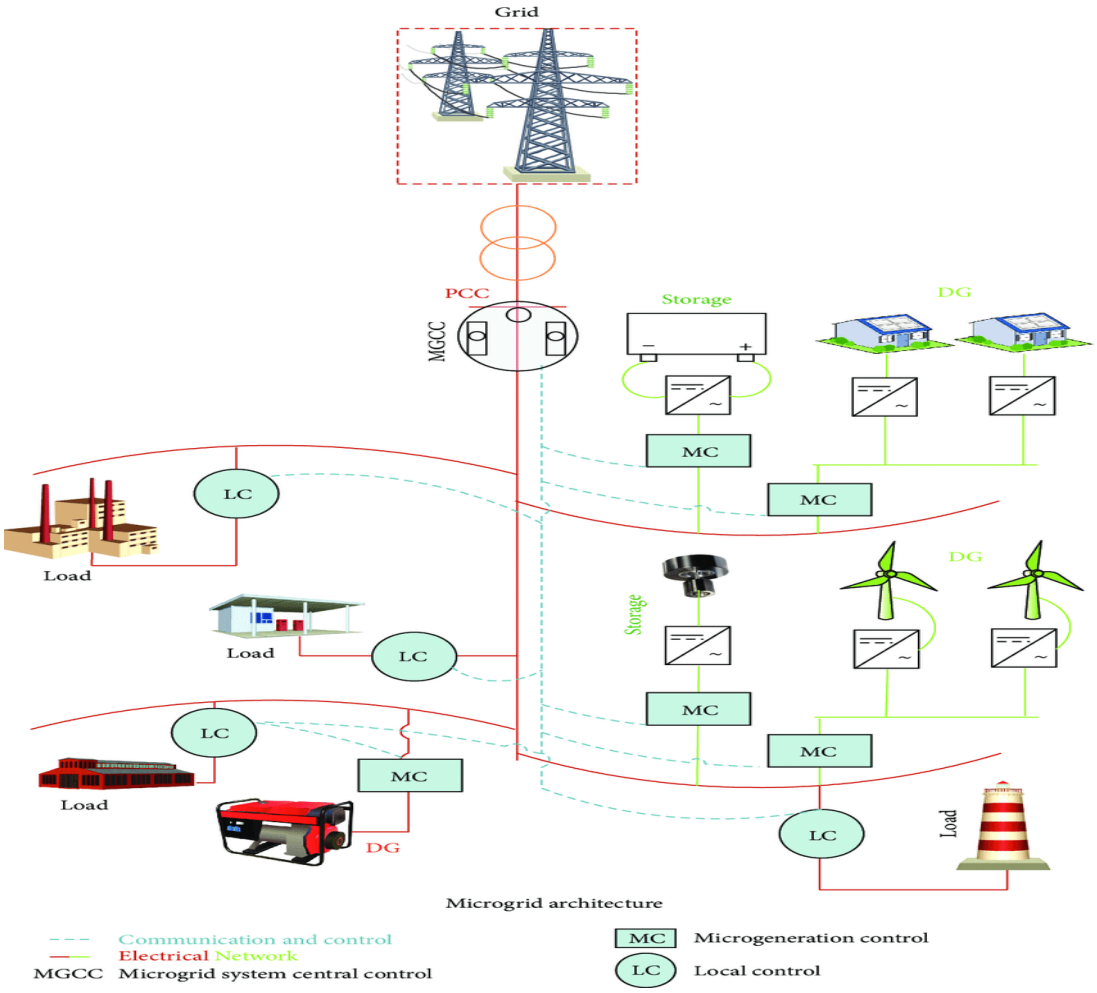

Figure 11. A simple microgrid architecture [58].

In a microgrid, local control contributes to increased efficiency.

2.6.2 Possible benefits and applications of Microgrids

In the future, as the number of DER units in low-voltage networks grows, many possibilities and advantages will be realized, but there will also be challenges. Table 3 summarizes the potential benefits of microgrids for various stakeholders (customers, utilities, and society) [59].

Table 3. Possible benefits of microgrids

Stakeholders	Possible Benefits
Customers	• Microgrids with multiple DG units can provide a more reliable energy supply to meet the growing number of sensitive customers' energy needs. • Using distributed energy sources in microgrids, such as combined heat and power, can provide financial benefits.
Utilities	• Microgrids make it possible to use electricity more efficiently than conventional centralized power systems. • Microgrids can minimize total greenhouse gas emissions as compared to centralized power systems. • In microgrids, the chances of using renewable energy sources have increased and have been diversified. • Microgrids can also help increase the reliability of electricity distribution.
Society	• Active network management through DER units and microgrids allows for more effective distribution of power usage. • Microgrids will delay distribution system upgrades by supplying dispatchable power for use during peak power conditions. • Microgrids are a component of smart energy systems that are capable of addressing potential energy issues and replacing aging energy infrastructure. • Microgrids can provide sensitive consumers with premium power at higher prices. • Microgrids allow the opportunity to save money and time that would otherwise be spent on building massive power plants.

As microgrids are expected to provide many more benefits to consumers, utilities, and societies, their potential applications are expanding in a variety of areas, including university campuses and high schools, hospitals, police stations, water treatment facilities, remote communities, residential areas not connected to grid, and military units [59].

As of 2017, the Asia Pacific region and North America had the highest microgrid power capacity markets, accounting for 40% and 34% of the global total microgrid market, respectively. The Middle East, Africa, Europe, and Latin America regions account for the remaining 26 percent. In contrast, the Antarctica region made no attempts at microgrid development, as shown in figure 12.

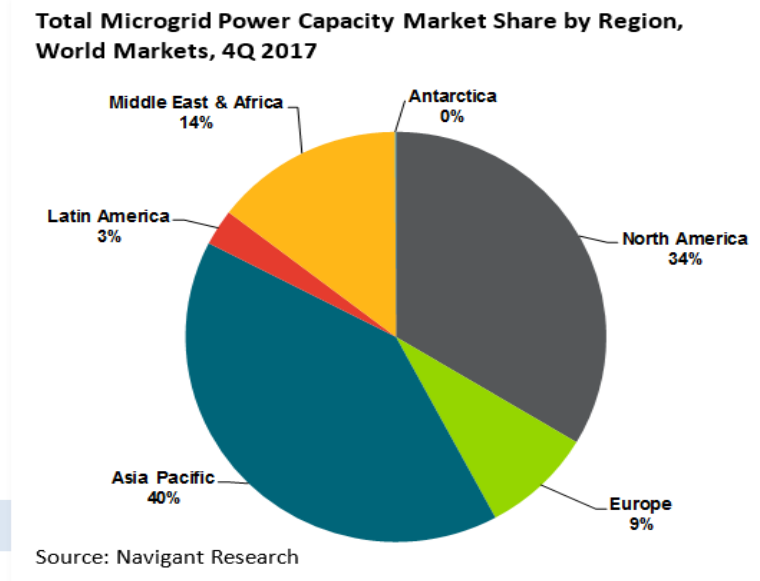

Figure 12. Total global microgrid capacity market share by region [60]

Microgrids can offer intriguing benefits in developing countries, especially in Sub-Saharan Africa, for addressing distribution and generation challenges [61].

2.6.3 Microgrid Components

The components of a microgrid must be compatible with its modes of operations, i.e., both islanded and grid-connected modes. A microgrid's major components include DGs, storage devices, loads, microgrid monitoring and control systems, and grid interconnectors [62], [63].

2.6.3.1 Distributed generations (DGs)

These are power-generating sources connected to a distribution grid and can be both renewable and nonrenewable energy sources. The renewable energy sources include solar PV, wind, biomass, solar thermal, and mini hydro, whereas nonrenewable energy sources include diesel, natural gas, combustion turbines, reciprocating engines, cogeneration, turbines, and microturbines [63]. DERs refer to a technology that incorporates both DGs and ESS.

The energy source and fuel storage requirements must meet microgrid criteria such as intended producing power, needed strength level, ramp rate, clean energy goals, and fuel availability. Incorporating renewable energy sources into microgrids is gaining popularity due to recent cost reductions [63].

Table 4 summarizes the characteristics of the most commonly used distribution energy generation sources in microgrids.

Table 4. Typical Characteristics of Microgrid DG Sources [63]

Characteristics	Solar	Wind	Micro-Hydro	Diesel	CHP
Availability	Determined by geographical position	Determined by geographical position	Determined by geographical position	Anytime	Based on source
Power	DC output	AC output	AC output	AC output	AC output
Control	can't be controlled	can't be controlled	can't be controlled	can be controlled	Based on source
Typical interface or power electronic	DC-DC-AC converter	AC-DC-AC converter	Synchronous of induction generator	Null	Synchronous generator
Power flow control	Maximum Power Point Tracker (MPPT) and DC link voltage control	MPPT, pitch and link voltage control	Can be controllable	Can be controllable	Automatic Voltage Regulation and governor

2.6.3.1.1 Solar PV systems

Photovoltaic (PV) is derived from the Greek words for "light" (photo) and "electrical" (voltaic). PV is a technology that converts sunlight directly to electricity. A solar cell, or PV cell, is the main component responsible for this conversion. When sunlight (photons) strikes a solar cell made of semiconductor material, it increases the energy of the semiconductor's electrons, allowing the electrons to move freely and produce current, voltage, and electricity [64], [65].

PV cells use only the sun's energy as a source of fuel. A PV module comprises a set of PV cells, while a PV panel is made up of PV modules, and a PV array is made up of PV panels that function as a complete power generator [65].

PV modules and arrays are rated in watts under standard test conditions, such as a cell (module) operating temperature of 25°C and incoming solar irradiation of 1000 W/m^2 [66].

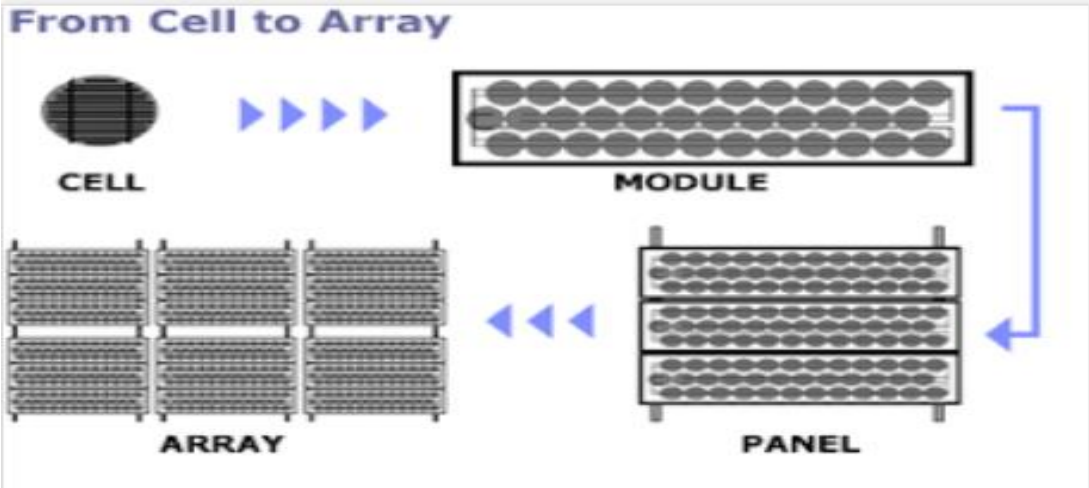

Figure 13. PV cell, module, panel, and array structures [67]

Prior to the discovery of other elements, silicon was the sole material available for making PV cells. Characteristics such as efficiency, cost, and material availability distinguish PV cells into three generations categories in table 5.

Table 5. Types of PV cell generations [68][69][70]

Generation	Solar cells
First-generation	• Monocrystalline or single-crystal silicon and • Polycrystalline or multi-crystalline.
Second-generation	• Amorphous silicon, • Cadmium telluride, • Copper Indium Gallium Selenide, and • Gallium Arsenide.
Third-generation	• Organic photovoltaics, • copper zinc tin sulfide (CZTS), • Perovskite solar cells, • Dye-sensitized solar cells (DSSCs), and • Quantum dot solar cells

Although more expensive than second and third-generation solar cells, first-generation solar cells are the most commonly used solar cells. This is owing to the material's better efficiency and widespread availability on Earth. The second-generation (thin film) has lower production costs than the first-generation, and they have better efficiency than the third generation. Solar cells of the third-generation solar cells have been developed to be less expensive than the first and second

generations. P-n junctions aren't used in third-generation solar cells [71]. Monocrystalline (mono c-Si) solar cells have the highest efficiency. They are the most expensive first-generation solar cells, followed by polycrystalline (poly c-Si) solar cells and then amorphous silicon [72].

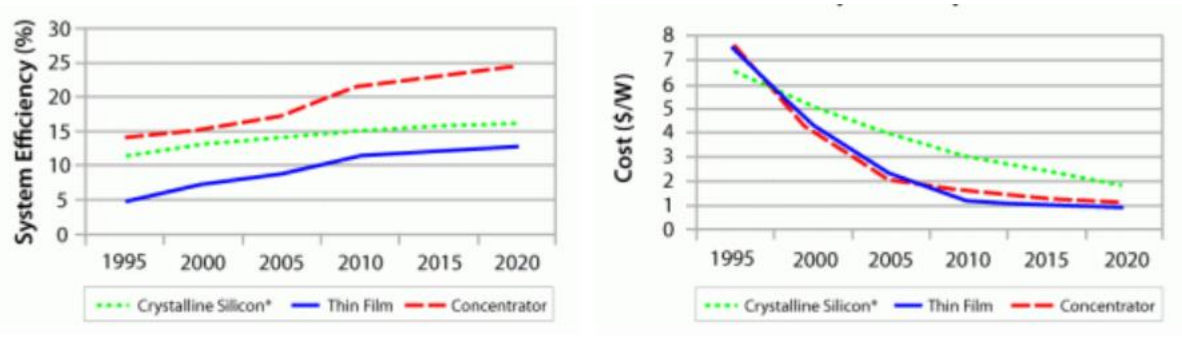

a) *b)*

Figure 14. a) PV cells efficiency b) cost comparisons [73]

2.6.3.1.1.1 Types of PV systems

Stand-alone PV systems and grid-connected PV systems are the two types of PV systems.

i. Stand-alone PV systems:

These types of PV systems rely solely on direct solar energy for service. It consists of PV modules, loads, and, in some cases, batteries for energy storage when the sun is not around to provide energy. This system also includes charge controls for controlling battery discharge and overcharging. The charge controller also powers DC loads using either the battery bank or direct supply from the solar array. Inverters help convert DC to AC power for AC loads since the power from the solar and stored in the batteries is DC [64]. Figure 15 shows a simplified block diagram of a stand-alone PV system.

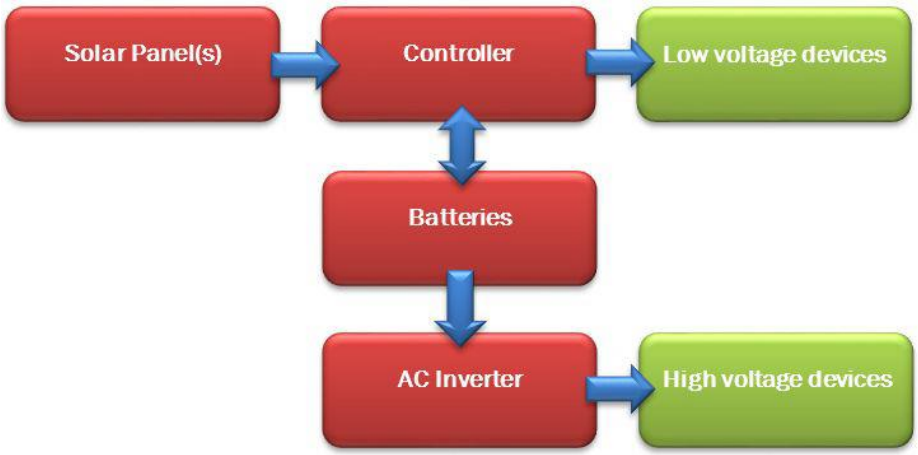

Figure 15. A simplified block diagram of a Stand-alone PV system [74]

The arrows in figures 15, 16, and 17 represents the flow of current. Stand-alone PV systems can power both low-voltage and high-voltage equipment.

ii. Grid-connected PV systems:

These PV systems may not need battery storage since they are connected to the power grid. In these systems, excess power can be sold to the grid, and the system can buy or use energy from the grid if the sun isn't available. These systems have more benefits than a stand-alone system, including lower infrastructure costs, no battery costs, improved energy efficiency, and fewer system components to balance. In this mode of operation, the inverter is a core component [64].

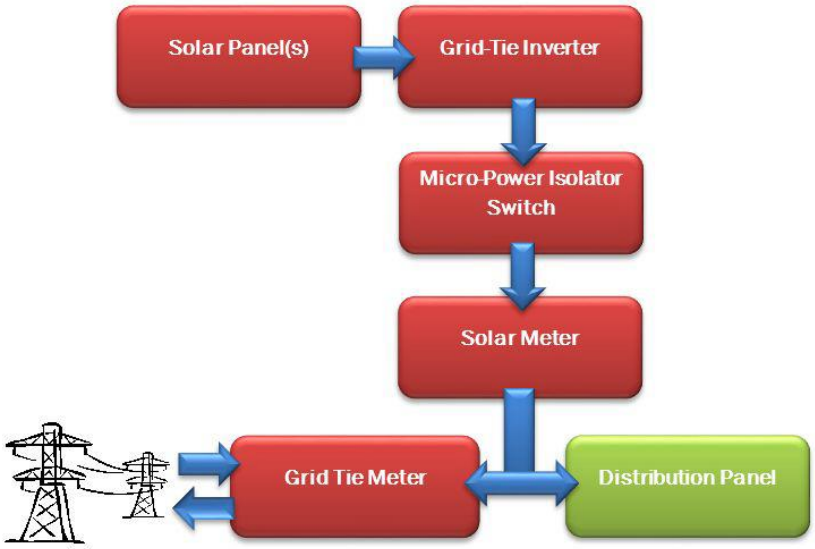

Figure 16. A block diagram of a grid-tied PV system using a single central inverter [74]

Figure 16 shows a grid-connected PV system with a single central inverter. Energy from the solar panels is fed into the main supply by the grid-tie inverter. In a grid-connected system, the single inverter's function regulates power flow into and out of the grid. The solar meter measures the amount of energy produced by the solar, whereas the grid-tied meter monitors the amount of electricity generated by the grid [74].

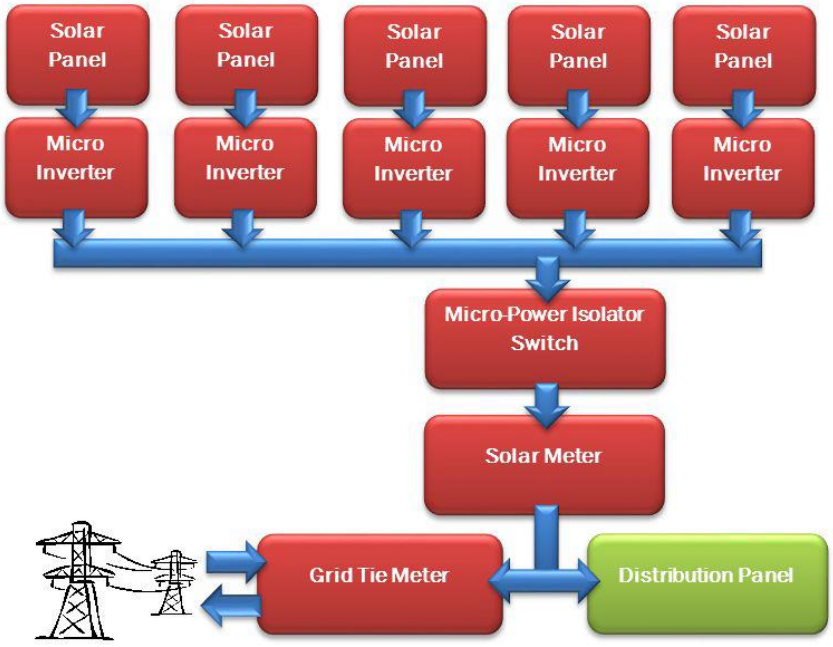

Figure 17. A block diagram of a grid-tied PV system using multiple micro-inverters [74]

In Figure 17, a grid-tied PV system with numerous interconnected micro-inverters, each PV module is connected to an inverter. The interconnected inverters convert low DC voltage to high AC voltage [74].

2.6.3.1.1.2 PV Modeling

PV panels can be modeled in a variety of ways depending on the system. When modeling PV systems, the three components of a PV panel's I-V curve, such as short-circuit current (I_{SC}), open-circuit voltage (V_{OC}), and maximum power point (mppt), are taken into account when modeling PV systems. PV current is determined by ambient temperature and solar insolation [75]. PV cell modeling incorporates calculating the I–V and P–V characteristic curves to simulate the real cell under various situations [76].

2.6.3.1.1.2.1 Equivalent electrical circuit

Figure 18 represents an equivalent circuit of a PV cell.

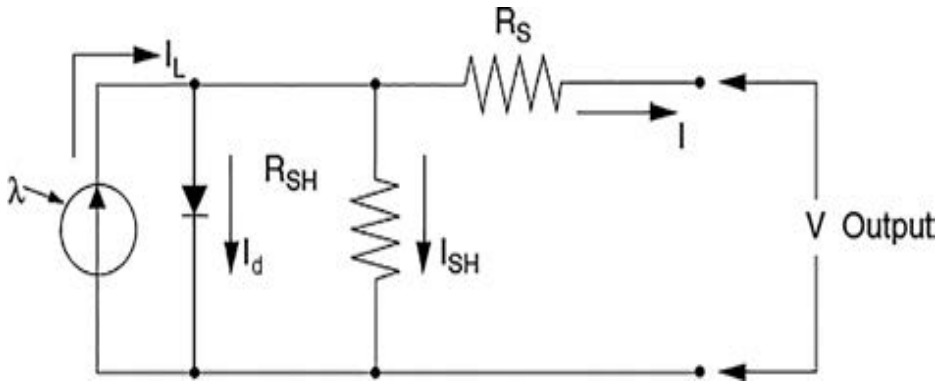

Figure 18. Solar PV cell equivalent circuit [77]

The expression, [74] gives the parameters in figure 18.

$$I = I_L - I_d - I_{sh} \quad (1)$$

where:

I = Output current of PV measured in amperes

I_L = solar current measured in amperes

I_d = Current through a diode measured in amperes

I_{sh} = Shunt-leakage current measured in amperes

When $I = 0$, the PV cell's open-circuit voltage V_{oc} is determined, and it is as follows:

$$V_{oc} = V + IR_{sh} \quad (2)$$

Where:

R_{sh} = shunt resistance

Since the diode current is given by

$$I_d = I_D\left\{exp\left(\frac{QV_{oc}}{AkT}\right) - 1\right\} \quad or \quad I_d = I_D\left\{exp\left(\frac{Q(V + IR_{sh})}{AkT}\right) - 1\right\} \quad (3)$$

Where:

I_D = diode saturation current measured in amperes

Q = electron charge whose value is $1.6 \times 10^{-9} Coulombs$

A = curve-fitting constant

k = Boltzmann constant whose value is $1.38 \times 10^{-23} J/°K$

T = absolute temperature measured in Kelvins

R_{sh} = shunt resistance measure in ohms

And the Shunt-leakage current can also be expressed

$$I_{sh} = \frac{V_{oc}}{R_{sh}} \quad or \quad I_{sh} = \frac{V + IR_{sh}}{R_{sh}} \tag{4}$$

When (3) and (4) are substituted into (1), the PV output current becomes:

$$I = I_L - I_D \left\{ exp\left(\frac{QV_{oc}}{AkT}\right) - 1 \right\} - \frac{V_{oc}}{R_{sh}}$$

$$or \tag{5}$$

$$I = I_L - I_D \left\{ exp\left(\frac{Q(V + IR_{sh})}{AkT}\right) - 1 \right\} - \left(\frac{V + IR_{sh}}{R_{sh}}\right)$$

Low shunt resistance develops during periods of low irradiance, resulting in lower current passing through the solar cell junction and lower solar cell voltage. Consequently, the last term, which denotes the shunt-leakage current, is negligible and ignored [75], [78].

Setting V_{oc} to zero, I_{sc} can be calculated, resulting in short circuit and solar produced currents of equal value. At constant temperature, the diode saturation current (I_D) is constant, and its mathematical expression is as follows [77].

$$I_D = \frac{I_{sc}}{exp(Q.V_{oc}) - 1} \tag{6}$$

If the short circuit current of the module is known from the data sheet of the cell at any solar irradiation, the cell current (I) is given as follows.

Given I_{sc}, I_L can be expressed as:

$$I_L = \left(\frac{G}{Go}\right) I_{sc,Go} \tag{7}$$

Where:

$G =$ Solar irradiance [W/m^2]

$I_{sc,Go} =$ Short circuit current at standard test condition measured in amperes

$Go =$ irradiation of the sun under standard test conditions [1000W/m^2]

Setting net current, $I = 0$, V_{oc} becomes:

$$V_{oc} = \frac{AKT}{Q} ln\left(\frac{I_L}{I_o} + 1\right) \tag{8}$$

Fill factor (FF) is a variable considered when modeling PV systems to quantify the performance of a PV module. mathematically, FF is written as [79].

$$FF = \frac{P_{max}}{V_{OC} * I_{SC}} \tag{9}$$

Where P_{max} = Maximum PV modules power.

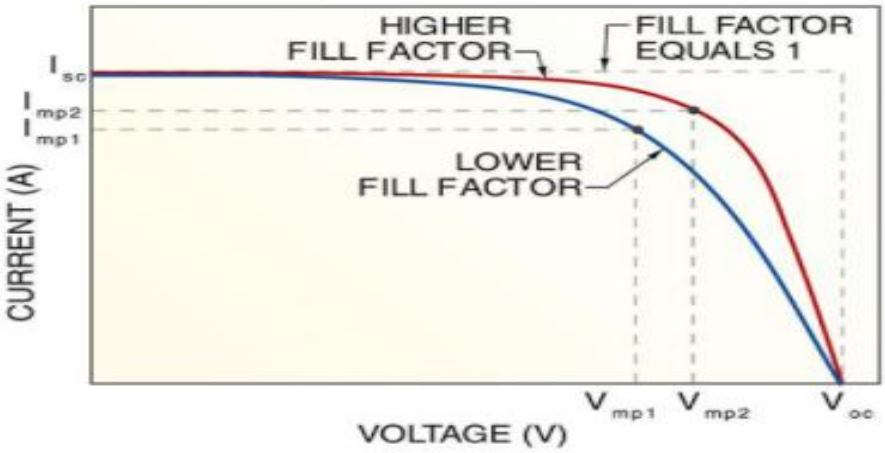

Figure 19. Remodeling of the I-V Curve with changing FF [79]

FF is essentially taken into consideration especially in locations with low solar irradiance. A maximum power can be achieved at maximum current and voltage [79], [80].

$$P_{max} = V_{MP} * I_{MP} \tag{10}$$

Where:

V_{MP} = Voltage achieved at point of maximum power [V]

I_{MP} = Current achieved at point of maximum power [V]

Mathematically, FF is also expressed as:

$$FF = \frac{V_{MP} I_{MP}}{V_{OC} I_{SC}} \tag{11}$$

Figure 20 depicts a PV module with I-V and P-V characteristic curves.

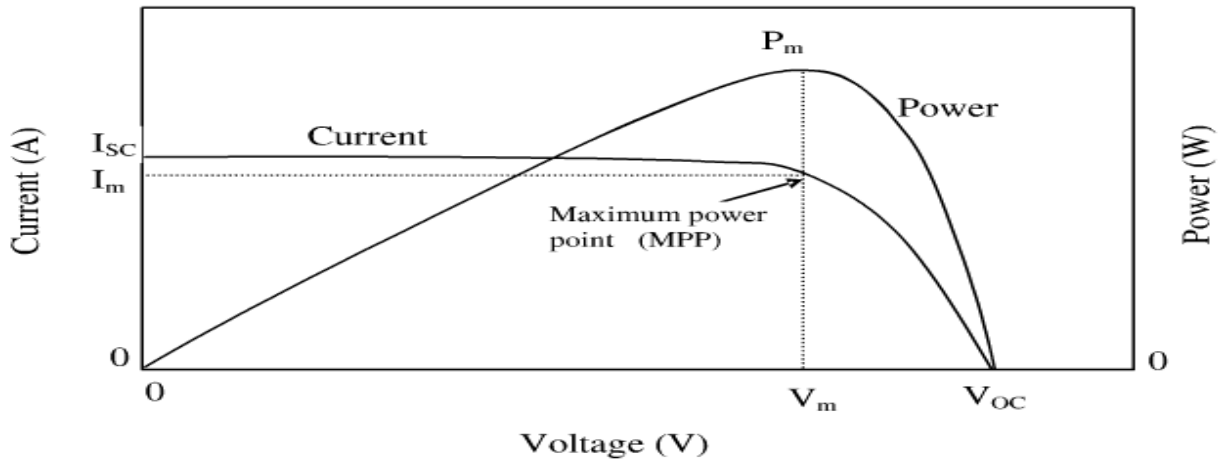

Figure 20. I-V and P-V characteristics curves of a PV cell [81]

2.6.3.1.1.2.2 Mathematical modeling of solar PV

Solar irradiance, temperature records, and PV module data are required to compute a PV system's power output. The energy generated by solar PV panels can be given by [82].

$$P_{PV-out} = P_{N-PV} \times \left(\frac{G}{G_{ref}}\right) \times \left\{1 + K_T\left(T_C - T_{ref}\right)\right\} \quad (12)$$

Where:

P_{PV-out} = PV power output

P_{N-PV} = rated power at reference state

G = solar radiation (W/m^2)

G_{ref} = solar radiation at reference state (G_{ref} = 1000 W/m^2)

T_{ref} = Cell temperature at reference state (T_{ref} = 25 °C)

K_T = temperature coefficient for monocrystalline and polycrystalline solar cell at maximum output $\left(K_T = -3.7 \times 10^{-3}\,(1/℃)\right)$.

T_C = PV cell temperature.

T_C is expressed as;

$$T_C = T_{amb} + 0.0256 \times G \quad (13)$$

Where:

T_{amb} = Ambient temperature

The efficiency of a PV system indicates how much of the available solar energy is converted into electrical energy by a solar cell. It is expressed as;

$$\eta_{PV} = \frac{P_{PV}}{A_{PV} * G_t} \quad (14)$$

Where:

η_{PV} = PV system efficiency

P_{PV} = Maximum power output [watts]

A_{PV} = Total panel area [m^2]

G_t = Incident radiation on PV system [kW/m^2].

2.6.3.1.2 Wind turbines

Wind turbines convert kinetic energy from the wind into mechanical energy and then into electricity. The output of a wind turbine is influenced by turbine size and wind speed. A small wind power plant could generate as much as 100 kW or less. Turbines rated less than 100 kW or between 100 kW and 1.5 MW are commonly used in small commercial and community wind projects, whereas turbines rated between 1.5 MW and 8 MW are used in utility-scale wind projects [83].

2.6.3.1.2.1 Types of wind turbines

The two wind turbines classified based on rotor are horizontal axis wind turbines (HAWT) and vertical axis wind turbines (VAWT). VAWT has advantages such as having a gearbox, easy transmission system and maintenance at ground level, and the ability to catch wind from any angle without redirecting the turbines based on wind direction. Nevertheless, it has disadvantages, such as lower efficiency, the need for a wide installation space, and poor self-starting abilities. VAWTs are only suited for small-scale projects, whereas HAWTs are the most often used wind turbine systems because they have a high efficiency, produce more energy than VAWTs, are self-starting, and have lower prices. The HAWTs' redirection capabilities are poor [71].

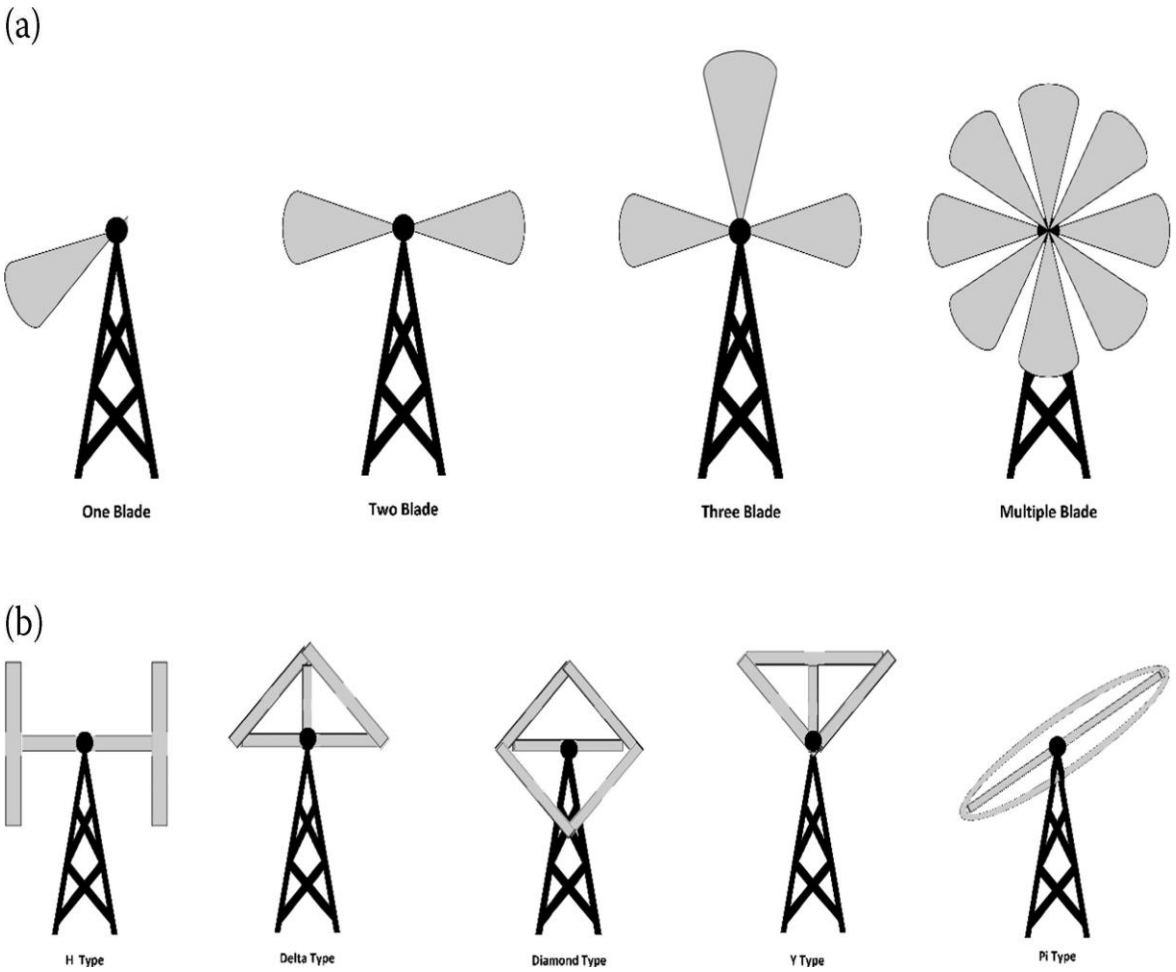

Figure 21. a) VAWTs b) HAWTs

The ideal rotor of a wind turbine can only collect 59 percent (Betz limit) of wind energy, according to the Betz law (1919), while Siemens reported in 2017 that modern wind turbines with three blades can collect up to 80 percent of wind energy [84].

2.6.3.1.2.2 Wind speed and energy relations

Motion, like a flowing wind, is linked to kinetic energy. The power in flowing air is given by;

$$\text{Power} = \frac{1}{2}(mass\ flow\ per\ second)V^2 \tag{15}$$

The theoretical wind power is calculated by [78]:

$$P = \frac{1}{2}\rho A V^3 \tag{16}$$

Where:

$P =$ power in wind (watts)

$\rho =$ density of air (kg/m^3)

$A =$ area swept by rotor blades (m^2)

$V =$ velocity of air (m/s).

Using equation (15), the mechanical power generated by the wind turbine can be expressed as.

$$P_o = \dot{m}(V^2 - V_0^2) \tag{17}$$

Where:

$P_o =$ wind turbine generated mechanical power [watts]

$V =$ upstream rotor wind speed [m/s]

$V_o =$ downstream rotor wind speed [m/s]

$\dot{m} =$ mass flow rate of air [kg/s].

Product of air density and average velocity can also give mass flow rate of rotor blades as in the expression:

$$\dot{m} = \rho A \frac{V + V_0}{2} \tag{18}$$

As a result, the mechanical power extracted by the rotor can be expressed as:

$$P_o = \frac{1}{2}\rho A V^3 \frac{\left[1 + \frac{V_o}{V}\right]\left[1 - \left(\frac{V_o}{V}\right)^2\right]}{2} \tag{19}$$

The efficacy of transferring wind energy into electrical energy is measured by a wind turbine's coefficient of power (CP). C_p is the ratio of a wind turbine's output power to the total energy available in the wind.

A wind turbine's power coefficient (C_P), also known as the Betz limit, is the ratio of wind turbine power production to total wind energy. CP is a measure of wind turbine efficiency.

$$C_P = \frac{\left[1 + \frac{V_o}{V}\right]\left[1 - \left(\frac{V_o}{V}\right)^2\right]}{2} \tag{20}$$

The ratio $\frac{V_o}{V}$ is one-third, so substituting one third in equation (20) gives the maximum efficiency of a rotor, i.e., 0.59. Betz limit maximum value lies between 0.4 and 0.5 for two-bladed rotors and between 0.2 and 0.4 for turbines with more blades and slow-motion turbines due to loss.

Thus equation (19) can be written as:

$$P_o = \frac{1}{2}\rho A V^3 C_P \quad (21)$$

A turbine rotor rotates through an area called the rotor-swept area. Area swept by the rotor blades of a horizontal turbine is given by:

$$A = \frac{\pi}{4}D^2 \; or \; A = \pi R^2 \quad (22)$$

Where:

$A =$ Area of the rotor [m^2]

$D =$ Diameter of the rotor [m]

$R =$ Radius of rotor [m].

While the area swept by the rotor blades of a vertical turbine is given by:

$$A = \frac{2}{3}WH \quad (23)$$

Where:

$W =$ Width of rotor [m]

$H =$ Height of rotor [m].

Wind is caused by air pressure, hence the greater the pressure difference, the more wind energy a turbine can generate, and vice versa. Temperature, pressure, and the amount of water vapor in the air determine air density.

Using the ideal gas law formular, the air density formula can be given by:

$$\rho = \frac{P}{RT} \quad (24)$$

$\rho =$ air density [kg/m^3]

$P =$ pressure of air [pascal]

$R =$ gas constant [287 J/kg˚k]

$T =$ absolute temperature of air [k].

Weibull probability distribution is a significant approach for expressing variance in wind speed. In the Weibull distribution function, the non-dimensional shape parameter (k) and the scale parameter (c) for wind speed can be expressed as [85].

$$f(v) = \frac{k}{c}\left(\frac{v}{c}\right)^{k-1} exp\left\{-\left(\frac{v}{c}\right)^{k}\right\} \quad (25)$$

Where:

$f(v) =$ Weibull density function in the wind speed

$k =$ Non-dimensional shape parameter

$c =$ Scale parameter [m/s]

$v =$ Speed of wind [m/s].

Broader wind speed distribution gives a smaller non-dimensional shape factor and narrower wind speed distribution gives a greater shape factor [77]. The wind speed distribution curve with K = 1 is called the exponential distribution used in reliability studies. K = 2 is called the Rayleigh distribution, present at most wind sites, and K >3 is called the Gaussian or the bell-shaped distribution. *At* K >3, the wind speed Weibull distribution curve approaches the nominal distribution [78].

The cumulative Weibull distribution function is as follows [85]:

$$F(v) = 1 - exp\left\{-\left(\frac{v}{c}\right)^{k}\right\} \quad (26)$$

The yearly mean speed of wind is calculated as [78]:

$$V_{mean} = \frac{1}{8760}\int_{0}^{\infty} fvdv \quad (27)$$

Where:

$V_{mean} =$ annual mean speed of wind

$8760 =$ hours in a year.

The relationship between the Weibull parameters and the average wind speed is defined as follows [85]:

$$v_{mean} = c\Gamma\left(1 + \frac{1}{k}\right) \tag{28}$$

Where:

Γ = Gamma function

The gamma function is defined as follows:

$$\Gamma(y) = \int_0^\infty e^{-x}\, x^{y-1}\, dx \tag{29}$$

The general form of the Rayleigh distribution using mean speed is summarized as [78].

$$f(v) = \frac{2v}{c^2} exp - \left(\frac{v}{c}\right)^2 = \frac{2v}{(v_{mean})^2} exp - \left(\frac{v}{v_{mean}}\right)^2 \tag{30}$$

Wind shear, also known as wind speed profile, is the variation in wind speed with height above ground level. The higher a wind turbine is above ground, the more wind energy it captures since wind speed is higher than lower. The power law is applied to the vertical wind speed profile as [78], [86]:

$$\frac{V_2}{V_1} = \left(\frac{h_2}{h_1}\right)^\alpha \tag{31}$$

Where:

V_2 = Wind speed estimated at hub height h_2 [m/s]

V_1 = Wind speed at reference height h_1 [m/s]

h_1 = Reference height above ground level in meters

h_2 = Hub height in meters

α = The power-law exponent varies depending on the location's height, time of day, season, terrain type, wind speed, and temperature.

The operation of turbines is described by three speeds [87]:

- Cut-in speed: This is the lowest wind speed at which a turbine begins to spin and generate practical power.

- ♠ Rated wind speed: This is the speed at which a turbine can achieve its maximum wind power output.
- ♠ Cut-out speed: Under the requirements of the design process and safety, this is the highest wind speed at which a turbine can deliver power. Furling speed is another name for cut-out speed.

To safeguard the wind turbine from harm, the manufacturer determines Furling speed. Figure 22 depicts a representation of an ideal wind power curve.

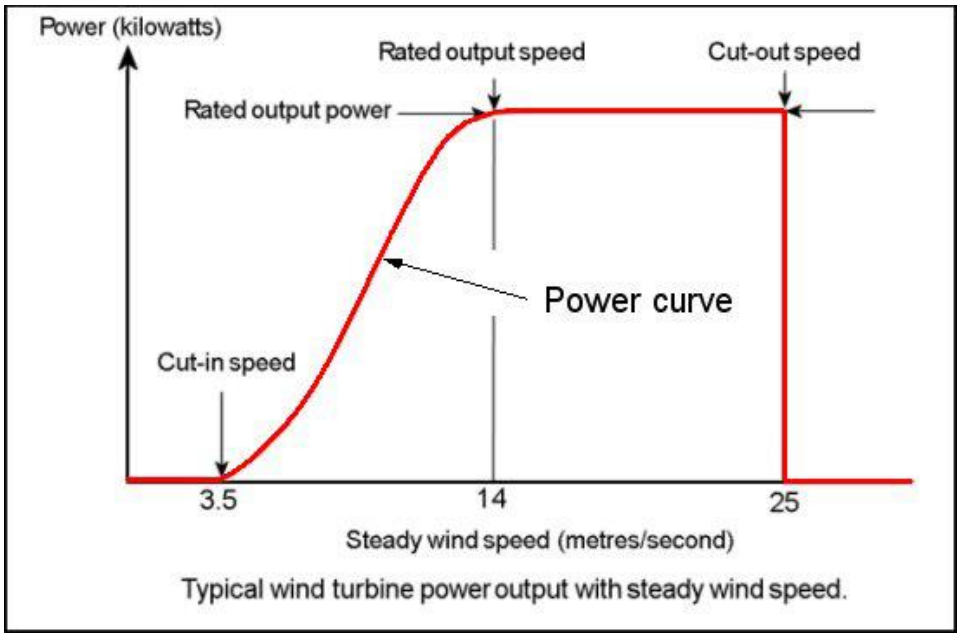

Figure 22. Typical wind turbine power characteristics curve [88]

2.6.3.1.2.2.1 Mathematical modeling of wind turbine

When estimating the power output of a wind turbine system, the wind speed distribution at a location, and the power output properties of a proposed turbine, are all factors to consider. Using the right model for wind turbine power output calculations is crucial [89]. A wind turbine's output power can be calculated by [90].

$$P_w(v) = \begin{cases} 0 \quad v \le v_{ci} \quad or \quad v \ge v_{co} \\ \dfrac{P_{rated-W}(v - v_{ci})}{(v_r - v_{ci})} \quad v_{ci} \le v \le v_r \\ P_{rated-W} \quad v_r \le v \le v_{co} \end{cases} \tag{32}$$

$$0 \le P_w \le P_{rated-W}^{max} \tag{33}$$

Where:

v_{ci} = Cut-in speed

v_{co} = Cut-off speed

v_r = Rated wind speed

$P_{rated-W}$ = Output power of wind turbine.

2.6.3.2 Loads

Based on reliability and outages or damage of power systems, microgrid loads can be classified into:

- Critical loads
- General loads
- sensitive loads
- Non-sensitive loads
- Controllable loads
- Non-controllable loads

The load of the customers must be understood before a microgrid can be designed to determine the best generating capacity and storage system to meet the demand for power (Asian Development Bank, 2020).

2.6.3.3 Storage system

Energy storage is a device that transforms electrical energy into storable energy and then transforms it back to electricity when required. Energy storage systems (ESS) are critical in microgrids because they improve system stability, reliability, and power quality [91].

An energy storage technology is selected based on the microgrid's size and necessary reaction time [63].

Figure 23 summarizes the various storage technologies and their storage system power ratings and discharge time at rated power.

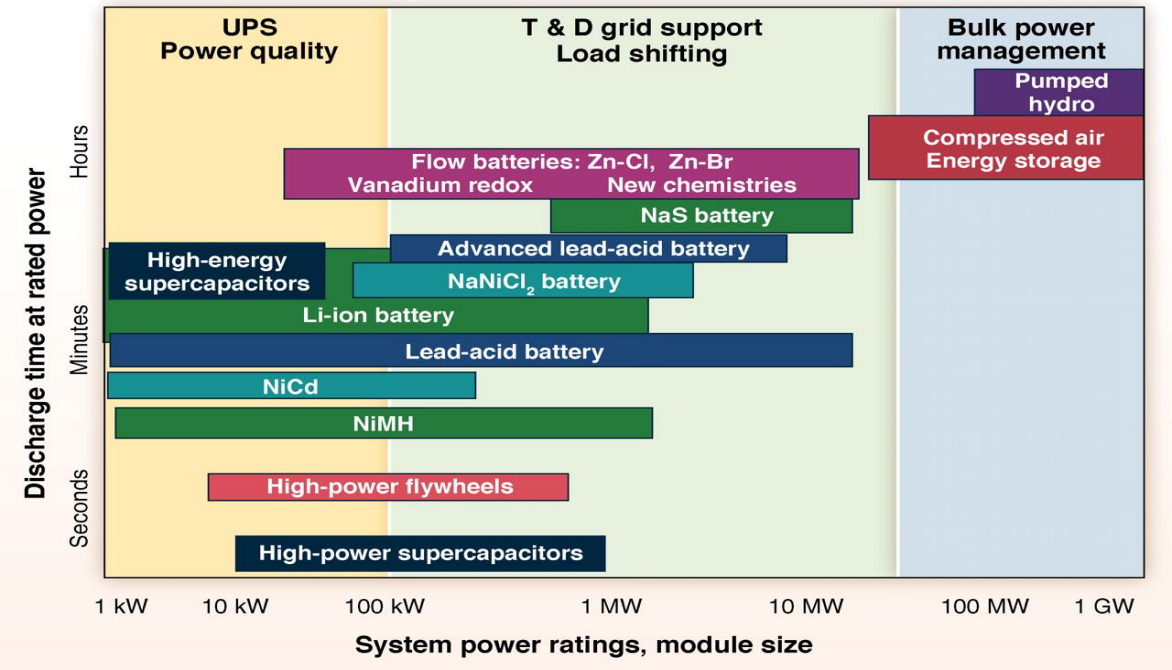

Figure 23. Comparison of Electrical Energy Storage (EES) systems used in Microgrids [92]

Due to the intermittent nature of most integrated sources in microgrids, such as solar and wind, ESS is a critical component of a renewable energy-based microgrid, as they improve power supply reliability. When energy storage is used or a grid is connected to a system, power issues are minimized. Figure 24 displays the benefits of ESS, which include reduced congestion, low power use, volatility, and security issues in the power system and maintaining stability and improving power quality.

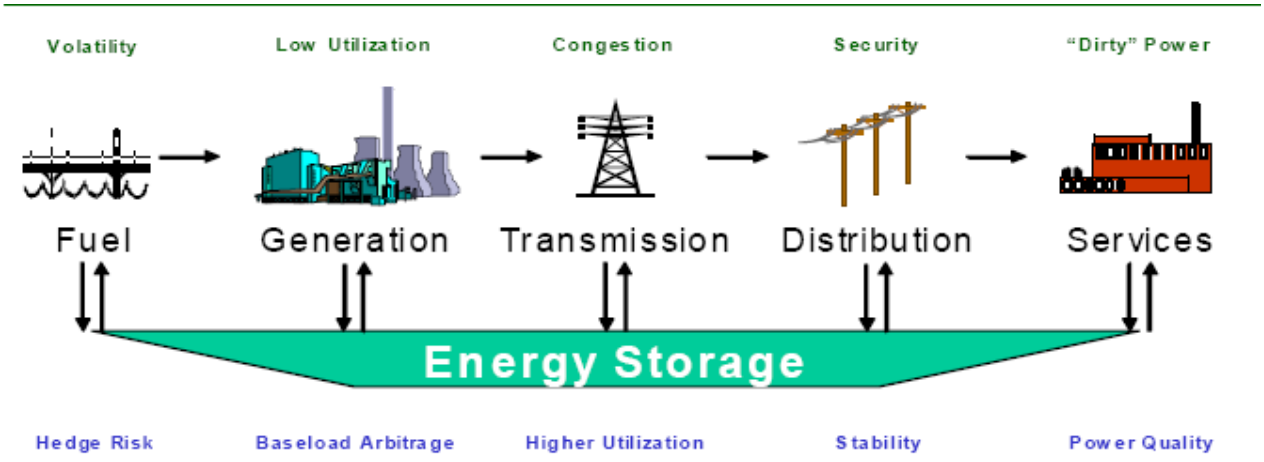

Figure 24. Energy storage benefits [93]

In this study, battery storage system will be considered in the modeling and design. The battery's capacity affects operating aspects such discharge rate, DOD, cut-off voltage, temperature, and the battery's age and cycle history. A battery's capacity is measured in Ampere-hours (Ah).

The following are the basic performance characteristics that govern battery design [78]:

- Charge and discharge voltages:

charging and discharging of batteries is a benchmark for how much energy is added or taken from the battery ESS in terms of power. The manufacturer determines a battery's charging and discharging rate. These characteristics are often shown on the battery label. A completely charged battery reaches maximum voltage and so has zero discharging Ah, however, a discharging battery has diminishing Ah until it is fully discharged and its charging Ah becomes zero. Prolonged charging of a fully charged battery induces gassing and causes the charging to be transformed into heat..

- Charge and discharge ratio:

The charge and discharge ratio are calculated by dividing the Ah input by the Ah output while keeping the charge constant.

- Round-trip energy efficiency:

The energy efficiency of batteries is the ratio of energy output to energy input at the battery's electrical terminals throughout a full charge and discharge cycle. Batteries are not ideal as such they lose energy inform of heat during charging and discharging processes.

- Charge efficiency:

The Ah injected internally between the plates to the Ah delivered to the exterior terminals during the charging process is known as charge efficiency. The charge efficiency of an empty cell estimated to be approximately 100 percent, and when the charging rate approaches one, the charge efficiency drops to zero.

- Internal resistance:

This is the obstructing of current flow from the battery. Externally, current runs from positive terminal to negative terminal in a battery, however internally, current flows from negative terminal to positive terminal, therefore parameters like electrolyte conductivity, ion mobility, and electrode surface area create resistance to current during this flow. Small cells, for example, have small

electrodes and hence have a higher resistance than large cells, which have large electrodes and a lower resistance.

- Memory effect:

A battery memory effect tends for a battery to remember the level at which it last provided the majority of its capacity. After numerous shallow discharge cycles, this effect causes the full capacity to be lost. To get rid of this effect, "reconditioning" is done once every few months, in which a battery is discharged to 1 Volt per cell and then completely charged to around 1.55 Volts per cell. Memory effect is experienced by some batteries, such as NiCd and Li-ion, but other types of storage technologies do not experience it.

- Effects of temperature:

Higher temperatures cause battery gassing, self-discharge, lower battery life, and lower capacity and charge efficiency. On the other hand, low temperatures reduce conductivity in the battery electrodes, lowering efficiency, and increasing internal resistance. Battery capacity drops at temperatures over 25°C or below 10°C, and at temperatures below zero, capacity drops sharply.

- Failure:

Battery failure is the result of a set of interconnected events that are influenced by the chemistry, design, environment, and actual working circumstances of the battery. Conditions such as below-zero temperatures, vibration, overcharging, deep discharging, heat, and fast charging can all cause a battery to fail.

2.6.3.3.1 Mathematical modeling of battery storage system

The majority of batteries used in hybrid systems are lead acid batteries because of the advantages they provide, such as the ability to charge and discharge without affecting storage capacity, and the fact that they are safer than wet acid batteries because the acid in lead acid batteries is stored in a gel and cannot be easily leaked, unlike in wet acid batteries [94]. The state of charge (SOC) at time t can be estimated during the charging phase as follows [94]:

$$SOC(t) = SOC(t-\Delta t) + (P_{PV}(t) * \eta_{DC-DC}) + P_{WG}(t) * \eta_{AC-DC} - \left(\frac{P_{load}(t)}{\eta_{wr} * \eta_{inv}}\right) * \frac{\eta_{cha}}{U_{bus}} * \Delta t \quad (34)$$

SOC at time t can be estimated during the discharging phase as follows:

$$SOC(t) = SOC(t - \Delta t) + (P_{PV}(t) * \eta_{DC-DC}) + P_{WG}(t) * \eta_{AC-DC} - \left(\frac{P_{load}(t)}{\eta_{wr} * \eta_{inv}}\right) * \frac{1}{U_{bus} * \eta_{dech}} * \Delta t \quad (35)$$

Where:

P_{load} = Power consumed by the load at t time. load power consumed at time t

t = Simulation time step (t = 1 hour)

η_{DC-DC} = efficiency of a DC-DC

η_{AC-DC} = efficiency of an AC-DC

η_{inv} = efficiency of a DC-AC converter

$\eta_{DC-DC} = \eta_{AC-DC} = \eta_{inv}$ = 0.95 (an assumed value)

η_{cha} = Battery efficiency during charging = 0.85

η_{dech} = Battery efficiency during discharging = 1

η_{wr} = Efficiency introduced to consider wire losses = 0.98

U_{bus} = Nominal DC bus voltage = 48 V.

2.6.3.4 Microgrid monitoring and control systems

Microgrid monitoring and control systems (MMCS) connect the microgrid's elements and balance the configuration. In a simple microgrid setup, the governor may be the only MMCS for a generator. In a comprehensive microgrid arrangement, on the other hand, the MMCS may incorporate sensing, meters, complex tools, and communication channels, energy storage, loads, and utility interfaces [63]. The microgrid's control system maintains frequency and voltage stability during load changes and network interconnections and regulates the converter's active and passive force [95].

2.6.3.5 Grid interconnectors

Grid interconnectors connect a microgrid to a utility grid to draw/inject additional power from/to the grid. Excess power production from the microgrid can also be pumped into the grid to save money, and the interconnections between the two also ensure that power reliability is improved. Direct through switchgear, power electronic interfaces, and static switches are the interconnection methods [96].

The point of common coupling (PCC) is the electrical junction where a microgrid connects and disconnects from the power grid. According to IEEE 2011 standard 1547 of interconnection policy, microgrids and their components, such as control systems and grid interconnectors, must meet

technical requirements such as anti-islanding, low-or high-voltage and frequency ride-through, and power quality, as well as operational requirements such as real and reactive power import and export. Microgrids, including their components such as control systems and grid interconnectors, must meet technical specifications such as anti-islanding, low-or high-voltage and frequency ride-through, power efficiency, and operational requirements such as actual and reactive power import and export, for the PCC [26].

2.6.4 Power electronics (PE) in microgrids

The PE interface connects DERs to electrical power systems using switches, control systems, inductive components, and capacitive elements. A microgrid PE interface is shown in Figure 25.

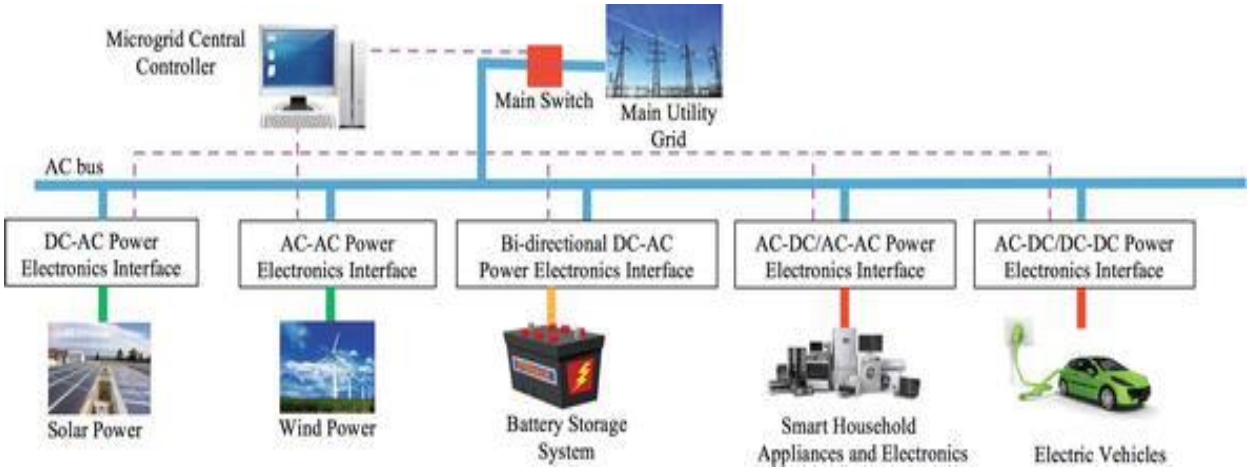

Figure 25. Microgrid PE interfaces [97]

2.6.4.1 Power electronic converters

Converters are significant power electronics and components in renewable energy systems because they ensure effective energy management and system stability.

Power electronic converters are primarily used for controlling, converting, and conditioning electricity flow from one form to another [98].

In hybrid renewable energy systems, power converters must meet some requirements, including high efficiency, low electromagnetic interference, cheap, appropriate voltage ratio, low current ripple, and maximum reliability [99]. Whether in grid-connected or islanded operation mode, modern grid-supporting power converters in a Microgrid should contribute to damping power oscillations and grid voltage and frequency regulation [100].

2.6.4.1.1 Classification of converters

The classification of converters include:

i. Inverter (AC to DC converters)

Inverters are often used to convert D.C. power from fuel cells, solar panels, and batteries into AC power. Hybrid inverters in hybrid renewable energy systems reduce over-reliance on these grid-connected systems. Hybrid inverters are also convenient for operating several renewable energy technologies, minimizing high electricity costs, and being efficient [101]. An A.C. voltage is the resultant power output supplied to loads when an inverter is connected between a D.C. link and a load in hybrid systems. Multilevel inverters, which use some power semiconductor design technologies and D.C. voltage sources, have gained greater interest in recent years. The cascaded, diode-clamped, and capacitor-clamped multilevel inverter topologies are the most popular [102]. Inverters are used in both domestic and industrial systems to supplement power disruptions in utility grids. However, they are prone to failure when battery capacity is limited, and large appliances are used that are considerably heavier than what the inverter is designed to handle. To employ hybrid inverters, the battery system voltage must match the inverter's D.C. voltage input requirements. The hybrid system's power capacity from renewable energy sources must charge batteries and supply sufficient capacity to the load [103]. However, choosing an inverter size that matches the size of the renewable energy systems based on intermittent sources demands a significant investment [104].

ii. Rectifiers

Rectifiers change the low voltage of a steady AC output to a variable voltage of dc output [105].

iii. Choppers (DC to DC converters)

A chopper is a stationary device that converts a constant DC input voltage to a changing DC output voltage. Chopper converters provide seamless control, high performance, and fast response, and are extensively used for deceleration and movement regulation in electric vehicles and mini transportation [106].

iv. AC voltage controllers

A fixed ac voltage is converted to a variable ac output voltage using these converters, also known as AC voltage controllers or AC regulators. The attainable AC has the same frequency as the input AC [107]. AC voltage controls are used to ensure a steady temperature during electric heating

processes. A tap changing transformer may convert fixed ac to variable ac without changing the frequency.

v. Cycloconverters

Cycloconverters use one-stage conversion to transform input power at one frequency into output power at a different frequency. They're employed in high-capacity drives [107].

2.6.5 Mechanisms for Microgrid optimization

Optimization is a strategy for improving efficiency, economics, resiliency, and robustness in microgrid energy management systems (EMS). An EMS is required in a microgrid employing more than two DERs to impose power allocation among the DERs, the cost of energy production, and emissions [108]. An example of EMS in a microgrid is shown in Figure 26.

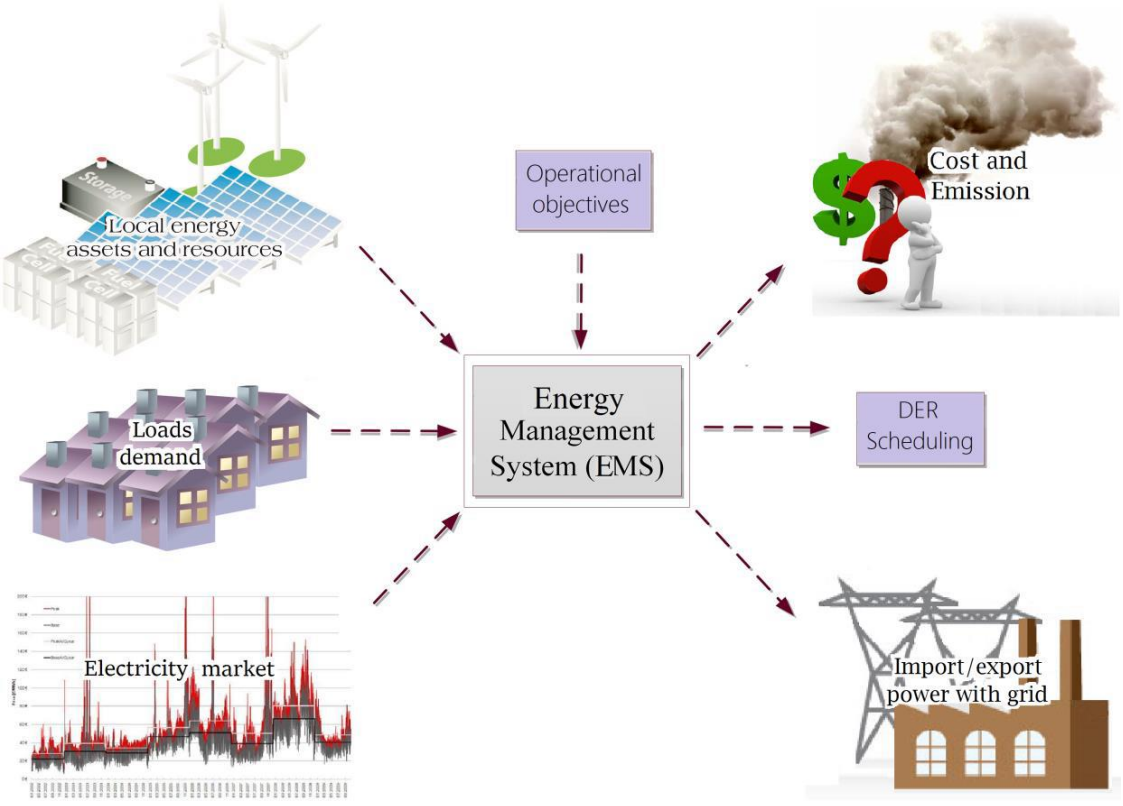

Figure 26. Energy management system in a microgrid [108]

For the optimization technique, this study considers a simulation-based approach using the HOMER tool. Creating an optimal conversion model yields consistent energy from renewable energy sources [66].

2.6.6 What is a smart grid?

A smart grid is a recent invention in the electric power system that seeks to improve electricity reliability considerably more than before while also ensuring cost minimization, increasing the use of sustainable energy sources, and reducing carbon emissions [109]. Figure 27 illustrates the share of benefits that smart grid can provide to different factions.

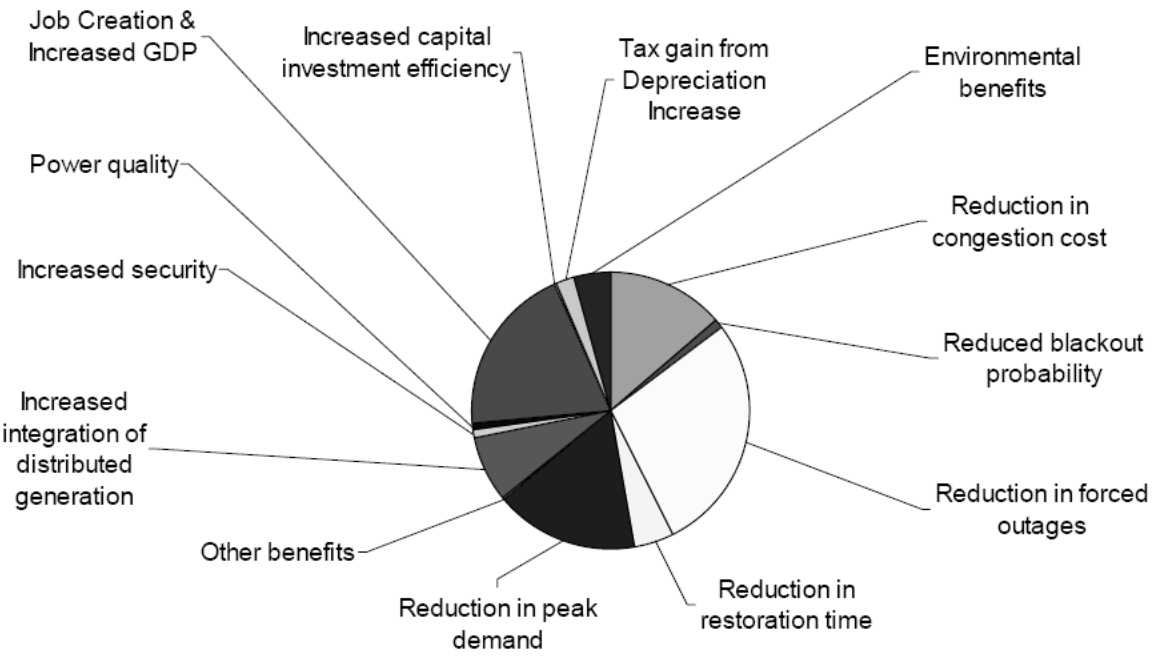

Figure 27. Benefits of smart grid schemes, broken down per value segment [110]

There is no unified definition of a smart grid; different research institutes, organizations, and authors define it differently.

According to DOE, A smart grid is an electrical distribution system linked to communications and information technologies from generation to consumption for better grid management, client service, and emission reduction. In contrast, the E.U defines a smart grid as an electric system that can smartly combine the behaviors of all users, including producers and consumers to provide sustainable, cost-effective, and secure electricity supply. The Electric Power Research Institute (EPRI) gave its definition of a smart grid as a system that incorporates information and communications technology into every part of energy generation, distribution, and consumption to cut costs and improve efficiency while minimizing environmental effects, improving markets, and improving dependability and service [111]

A microgrid is part of a smart grid. Figure 28 depicts various components or technologies of a smart grid.

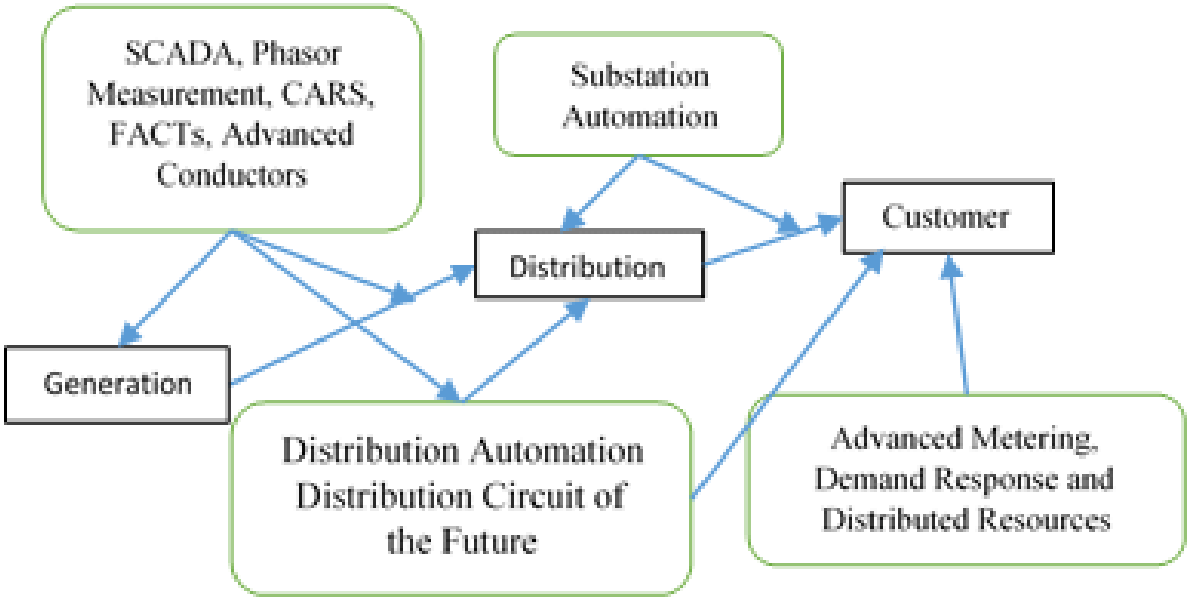

Figure 28. Smart grid components [112]

The implementation of the smart grid concept envisions the interaction and integration of several stakeholders, including Consumers, System operators, manufacturers, ICT service providers, Centralized and decentralized energy producers, energy and service providers, research and innovation centers, education and training institutions, regulation authorities, standardization organizations [110].

2.6.7 Classification of microgrids

Microgrids are classified according to their function demand, capacity, and AC/DC form [49].

2.6.7.1 Function demand.

This category has three microgrids: simple microgrid, multi-DG microgrid, and utility microgrid [49].

2.6.7.1.1 Simple microgrid

This microgrid has a simple architecture to power independent institutions, with only one DG required for its configuration. It aims to keep vital loads powered up at all times. A simple microgrid has a capacity of 2MW or less [49].

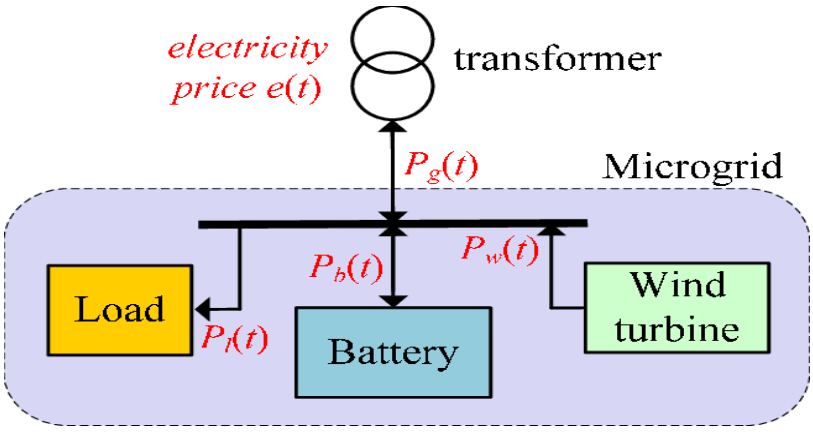

$Pw(t)$ = power output of the wind turbine at time t, and $Pl(t)$ = power consumption of the load, $Pg(t)$ = grid output power of and $Pb(t)$ = power output of battery storage.

Figure 29. A simplified simple microgrid structure[113]

2.6.7.1.2 Multi-DG microgrid

As the name implies, a multi-DG microgrid comprises two or more DGs or a series of simple microgrids. The design mechanisms of a Multi-DG microgrid, unlike simple microgrids, are more complex to implement [49]. A typical multi-DG microgrid consists of DGs, ESS, and load [114].

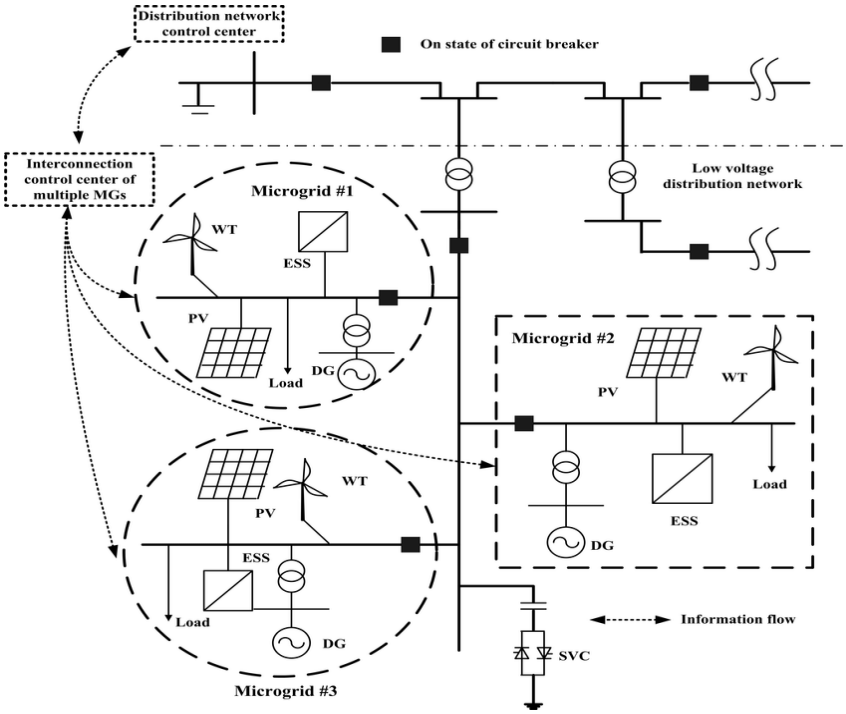

Figure 30. A typical configuration of multi-DG microgrids [114]

2.6.7.1.3 Utility microgrid

During peak hours, a utility microgrid is used to sustain critical loads of consumers. A utility microgrid is grid connected thus it can take and pump power into and out of a grid, and they typically use renewable energy sources as DGs, increasing reliability. A utility microgrid is designed to run in an island mode if the main grid fails automatically. The key components of a utility microgrid are DGs, ESS, a Central Management Controller (CMC), and transmission lines, as shown in figure 31. When energy supply from DG sources is insufficient, CMC can take electricity from the utility grid [115].

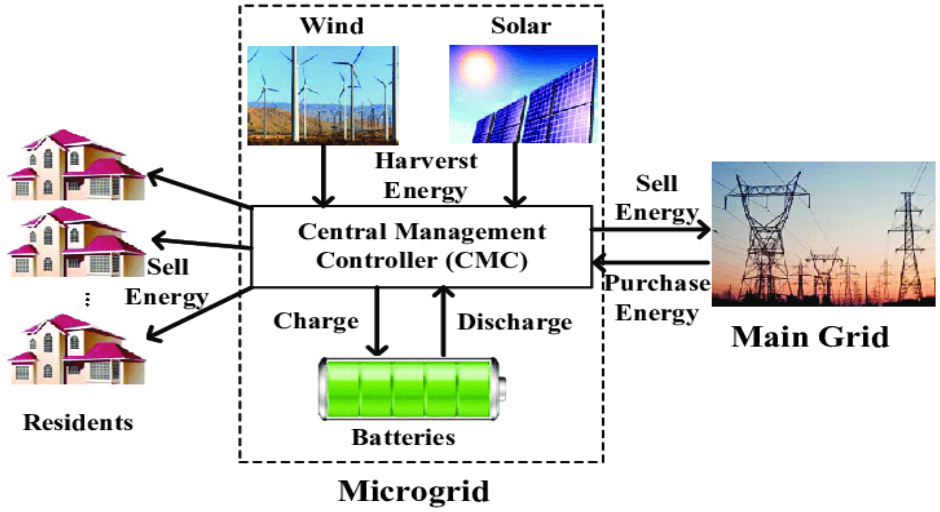

Figure 31. A typical utility microgrid's structure [115]

2.6.7.2 Capacity

The simple microgrid, corporate microgrid, feeder area microgrid, substation area microgrid, and independent microgrid are the several types of microgrids that fall under this category; a simple microgrid has already been highlighted. The other four types of microgrids in this group, apart from the independent microgrid, are grid-connected microgrids.

2.6.7.2.1 Corporate microgrid.

The capacity of a cooperate microgrid ranges from 2 to 5 MW. The capability of a cooperative microgrid differs significantly from that of a simple microgrid.

2.6.7.2.2 Feeder area microgrid.

This microgrid, also known as a feeder-based microgrid, is a cutting-edge microgrid designed to replace outdated infrastructure and modernize feeders that are no longer suitable for microgrids. It

can operate in two modes: autonomous and grid-tied, with the latter being the most common for economic reasons and islanding. A feeder-based microgrid improves distribution system reliability and stability, improves control system flexibility, and reduces the probability of faults. It also provides enhanced security against cyber-attacks and improves DG power flow [116]. The feeder-based microgrid has a capacity of 5–25 MW [49].

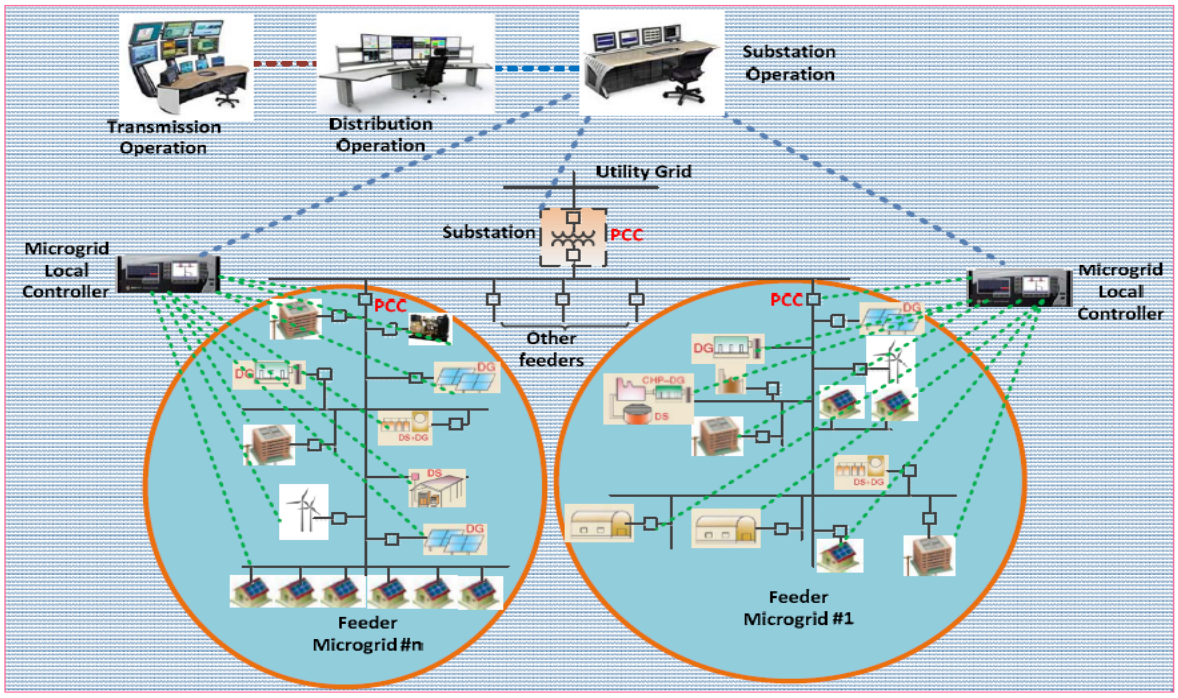

Figure 32. A feeder based microgrid example [116]

2.6.7.2.3 Substation area microgrid

This form of microgrid can handle more than 20MW of power. It employs CHP trigenerations and local loads, such as those found in homes, businesses, and industries.

2.6.7.2.4 Independent microgrid

Independent microgrids are typically designed for autonomous operation and power small loads with low electricity demands. Wind-based independent microgrids, PV-based independent microgrids, and biomass-based independent microgrids are examples of independent microgrids [49], [117].

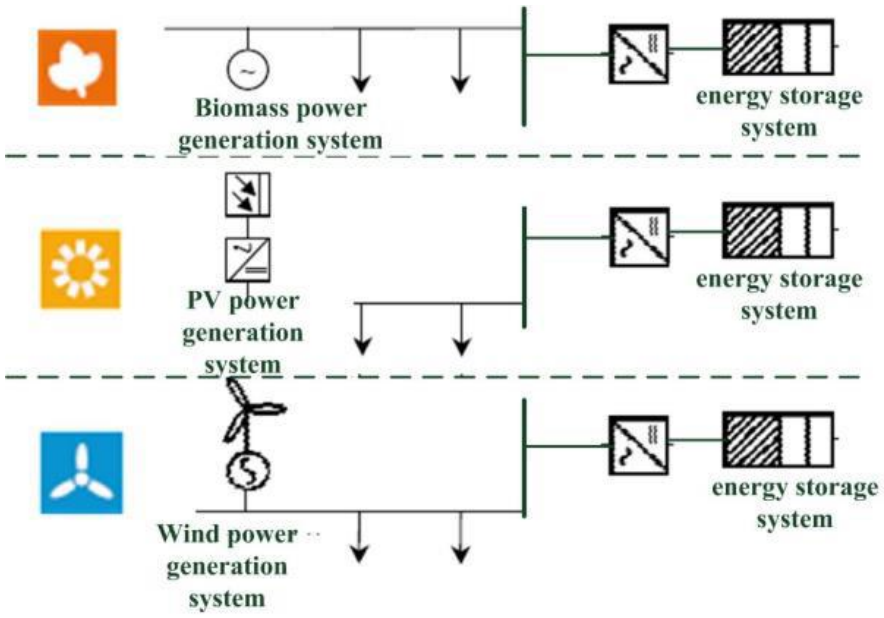

Figure 33. Independent microgrid consisting of biomass-based independent microgrid, PV-based independent microgrid and wind-based independent microgrid [117]

2.6.7.3 AC/DC classification

AC microgrids, DC microgrids, and AC/DC HBMGs are the three types of microgrids in this category.

2.6.7.3.1 AC microgrid

The AC bus, part of an AC microgrid, connects the DGs and EESs via the PEs. Using a static switch to link the microgrid to the power grid can operate in both islanded and grid-tied modes [117]. An AC to DC rectifier in an AC microgrid converts AC power to DC to feed DC loads, while AC loads are connected to the AC microgrid [118].

Some of the benefits of an AC microgrid include enabling voltage step-up for long-distance distribution and isolating it from the grid in the event of a grid fault [118]. In addition, the design and installation of an AC microgrid are much easier [119].

Unwanted current output from bi-directional power flow, low efficiency during energy conversion from AC to DC while supplying DC loads, complex control mechanisms, and frequency deviations due to only small synchronous generators are some of the challenges associated with AC microgrids [118], [120].

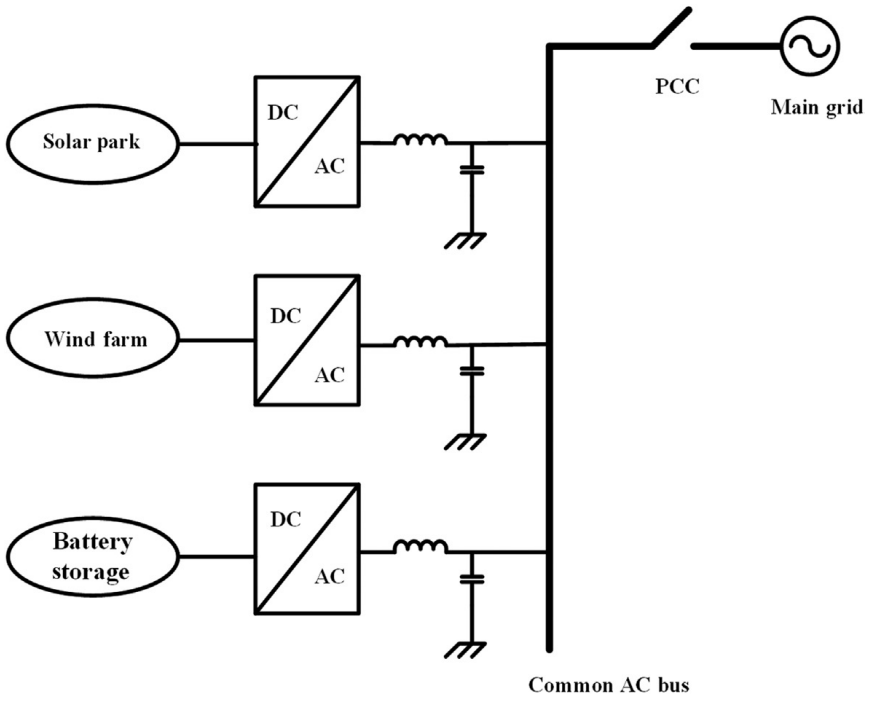

Figure 34. AC microgrid architecture [121].

2.6.7.3.2 DC microgrid

DC microgrids are intended to connect DC-output sources such as solar PV, fuel cells, and batteries to directly supply DC loads using a DC bus, preventing the conversion loss in AC microgrids and thus increasing DC microgrid performance. Furthermore, since existing energy is stored in the DC capacitor and voltage control of the AC/DC converter, synchronization in a DC microgrid is not required. The DC bus voltage is unaffected in the event of grid interruptions [100].

A DC microgrid's downside is that inverters must convert DC electricity to AC power to feed AC loads connected to the DC microgrid [49].

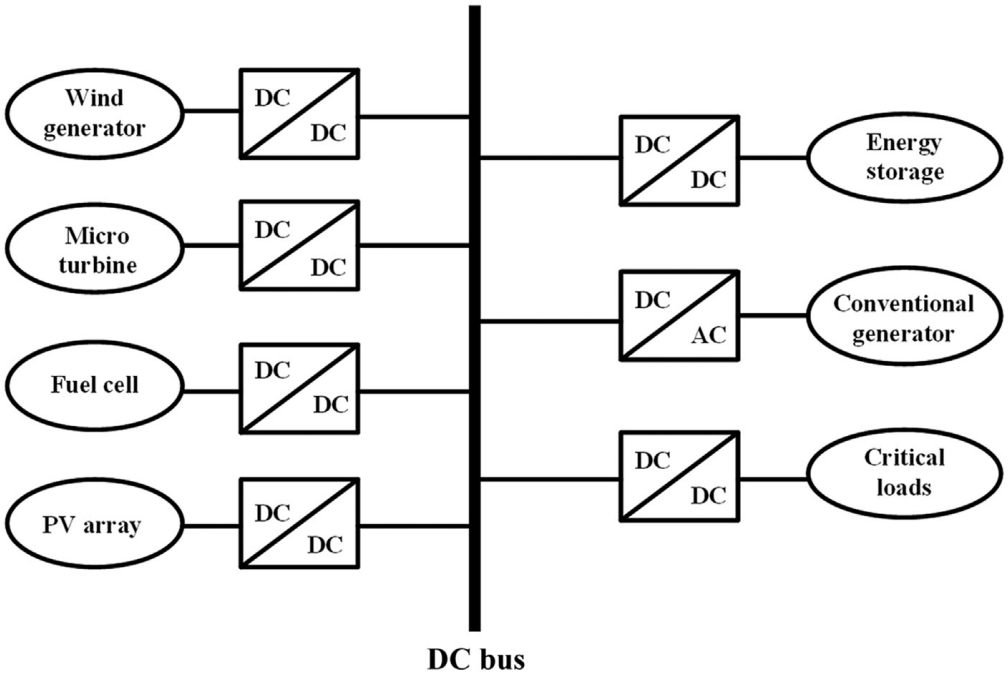

Figure 35. DC microgrid architecture [121]

2.6.7.3.3 AC–DC HBMG

The AC-DC HBMG, also known as a HBMG, is a microgrid that incorporates both an AC bus microgrid and a DC bus microgrid linked to each other by a bidirectional AC/DC converter, which allows power to flow in both directions between the buses while minimizing energy loss during conversion. Thus, efficiency is improved [121]. The renewable HBMG improves power stability, reliability, dispatchability, and solutions for critical loads and is a more cost-effective alternative [122].

A renewable energy HBMG can integrate renewable energy sources, including solar and wind combinations, solar and hydropower combinations, solar and biomass combinations, wind and hydropower combinations, and so on.

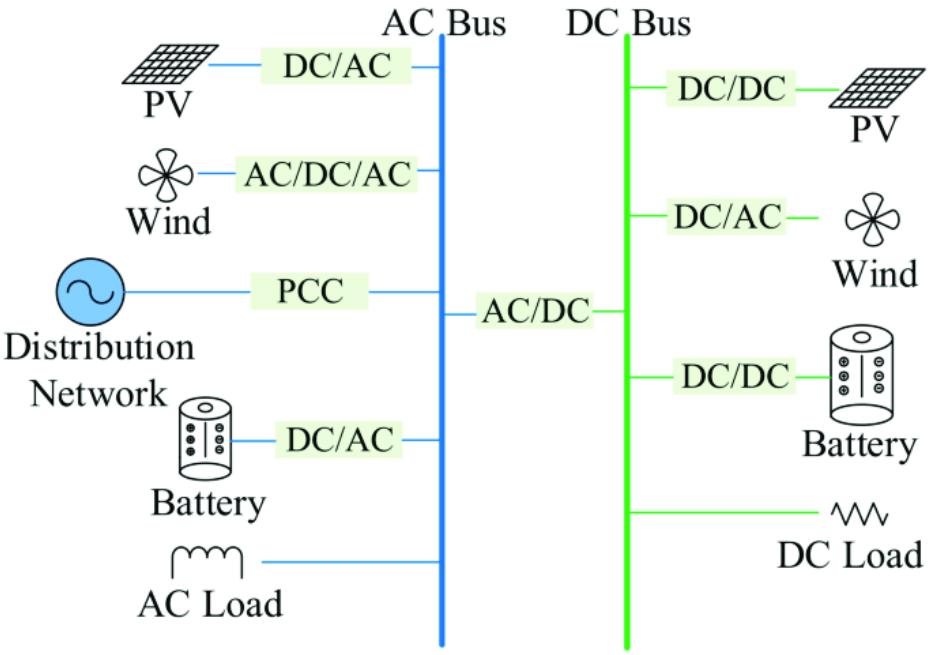

Figure 36. AC/DC microgrid architecture [123]

CHAPTER THREE

3 Methodology of the proposed system

This chapter explains the research techniques, including data modeling, component descriptions, site resources, economic parameters, and a brief introduction to the software.

3.1 HOMER as a Tool for HBMG

Some of the most commonly used microgrid optimization software tools include HOMER, HYBRID2, HOGA, TRNSYS, HYDROGEMS, HYBRIDS, INSEL, ARES, RAPSIM, SOMES, and SOLSIM. HOMER is a microgrid system optimization, simulation, and sensitivity analysis software developed by the National Renewable Energy Laboratory (NREL) in the United States of America [124].

- HOMER can simulate hundreds of thousands of solutions depending on the situation at hand. It can simulate the intended system based on the estimation of installation cost, replacement cost, Operation and Maintenance (O&M) cost, fuel, and interest rate.
- Following the simulation step, the optimization step displays a sorted list of configuration results based on Total Net Present Cost (TNPC). HOMER examines the many types of system configurations from the lowest to the highest TNPC. The system configuration based on TNPC, on the other hand, varies depending on the sensitivity variable chosen by the user.
- The sensitivity phase is an optional step in which sensitivity variables such as wind speed, solar radiation, fuel costs, and so on are presented to see how the optimal system changes when these variables [125], [126].

HOMER considers several elements, including technological feasibility, climate, load consumption, and economics parameters analysis.

The HOMER tool necessitates the collaboration of stakeholders such as renewable energy advocates, power engineers, utility operators, and financiers as shown in figure 37.

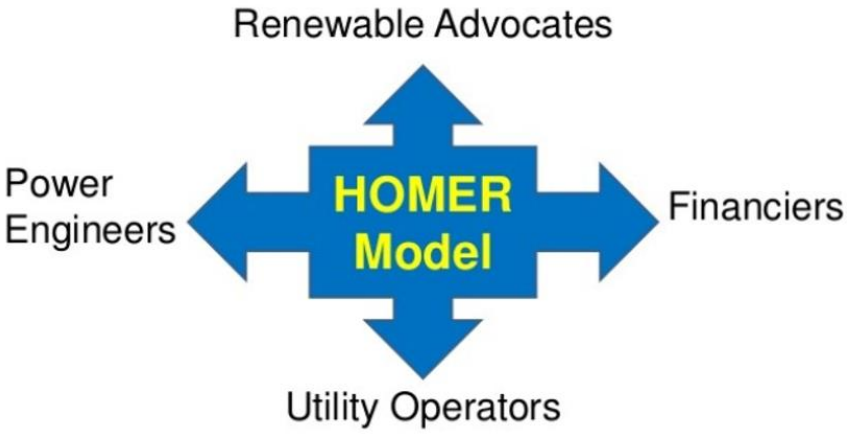

Figure 37. HOMER as a communication tool that brings together various stakeholders [127]

3.2 Case study – Faculty of Technology of University of Tlemcen

The Faculty of Technology of the University of Tlemcen is located in Chetouane, in the province of Tlemcen, Algeria. A natural gas-driven utility grid presently supplies the faculty. The city of Tlemcen, located in the northwest of Algeria, experiences four seasons in a year. The four seasons include [128]:

- The spring season begins in March and ends in May, and it follows the winter season. It's usually marked by scattered clouds in the sky, warm air temperatures, and a drop in precipitation levels. For the three months of the Spring season, the average minimum temperature is around 12°C, and the average maximum temperature is around 20°C.
- Summer season: This season begins in June and finishes in August, shortly following spring. It is characterized by aridity and a lack of rain and dry high air temperature and pressure. Throughout these months, temperatures can reach 30°C to 35°C or even higher on some days, with a low average temperature of around 20°C.
- Autumn season: This season begins in September and extends in November, and it follows the summer season. Low cloud formations and sporadic rainfall are typical characteristics. The overall average minimum temperature for the three months of winter is around 16°C, while the entire average maximum average temperature is around 23°C.
- Winter season: This season follows the autumn season, beginning in December and ending in February It is characterized by plentiful rainfall, and mountainous regions experience snow and chilly air at times.

3.3 Estimation of Electric Load

The primary load data in this research was collected from the faculty of technology, the University of Tlemcen, which comprises several categories, including lecture rooms load, library load, outdoor lighting load, the Pan African University Institute of Water and Energy Sciences (PAUWES) building data load, and the faculty kitchen data load. The estimated loads/appliances include Cast Iron Radiators (CIR), lamps or lighting, projectors, air conditioners (A/C), desktop computers, and kitchen appliances. The lamps include Compact Fluorescent Lamps (CFL), 2 lamp Fluorescence Lamps (2 lamp FL), T6 lamp Fluorescent Lamp (T6 lamp FL), 3 headed outdoor street lamps, Polycarbonate outdoor post lantern with frosted acrylic glass, LED round gate lights, LED road lamps, and LED outdoor street lights. The load profile consumption is broken down into four seasons.

Seasonal fluctuations, combined with faculty schedules, cause some load consumption to vary throughout the year. For example, since the winter season is marked by cold temperatures, the cast iron radiators (CIR) are turned on while the air conditioners (A/C) are turned off. In the summer season, characterized by high temperatures, the faculty usually takes a long or end-of-academic-year vacation that usually lasts the entire summer season. Though the faculty remains closed for the summer, some offices are likely to remain open since the administration may compile student results, prepare for the next academic year, or fulfill certain formal obligations. As a result, summer loads such as air conditioning and office loads will use power. In the autumn and spring seasons, the load consumption is estimated to be the same and seasonal loads such as CIR and A/C are non-operational because of the moderate temperatures in these two seasons. The load consumption of outdoor lighting remains consistent throughout the year. The detailed load profile data for winter, spring, summer, and autumn seasons are presented in Appendix A (A.1, A.2 and A.3).

Table 6. depicts hourly load profile data calculated from Appendix A (A.1, A.2 and A.3) for the Faculty of Technology of the University of Tlemcen, used in this study.

Table 6. Time series load profile of the case study

Hour	ELECTRICAL LOAD (kW)			
	Winter Months	Spring Months	Autumn Months	Summer Months
0	8.21	8.21	8.21	8.21
1	8.21	8.21	8.21	8.21
2	8.21	8.21	8.21	8.21
3	8.21	8.21	8.21	8.21
4	8.21	8.21	8.21	8.21
5	8.21	8.21	8.21	8.21
6	28.47	28.47	28.47	8.21
7	31.26	31.26	31.26	0.07
8	45.001	45.001	45.001	1.979
9	173.109	73.581	73.581	1.979
10	162.609	63.081	63.081	1.979
11	160.309	60.781	60.781	1.979
12	132.999	33.471	33.471	25.979
13	128.799	29.271	29.271	25.229
14	140.389	40.861	40.861	28.469
15	140.389	40.861	40.861	28.469
16	27.541	27.541	27.541	1.979
17	10.8	10.8	10.8	0.14
18	10.8	10.8	10.8	0.14
19	8.21	8.21	8.21	8.21
20	8.21	8.21	8.21	8.21
21	8.21	8.21	8.21	8.21
22	8.21	8.21	8.21	8.21
23	8.21	8.21	8.21	8.21

3.3.1 Electrical load Simulation in HOMER

The load data entered into the HOMER is based on various appliances and their durations over 24 hours at the faculty. As illustrated in figure 38, HOMER utilizes the load data to simulate daily, seasonal, and yearly profiles to calculate average and peak loads.

Figure 38. Load profile of the faculty under consideration

The average daily energy consumption is 601.11kWh/day and a peak load of 296.32 kW was produced after taking into account a random variation in the load with a 10% day-to-day base and a 20%-time step.

3.4 System Configurations of the Proposed HBMG System for the Faculty

Figure 39 depicts the suggested configured system setups for the faculty. Solar and wind are the renewable energy sources considered in the design, with three scenarios considered for the analysis, one of the scenarios considered is a standalone system, the other scenario is a grid-connected system without batteries and the third scenario is a grid-connected with batteries as an additional backup. The configured systems are connected to the grid to improve system power stability and reliability and to provide backup power in the event of low or no electricity from the deployed renewable sources.

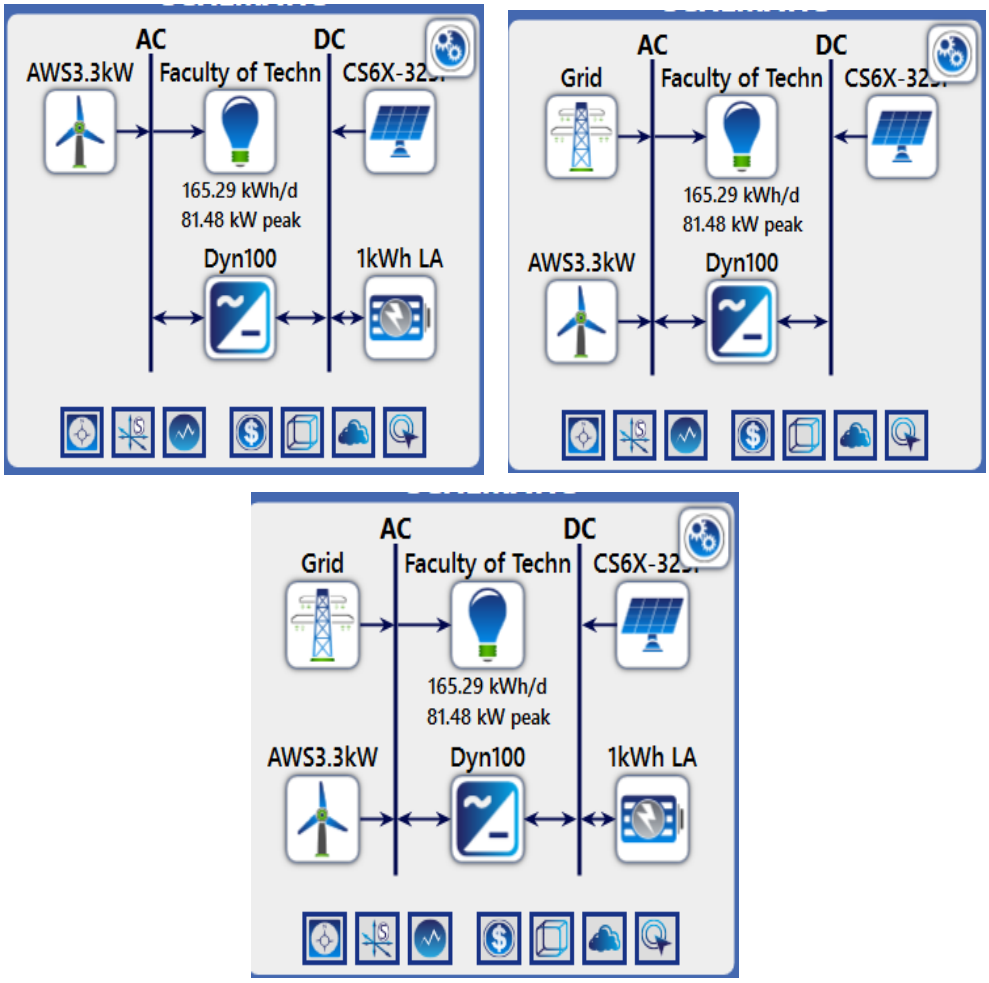

Figure 39. Schematic diagrams of the proposed HBMG systems with the figure on the top left showing a stand-alone system. The figure on the top right shows a configured grid connected system without batteries. The figure on the bottom is a grid connected-configured with batteries.

3.5 Resources of the Location

Chetouane is located at the coordinates 34°55.'4N and 1°18.0'W, and the time zone is GMT/UTC (UTC+01:00) is used to access the location resources. The solar, wind, and temperature resource data is obtained through HOMER from the National Aeronautics and Space Administration **(**NASA) prediction of worldwide energy resources. The HOMER tool requires the site's average monthly temperatures to calculate feasibility [129].

3.5.1 Solar resource

Global Horizontal Irradiance (GHI) represents the total quantity of solar radiation incidents on a horizontal surface. The average monthly GHI is based on data collected over 22 years. The

clearness index is a dimensionless value between 0 and 1 that defines the clearness of the atmosphere. The clearness index has a high value when the weather is clear and sunny, and a low value when the weather is cloudy. The annual average radiation is 4.92 kWh/m^2/day. In general, Chetouane solar radiation is adequate from March to October, i.e., adequate energy can be harnessed during this time. However, from November to January, the solar radiation is small. The average solar radiation trend and clearness index over a year is given in table 7 and Figure 40.

Table 7. Monthly average global horizontal irradiance data of Chetouane

Month	Jan	Feb	Mar	Apr	May	Jun	Jul	Aug	Sept	Oct	Nov	Dec
Daily Solar Radiation kWh/m^2/day	2.82	3.73	4.67	5.87	6.64	7.23	7.30	6.32	5.13	3.92	2.90	2.50
Clearness index	0.553	0.581	0.567	0.589	0.598	0.627	0.647	0.611	0.583	0.565	0.539	0.533

With a daily solar radiation of 7.3 kWh/m^2/day and a clearness index of 0.647, July has the highest solar radiation and clearness index, while December has the lowest radiation and clearness index, with a radiation of 2.5 kWh/m^2/day and a clearness index of 0.533. The GHI data is the average monthly radiation collected over 22 years from July 1983 to June 2005.

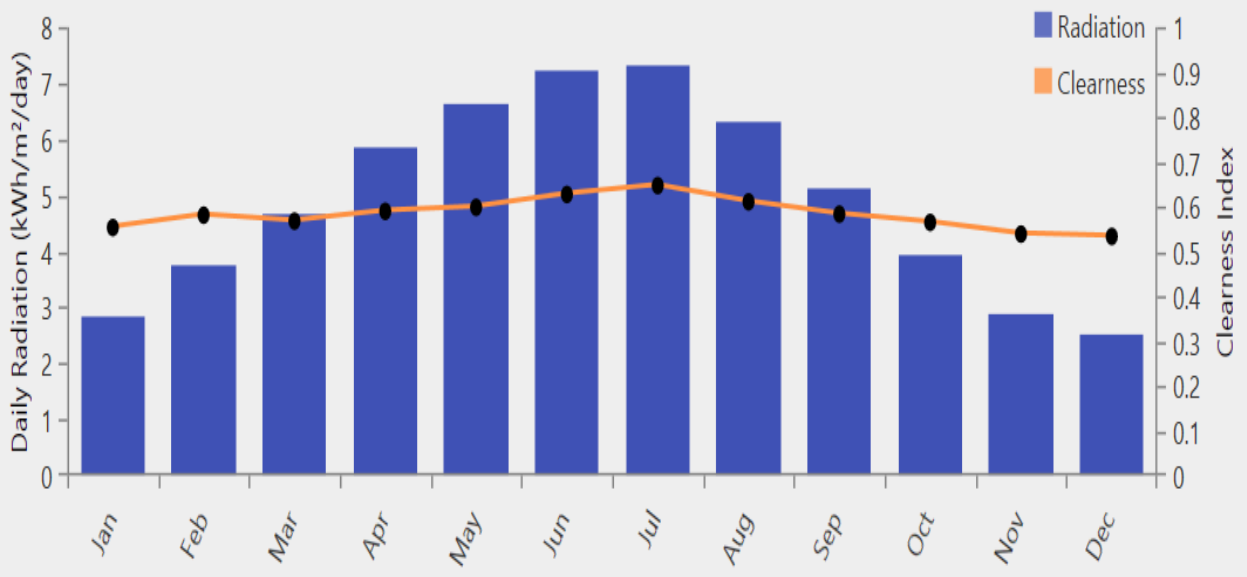

Figure 40. Chetouane monthly daily solar radiation and Clearness index

Over a year, the daily variations of the global horizontal solar radiation source tracked on an individual basis are shown in figure 41.

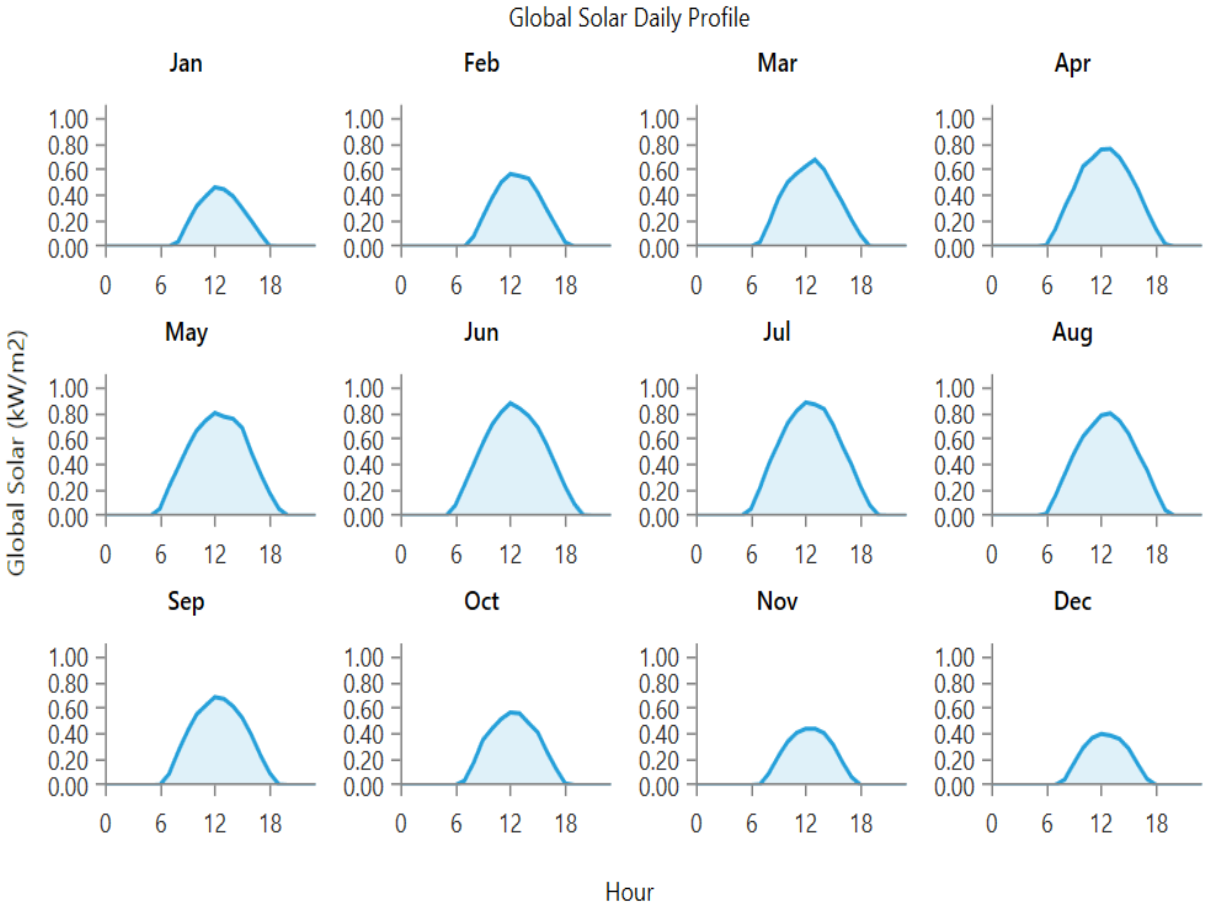

Figure 41. Individual daily changes of global horizontal solar radiation source throughout 12 months

3.5.2 Wind resource

Measured from a height of 50m above the surface, the average wind speed over 30 years from January 1984 to December 2013 is presented in table 8 and figure 42. The average yearly wind speed is 5.18 m/s, with the lowest average wind speed of 4.19 m/s occurring in August and the highest average wind speed of 6.09 m/s prevailing in December.

Table 8. Monthly Average Wind Speed

Month	Jan	Feb	Mar	Apr	May	Jun	Jul	Aug	Sept	Oct	Nov	Dec
Monthly average wind speed m/s	6.03	5.93	5.63	5.58	4.86	4.42	4.20	4.19	4.41	4.90	5.92	6.09

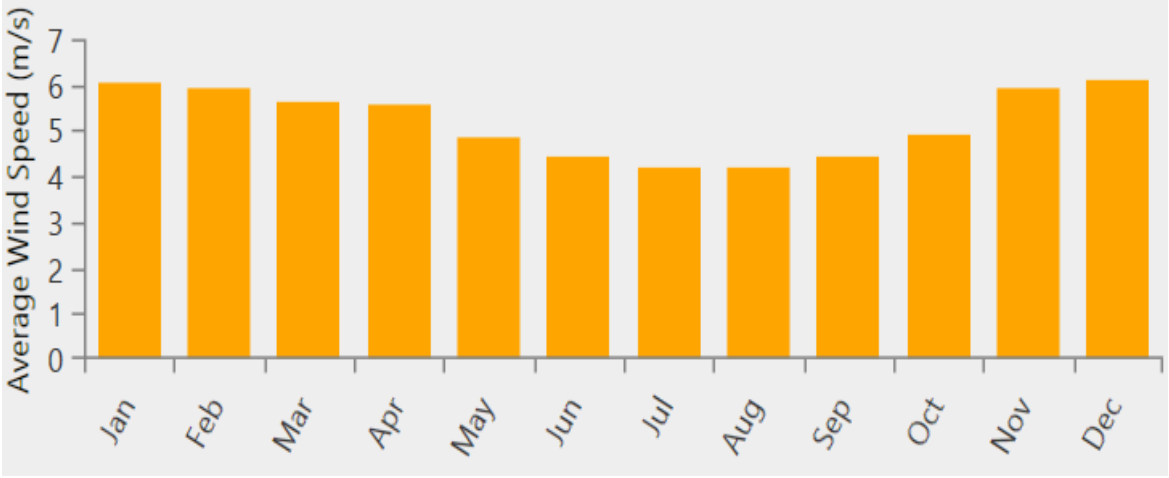

Figure 42. Average wind speed data for Chetouane

Figure 43 shows the 24-hour wind speed variance across the year.

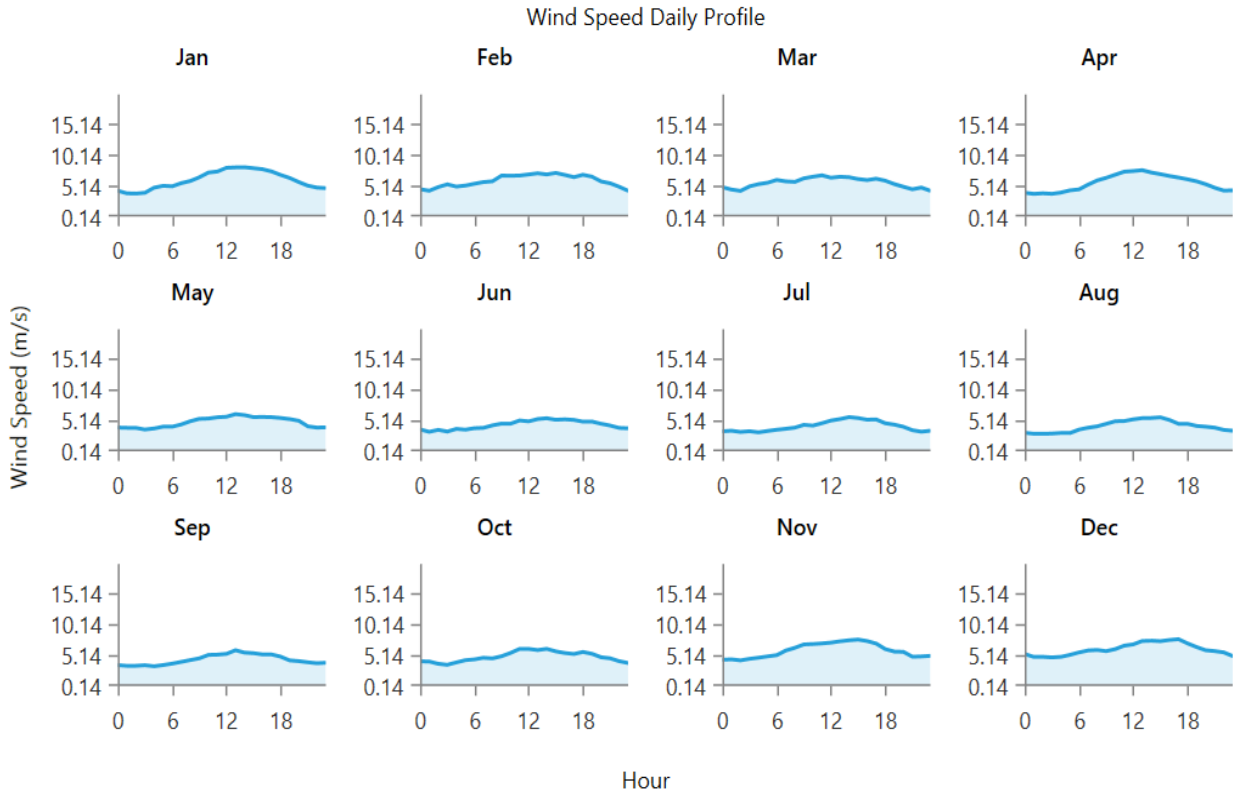

Figure 43. Individual daily changes of wind speed source throughout 12 months

Given that most micro wind turbines have a minimum set-in motion wind speed of roughly 2 m/s, the wind speeds of Chetouane are viable for wind power generation.

3.5.3 Temperature

The consequence of rising temperatures increases in PV cell temperature, which can result in a PV module's performance degrading. Thus, cooling can help preserve the efficiency of a PV module by regulating the temperature of the PV cell at severe temperatures. As in table 9 and figure 44, the temperature data for Chetouane indicates that losses during solar energy generation are minimal, based on the commonly used temperature coefficient to measure the loss of efficiency in PV modules set for over 25°C by solar panel manufacturers. The monthly temperatures were gathered during 30 years, from January 1984 to December 2013.

Table 9. Monthly average temperature data

Month	Jan	Feb	Mar	Apr	May	Jun	Jul	Aug	Sept	Oct	Nov	Dec
Daily temperature °C	7.49	8.71	11.33	13.62	17.45	22.32	26.27	26.39	21.85	17.22	11.77	8.63

The annual average temperature is 16.09°C on a scaled basis. The minimum average daily temperature is 7.49°C in January, while the maximum average daily temperature is 26.39°C in August.

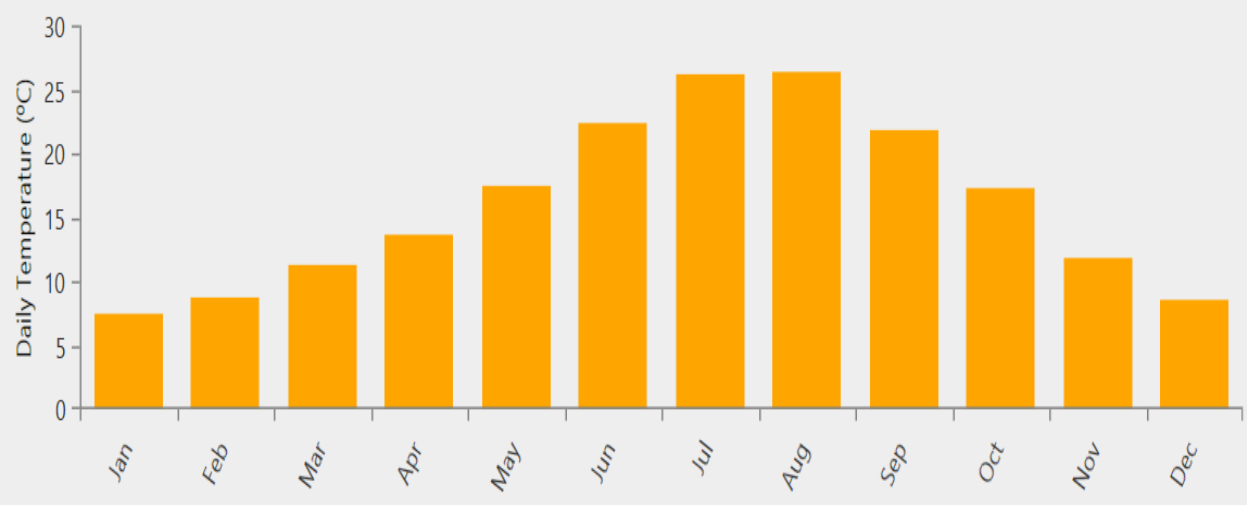

Figure 44. Average monthly mean temperatures data for Chetouane

The temperature data is higher from May to October and lower from November to March.

3.6 Properties of Components

The components used in this study were chosen straight from the HOMER library, and each has its own set of costs, capacity, lifespan, and other properties.

3.6.1 Solar PV properties

The CanadianSolar MaxPower CS6X-325P PV was selected after considering multiple simulation results from several PV modules to arrive at the most optimal solution. There are no replacement costs for the PV system over the project's 25-year life cycle since the PV system's life span is the same as the project's life cycle. Due to conditions such as ambient temperature influence, dust, shading, wiring losses, and PV degradation, the PV panels are bound to suffer losses. This PV's derating factor is 88%, and its temperature coefficient is -0.41% per degree Celsius. The efficiency of this PV system in standard conditions is 16.94%. There are 72 polycrystalline cells in this PV module with a capacity of 325 watts. Polycrystalline PV panels are less expensive than single crystalline silicon cells and perform better in slightly shadowed circumstances. No tracking system is employed for the PV system in this HBMG design. The PV system is set at $700 per kW, with an O&M fee of $10 per year. Appendix B (B.1) contains additional PV specifications.

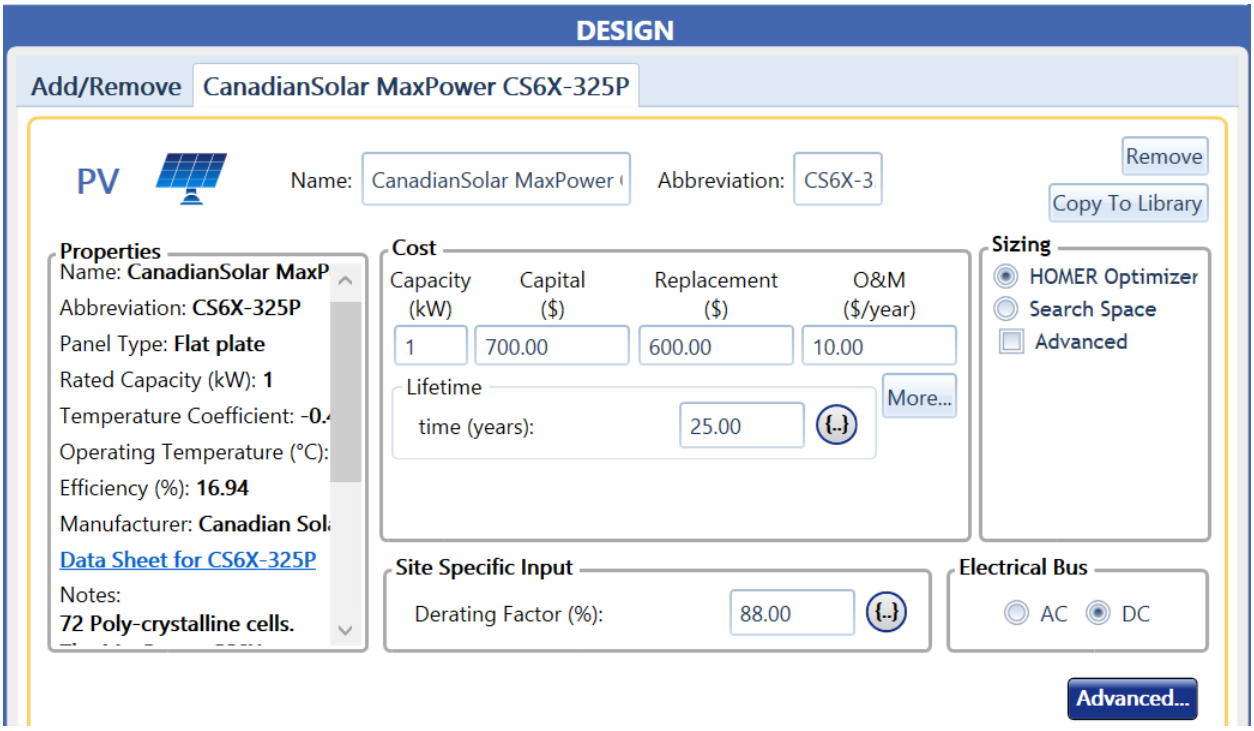

Figure 45. Simulated PV system considered for optimization

3.6.2 Wind Turbine properties

For the simulations in this study, an AWS HC 3.3kW rated capacity Wind turbine is used, and the capital cost is set at $ 7000 per kW, replacement cost at $ 6000 and O&M at $ 10 per year for economic analysis, with an O&M cost of $ 100 per year. Hub height of this turbine is 12 m and life span is 20 years. Appendix B (B.2) has additional wind turbine specifications.

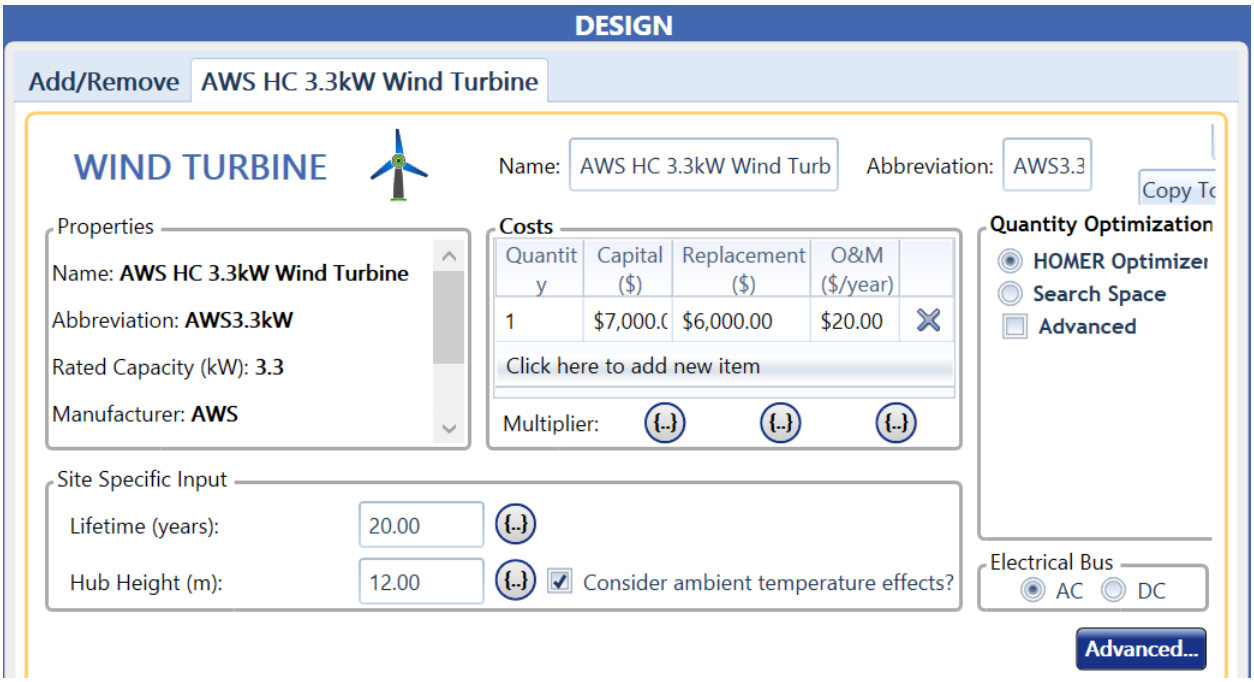

Figure 46. Simulated wind system considered for optimization

3.6.3 Battery Storage properties

For this simulation, a generic 1kWh lead acid battery with a nominal voltage of 12V, a maximum capacity of 83.4 Ah, an efficiency of 80%, a maximum charge current of 16.7A, and a lifetime of 10 years was used. As both the PV and the battery are connected to the DC bus in one configuration, their output voltages should be the same, thus the battery's 12V is connected in three strings to provide a 36V voltage, just like the PV system voltage. The cost of this battery is defined at $ 600, and its initial state of charge is 100%, with a minimum state of charge of 40%.

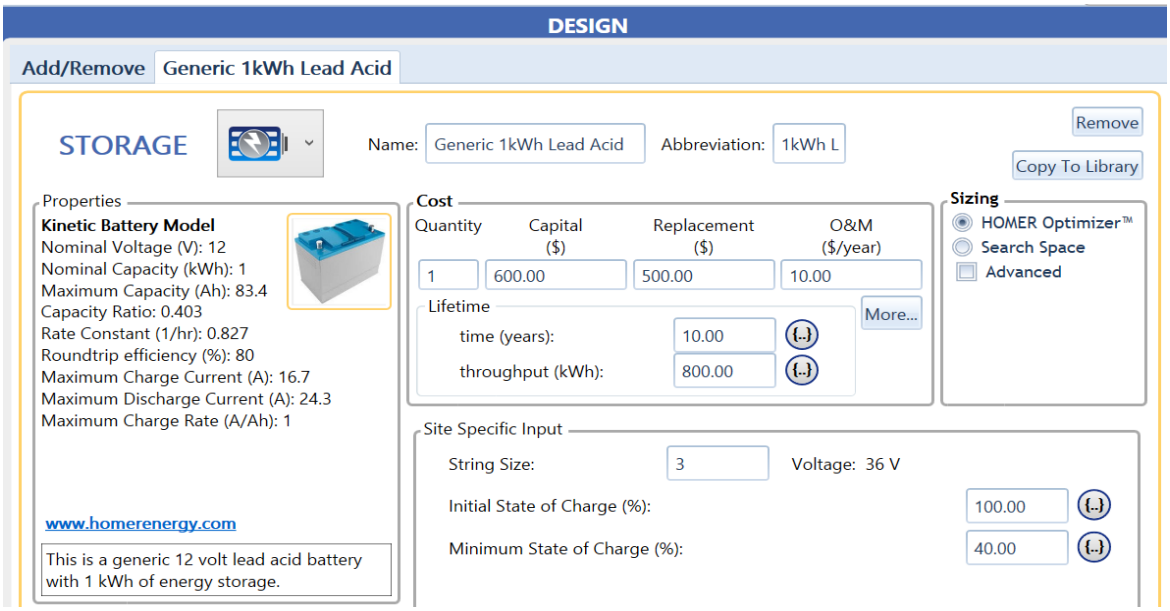

Figure 47. Simulated battery system considered for optimization

3.6.4 Converter

A bi-directional converter allows power to flow in both directions, making it easier to convert AC to DC for battery charging and supply AC to supply AC loads by converting DC to AC. A Dynapower SPS-100 with a capacity of 100 kW and an efficiency of 96.5% with a relative capacity of 100% was investigated. The converter has a 15-year life expectancy, with a considered capital cost of $ 700, a replacement cost of $ 600, and an annual O&M expense of $ 30. The capacity of this converter is slightly higher (approximately 19%) than the peak load.

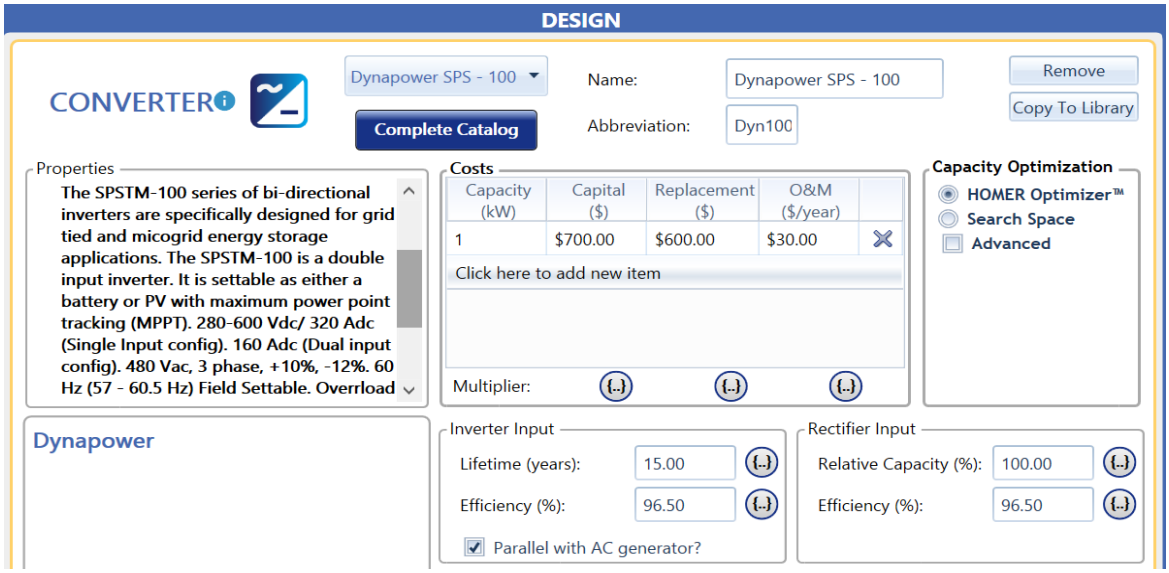

Figure 48. Simulated converter system considered for optimization

3.6.5 Main grid connection

Due to the unpredictability of solar and wind resources and the possibility of system failure, connecting to a grid allows the grid to supply electricity and provide backup for the system. The system's connection to the grid also allows the system's excess energy to be sold to the grid. The advanced grid module in HOMER enhances the grid by adding real-time rates, schedule rates, grid extension, and reliability choices. The advanced grid modeling by schedule rates was selected for this study. It enables grid-connected systems with programmed pricing to establish grid prices on a regular schedule based on day, month of the year, and weekdays or weekends. The grid purchase price is assumed to be $ 0.10/kWh, whereas the sell-back price is assumed to be $ 0.05/kWh.

3.7 Economics Analysis

Net Present Cost (NPC) and the Levelized Cost of Energy or Cost of Energy (COE) are the two key economic factors utilized in the HOMER tool for economic analysis and optimal configurations. NPC is the most cost-effective metric in the HOMER tool for optimization [130].

3.7.1 Net Present Cost

NPC is the total cost and revenue of a project across its whole life cycle, and it is represented by the expression [131];

$$NPC = \frac{C_{T-ann}}{CRF(i,t)} \tag{36}$$

Where;

C_{T-ann} = Annualized total cost of the system.

CRF = Capital recovery factor

i = Annual interest rate or discount rate

t = Project life time.

The annual effective interest rate is a percentage of the balance at the end of the year in which interest is paid or earned and it is represented as;

$$i = \frac{i' - f}{1 + f} \tag{37}$$

Where;

i' = Nominal interest rate

f = Annual inflation rate.

The capital recovery factor is the number of yearly payments required at a discount rate in order

to achieve present value after a given number of years. It is given by;

$$CRF(i,n) = \frac{i(1+n)^n}{(1+n)^n - 1} \quad (38)$$

Where;

n = number of years.

3.7.2 Levelized Cost of Energy

The Levelized Cost of Electricity (COE) is an economic metric that compares the long-term costs of producing electricity using various generation techniques and it is mathematically expressed as [130];

$$COE = \frac{C_{T-ann}}{E_{off-grid} + E_{on-grid}} \quad (39)$$

Where;

$E_{off-grid}$ = Grid-supplied electrical energy.

$E_{on-grid}$ = microgrid's total quantity of electricity sold to the grid

3.4.3 Economic feeds

The project lifetime is designed to run for 25 years with a discount rate set at 4.00% and the inflation rate set at 2.4%, and the annual capacity shortage is assumed to be zero for the grid-tied systems and 10% for the stand-alone system.

3.8 Sensitivity Analysis Inputs

Sensitivity is a technique for analyzing how the optimal components change over time and measuring the impact of each change on the project's result. In this study, three solar radiation and wind speed sensitivity variables are considered, with one of the values being the average solar radiation and average wind speed of the site, and the other two values varying slightly from lower solar radiation values and wind speed values to higher solar radiation values and wind speed values. Table 10 lists the sensitivity variables that were used in the simulations.

Table 10. Sensitivity analysis inputs under consideration

Solar radiation	**Value ($kWh/m^2/day$)**	**Wind speed**	**Value (m/s)**
Solar Scaled Average Radiation	4.92	Wind Scaled Average Speed	5.18
Lower Solar radiation value considered	3	Lower Wind speed value considered	4.2
Higher Solar radiation value considered	7	Higher Wind speed value considered	6

In addition to the specified values for the sensitivity analysis, HOMER took values between the specified values into account.

CHAPTER FOUR

4 Result Analysis and Discussion

This chapter presents results and discussions of the three designed systems considered in this study. Despite multiple simulation results from utilization of various solar radiation and wind speed values, optimization results based on the lowest NPC of an average scaled solar radiation value of 4.92 kWh/day and an average scaled wind speed value of 5.18 m/s are considered for the three configuration systems. This chapter also presents a sensitivity analysis of the variables under consideration.

4.1 The Scenarios

As stated in chapter three, the three HBMG systems chosen for this analysis are classified as:

- ✓ Standalone HBMG system (scenario one (1))
- ✓ Grid connected HBMG system without battery system (scenario two (2))
- ✓ Grid connected HBMG system with battery system (scenario three (3))

4.1.1 Standalone system (scenario one (1))

The chosen standalone HBMG system consists of solar, wind, and batteries as the DERs. A total of 22476 solutions were simulated in this scenario, with 9896 solutions proving feasible and 12580 proving infeasible due to the capacity shortage constraint.

Table 11. Categorized optimization Result of standalone HBMG

Export...

Optimization Results

Left Double Click on a particular system to see its detailed Simulation Results.

Categorized Overall

Architecture						Cost				System		CS6X-325P		AV
CS6X-325P (kW)	AWS3.3kW	1kWh LA	Dyn100 (kW)	Dispatch	NPC ($)	COE ($)	Operating cost ($/yr)	Initial capital ($)	Ren Frac (%)	Total Fuel (L/yr)	Capital Cost ($)	Production (kWh/yr)	Capital (($)
97.8	9	117	39.4	CC	$400,062	$0.335	$8,307	$229,234	100	0	68,458	166,356	63,000
161		174	50.5	CC	$511,017	$0.432	$12,584	$252,241	100	0	112,487	273,350	
	30	168	35.4	CC	$589,404	$0.502	$12,342	$335,588	100	0			210,000
523	49		50.6	CC	$987,024	$0.832	$11,776	$744,858	100	0	366,450	890,494	343,000

From table 11, the simulation findings also show a $ 400062 NPC, a $ 0.335 LCOE, a $ 8,307 annual operating cost, and a $ 229,234 initial cost. Since only renewable energy sources were used in the scenario, the renewable energy fraction is 100%.

Figure 49 summarizes the total cost of the standalone HBMG, indicating details of the economic variables about each component that adds up to the NPC value. Compared to the other components in this design, the overall cost of a generic lead-acid battery is the highest.

In the stand-alone HBMG, a PV system with a total rated capacity of 97.8 kW offers the majority of the energy generated with an annual generation of 166356 kWh. In comparison, a wind system with a total rated capacity of 29.7 kW offers an annual production of 61141 kWh.

Component	Capital ($)	Replacement ($)	O&M ($)	Fuel ($)	Salvage ($)	Total ($)
AWS HC 3.3kW Wind Turbine	$63,000.00	$39,602.82	$3,701.60	$0.00	($27,486.56)	$78,817.85
CanadianSolar MaxPower CS6X-325P	$68,457.70	$0.00	$20,111.35	$0.00	$0.00	$88,569.05
Dynapower SPS - 100	$27,576.37	$18,732.24	$24,303.97	$0.00	($5,347.30)	$65,265.28
Generic 1kWh Lead Acid	$70,200.00	$93,001.24	$24,060.40	$0.00	($19,851.41)	$167,410.23
System	$229,234.07	$151,336.30	$72,177.32	$0.00	($52,685.27)	$400,062.42

Figure 49. Cost summary of standalone HBMG

Meanwhile, Figure 50 summarizes the cost flow of the standalone HBMG with the project cost represented by the figures below zero. The high investment was experienced in year zero at a value of $66838.38. Except in years 0, 10, 15, and 20, the project incurred same operational costs of $3509.81 per year in the rest of the years. In year 10 (the replacement costs for batteries), year 15 (the replacement costs for converters), and year 20 (the replacement costs for wind turbines and

batteries), values of $58500, $23636.89, and $112,500, respectively, are experienced. The project's salvage value of $77628.96 occurs at the end of the project.

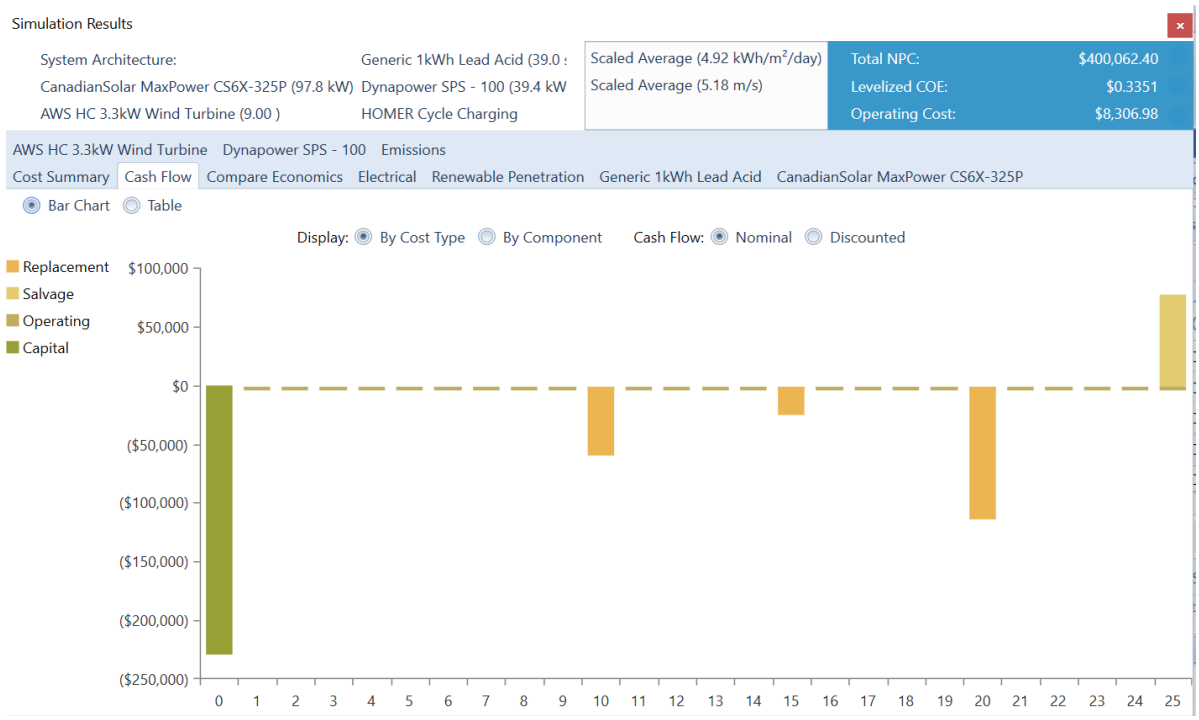

Figure 50. Cash flow of standalone HBMG

4.1.2 Grid-connected system without batteries (scenario two (2))

This scenario includes a solar, wind, and grid combination, and a total of 6396 solutions were simulated in this scenario, with all of the solutions being feasible.

The simulation results in table 12 show an NPC of $103419, a LCOE of $0.0505, an annual operating cost of $1841, and an initial cost of $65563. The renewable energy fraction is 77.5%.

Table 12. Categorized optimization Result of grid-connected without batteries HBMG

Export...

Optimization Results

Left Double Click on a particular system to see its detailed Simulation Results.

Categorized Overall

Architecture						Cost				System		CS6X-325P		AWS
CS6X-325P (kW)	AWS3.3kW	Grid (kW)	Dyn100 (kW)	Dispatch	NPC ($)	COE ($)	Operating cost ($/yr)	Initial capital ($)	Ren Frac (%)	Total Fuel (L/yr)	Capital Cost ($)	Production (kWh/yr)	Capital Cost ($)
35.1	4	999,999	18.6	CC	$103,419	$0.0505	$1,841	$65,563	77.5	0	24,547	59,651	28,000
46.5		999,999	24.4	CC	$107,626	$0.0547	$2,820	$49,634	68.8	0	32,556	79,113	
	8	999,999		CC	$110,253	$0.0613	$2,638	$56,000	62.1	0			56,000
		999,999		CC	$124,066	$0.100	$6,033	$0.00	0	0			

Figure 51 summarizes the total cost of the grid-connected HBMG without batteries, including details of the economic variables about each component that add up to the NPC value. Among all the components in this scenario, wind turbines have the highest total cost. In this HBMG, the PV system with a total rated capacity of 35.1 kW generates most of the energy (59,651 kWh per year). In comparison, a wind system with a total rated capacity of 13.2 kW generates 27,174 kWh per year.

Component	Capital ($)	Replacement ($)	O&M ($)	Fuel ($)	Salvage ($)	Total ($)
AWS HC 3.3kW Wind Turbine	$28,000.00	$17,601.25	$1,645.16	$0.00	($12,216.25)	$35,030.16
CanadianSolar MaxPower CS6X-325P	$24,547.09	$0.00	$7,211.39	$0.00	$0.00	$31,758.48
Dynapower SPS - 100	$13,016.25	$8,841.75	$11,471.65	$0.00	($2,523.96)	$30,805.69
Grid	$0.00	$0.00	$5,824.69	$0.00	$0.00	$5,824.69
System	$65,563.34	$26,443.01	$26,152.89	$0.00	($14,740.22)	$103,419.02

Figure 51. Cost summary of grid connected without batteries HBMG

The cash flow of scenario two is shown in Figure 52. Year zero sees a lot of investments, totaling $65,563.34. Throughout the 24 years, except in year 0, a consistent annual operating cost of $1,271.75 is realized. Year 15 (converter replacement costs) and year 20 (wind turbine replacement costs) have values of $1,1156.79 and $24,000, respectively. At the end of this project, the project salvage value of $21718.93 will be reached.

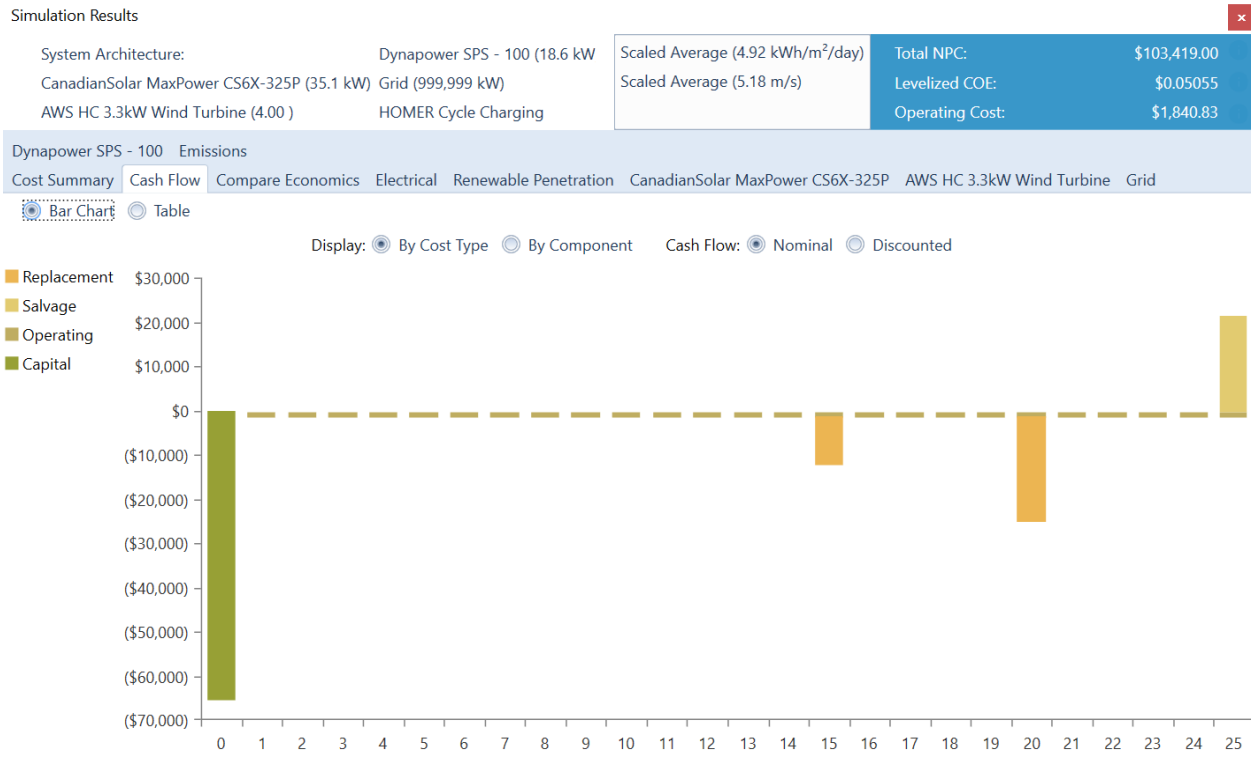

Figure 52. Cash flow of grid connected without batteries HBMG

4.1.3 Grid connected system with batteries (scenario (3))

The third scenario is based on a solar, wind, and grid combination, and it includes a total of 25812 solutions, all of which are feasible.

Table 13 shows that the NPC is $ 107712, the LCOE is $ 0.0529, the yearly operating cost is $ 1988, and the initial cost is $ 66838. Renewable energy accounts for 77.2% of total energy consumption in this scenario.

Table 13. Categorized optimization Result of grid connected with batteries HBMG

Export...

Optimization Results

Left Double Click on a particular system to see its detailed Simulation Results.

Categorized Overall

Architecture								Cost				System		CS6X-325P	
CS6X-325P (kW)	AWS3.3kW	1kWh LA	Grid (kW)	Dyn100 (kW)	Dispatch	NPC ($)	COE ($)	Operating cost ($/yr)	Initial capital ($)	Ren Frac (%)	Total Fuel (L/yr)	Capital Cost ($)	Producti (kWh/y
35.1	4		999,999	18.6	CC	$103,419	$0.0505	$1,841	$65,563	77.5	0	24,547	59,651
46.2			999,999	24.1	CC	$107,625	$0.0550	$2,840	$49,231	68.5	0	32,358	78,631
34.6	4	3	999,999	18.3	CC	$107,712	$0.0529	$1,988	$66,838	77.2	0	24,218	58,850
	8		999,999		CC	$110,253	$0.0613	$2,638	$56,000	62.1	0		
44.8		3	999,999	23.6	CC	$111,912	$0.0579	$3,026	$49,694	67.7	0	31,368	76,226

The entire cost of the grid-connected with batteries HBMG, including details of the economic variables that add up to the NPC value, is summarized in figure 53. Wind turbines have the highest total cost in this scenario when compared to all other components.

The PV system, with a total rated capacity of 34.6 kW, generates the majority of the energy (58850 kWh per year). In contrast, the wind system, with a total rated capacity of 13.2 kW, generates 27174 kWh per year in this HBMG.

Simulation Results

System Architecture: Generic 1kWh Lead Acid (1.00 ;
CanadianSolar MaxPower CS6X-325P (34.6 kW) Dynapower SPS - 100 (18.3 kW
AWS HC 3.3kW Wind Turbine (4.00) Grid (999,999 kW)

Scaled Average (4.92 kWh/m²/day)
Scaled Average (5.18 m/s)

Total NPC: $107,712.10
Levelized COE: $0.05294
Operating Cost: $1,987.59

AWS HC 3.3kW Wind Turbine | Grid | Dynapower SPS - 100 | Emissions

Cost Summary | Cash Flow | Compare Economics | Electrical | Renewable Penetration | Generic 1kWh Lead Acid | CanadianSolar MaxPower CS6X-325P

Cost Type
- Net Present
- Annualized

Categorize
- By Component
- By Cost Type

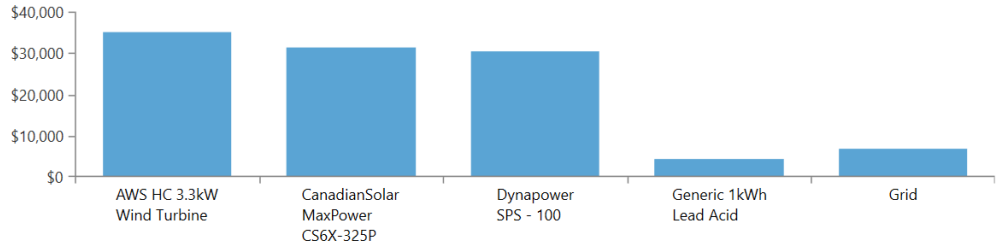

Component	Capital ($)	Replacement ($)	O&M ($)	Fuel ($)	Salvage ($)	Total ($)
AWS HC 3.3kW Wind Turbine	$28,000.00	$17,601.25	$1,645.16	$0.00	($12,216.25)	$35,030.16
CanadianSolar MaxPower CS6X-325P	$24,217.65	$0.00	$7,114.61	$0.00	$0.00	$31,332.26
Dynapower SPS - 100	$12,820.73	$8,708.94	$11,299.33	$0.00	($2,486.05)	$30,342.95
Generic 1kWh Lead Acid	$1,800.00	$2,384.65	$616.93	$0.00	($509.01)	$4,292.57
Grid	$0.00	$0.00	$6,714.13	$0.00	$0.00	$6,714.13
System	$66,838.38	$28,694.84	$27,390.16	$0.00	($15,211.31)	$107,712.06

Figure 53. Cost summary of grid connected with batteries HBMG

The cash flow of scenario three is depicted in figure 54. Year zero witnessed a lot of investments, with a total value of $665838.38. Except for years 0, 10, 15, and 20, the project's annual operating costs are the same at a value of $1331.92 for the remaining years. In years 10, 15, and 20, the costs of replacing batteries, converters, and wind turbines and batteries are $1500, $10989, and $25500, respectively. At the end of this project, a salvage value of $ 22413.07 will be acquired.

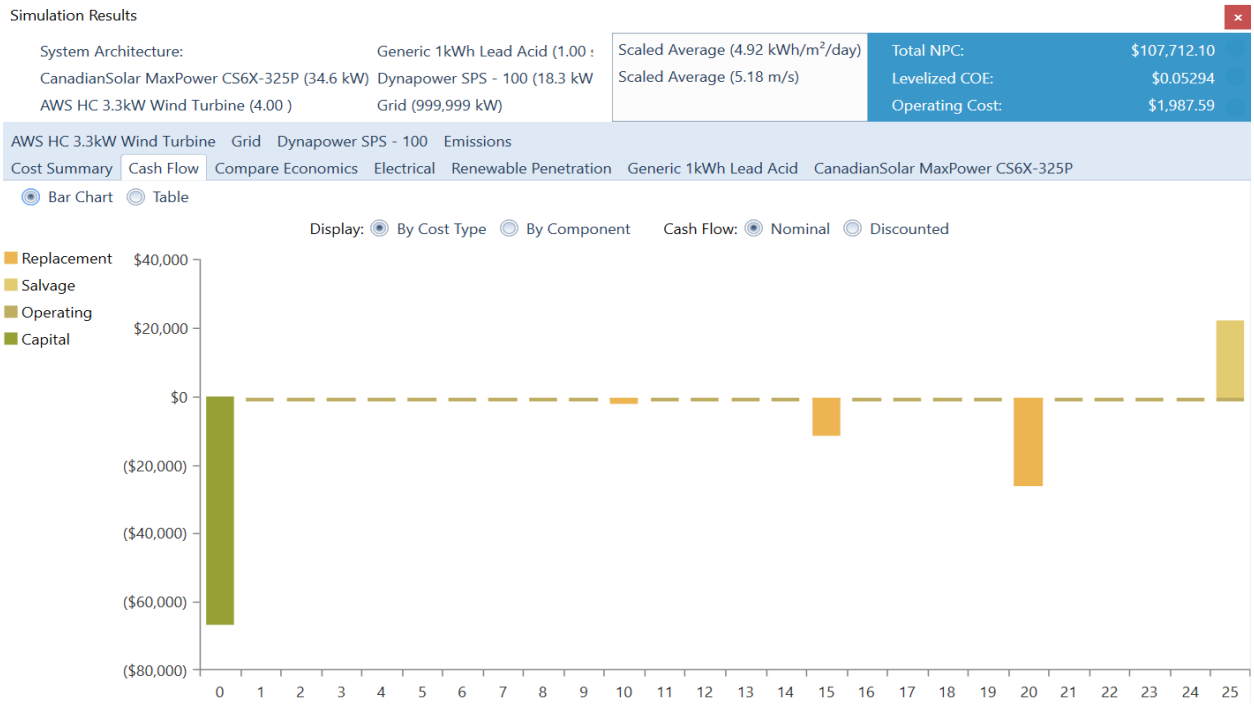

Figure 54. Cash flow of grid connected with batteries HBMG

4.2 The First Approach (Techno-economic) to Scenario Comparison to Choose the Most Viable HBMG System

Variables such as NPC, LCOE, initial costs, operating costs, capacity shortage, unmet electrical load, renewable fraction, return on investment, and excess electricity for the three scenarios were considered and compared in this study to choose the best optimal system as in figure 55 and figure 56.

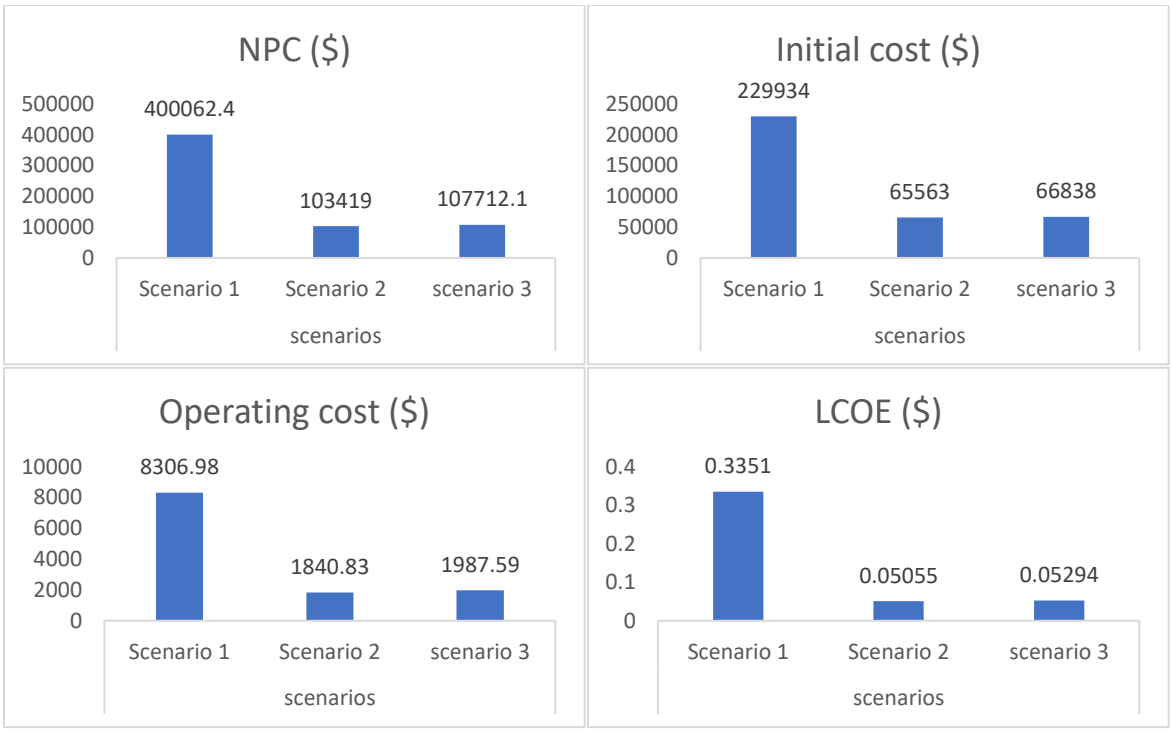

Figure 55. Comparison of Scenarios based on NPC, initial costs, operating costs, and LCOE

Based on the NPC (total capital costs of components, their replacement costs, their O&M, and salvage value), scenario 2 has the lowest NPC followed by scenario 3 while scenario 1 has the highest NPC value. The initial capital and operating expenditures for scenario 1 are higher than those for scenarios 2 and 3. Scenario 2 requires a lower initial investment and lower operating expenses, whereas scenario 3 demands a slightly higher initial investment and slightly higher operating costs. A system with a lower LCOE and NPC is considered to be good. The LCOE of scenario 2 is the lowest, followed by scenario 3, while the LCOE of scenario 1 is the highest.

Excess electricity is one of the variables evaluated. In this case, scenario 1 creates more surplus electricity that cannot be used to fulfill the load and is thus deemed waste or dumped electricity. Scenario 2 produces the least amount of excess electricity, followed by scenario 3 with the second least quantity of excess electricity. Both scenarios 2 and 3 have no capacity shortages because they are connected to the grid; however, Scenario 1 experiences a 10.1 % capacity shortage.

A return on investment (ROI) of the scenarios, a profitability indicator that defines how much profits a project can generate from an investment cost, is another variable included in the comparison. Scenario 2 has a ROI of 2.4%, scenario 3 has a ROI of 2.1%, and scenario 1 has zero ROI. Some of the electrical loads are sometimes not met by the system generating capacity, as

shown in scenario 1 where 3.77% of the load does not get electricity due to intermittent generating sources without a backup grid connected. In contrast, all electrical loads are met by the generation capacity in scenarios 2 and 3.

The renewable fraction, or the proportion of energy delivered to the load from renewable sources, is another objective set in this study. Scenario 1 delivers 100% renewable energy to the load, whereas scenarios 2 and 3 deliver 77.5% and 77.2% of renewable energy to the load, respectively. Scenario 1 has a 100% renewable fraction because the load is solely satisfied by renewable sources, unlike scenarios 2 and 3 where the load can draw power from the grid during intermittency or system failure.

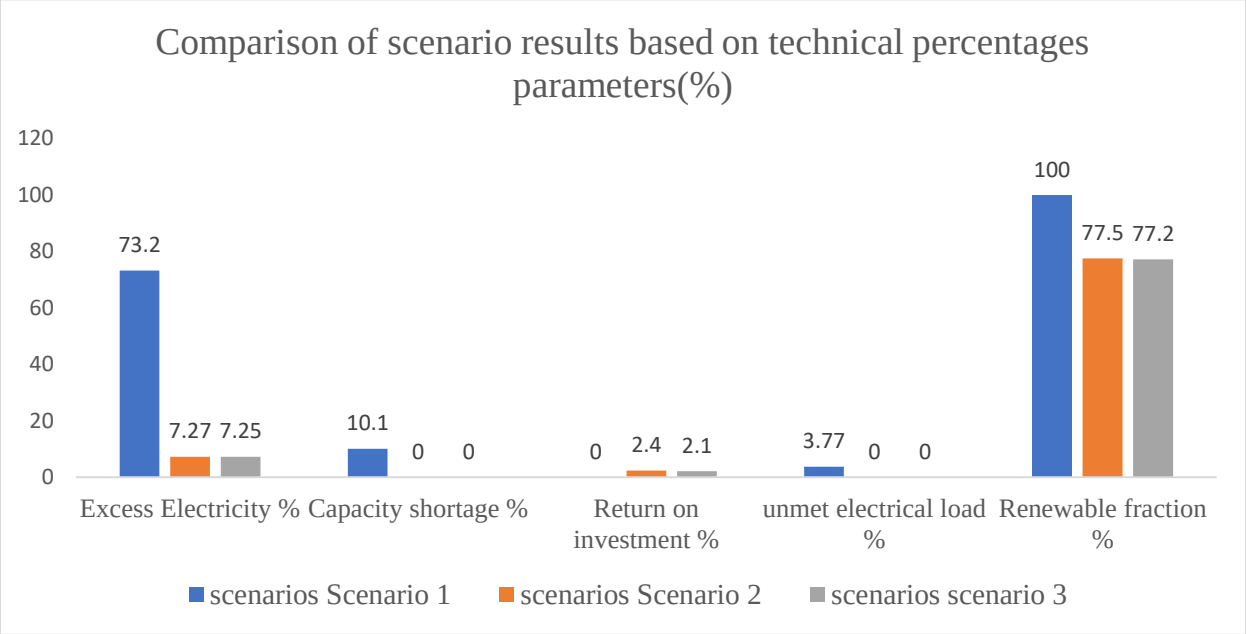

Figure 56. Comparison of scenarios based on excess electricity, capacity shortage, return on investment, unmet electrical load, and renewable energy fraction

The capacity shortage and unmet capacity load in scenarios 2 and 3 demonstrate that scenarios 2 and 3 are both reliable HBMG systems. In terms of efficiency, scenarios 2 and 3 are realistic possibilities because the quantity of excess electricity in scenario 1 (73.2%) is about 90% more than the excess electricity in scenarios 2 (7.27%) and 3 (7.25%).

The winner scenario, as shown in figure 56, is determined by selecting the scenario with the lowest NPC, the lowest LCOE, the lowest operating costs, the lowest initial costs, the lowest excess

electricity production, the lowest capacity shortage, the highest ROI, and the lowest unmet electrical demand.

4.3 The Second Approach (awarding/allocation of points) to Scenario Comparison to Choose the Most Viable HBMG System

An assumption was made to award points for the scenarios in each case compared to the first approach, with the best scenario receiving 150 points in each case, the second-best scenario receiving 100 points, and the third-best scenario receiving 50 points in each case. For example, scenario 2 receives 150 points for the lowest NPC comparison because it is the winner with the lowest NPC. In comparison, scenario 3 receives 100 points for coming in second place with the lowest NPC, and scenario 1 receives 50 points for having the highest NPC, and so on for all the cases under consideration.

Table 14. Compared cases with allocated points

Compared cases	Scenario points		
	Scenario 1	**Scenario 2**	**Scenario 3**
Lowest NPC	50	150	100
Lowest LCOE	50	150	100
Lowest Operation cost	50	150	100
Lowes Initial cost	50	150	100
Lowest excess electricity production	50	150	100
Lowest capacity shortage	50	150	100
Highest return on investment	50	150	100
Lowest unmet electricity load	50	150	100
Highest renewable fraction	150	100	50
Total points	**550**	**1300**	**850**

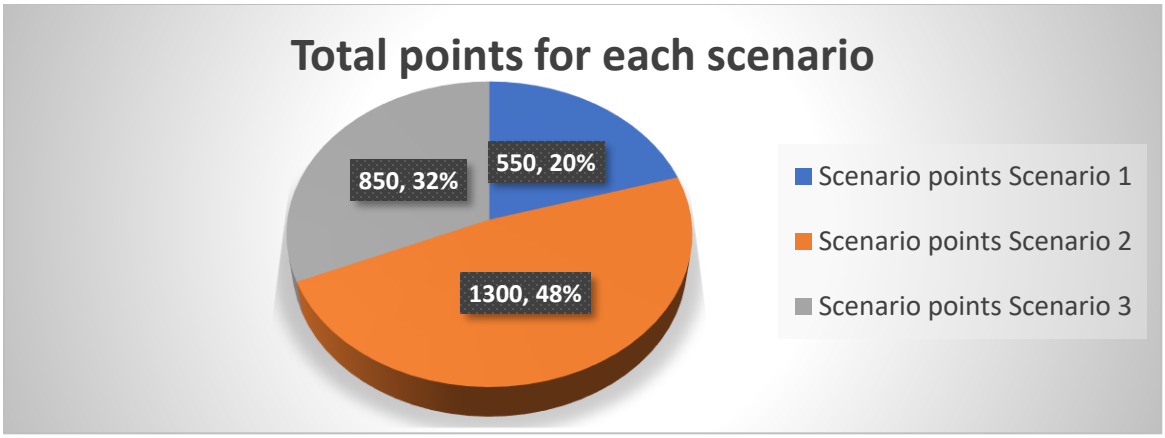

Figure 57. A Pie chart showing total points and percentage share for each scenario

Based on all of the factors combined in the first approach to scenario comparison and the allocation of points in the second approach to scenario comparison**,** scenario 2 is the overall winner, emerging on top with 1300 points, or 48% of the total points. Scenario 3 came in second with 850 points, or 32% of the total points, and scenario 3 came in third with 550 points, or 20%. Scenario 2 is connected to the grid and has higher power reliability than scenario 1. scenario 2 is chosen as the most feasible and optimal solution. Taking into account all of the comparisons between the scenarios in comparison case 1 and 2, scenario 2 is selected as the most feasible and optimal solution overall.

4.4 Further Analysis of the Selected System, Scenario 2

4.4.1 More economical results of Scenario 2

Table 15 shows some of the economic characteristics for scenario 2.

Table 15. Economic metrics for the optimal System

METRIC	VALUE
PRESENT WORTH ($)	$20,647
ANNUAL WORTH ($/YR.)	$1,004
RETURN ON INVESTMENT (%)	2.4
INTERNAL RATE OF RETURN (%)	4
SIMPLE PAYBACK (YR.)	13.77
DISCOUNTED PAYBACK (YR.)	18.06

4.4.2 Energy generation and consumption

The share of monthly electricity production by each component involved in the optimum system is presented in figure 58.

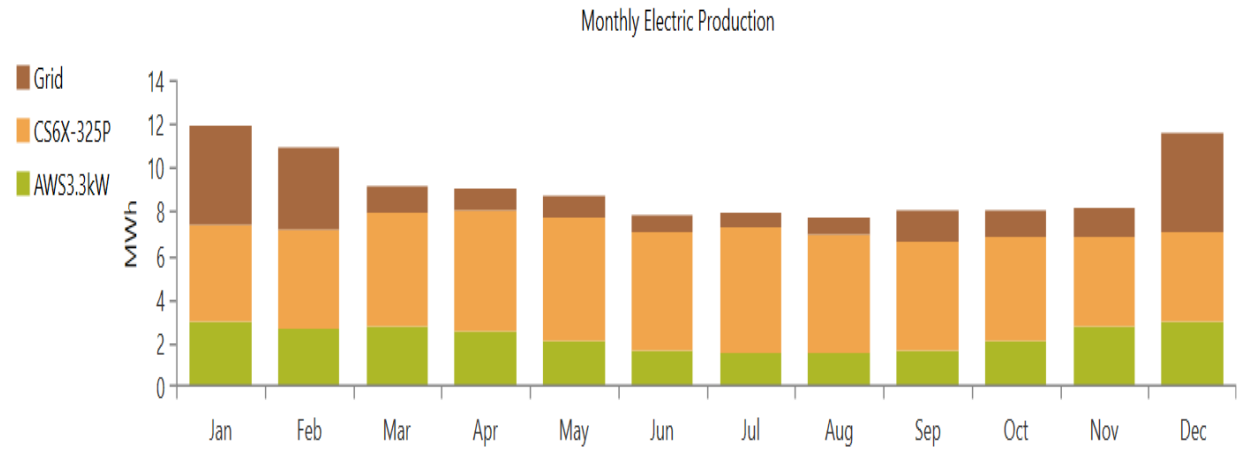

Figure 58. Monthly share of Electricity Generation from the Optimum System (scenario 2) with a 77.5% renewable fraction

Wind turbine energy production increases in the winter, as can be observed in figure 58. This is because winter brings higher temperature gradients, particularly when cold currents from the polar regions blow in. The solar output, on the other hand, is lower in the winter season compared to the summer, autumn, and spring seasons, due to lower number of sunshine hours in winter season compared to the summer, autumn, and spring seasons. The penetration of solar is more than the penetration of wind as in table 16.

Table 16. Selected optimal system simulation results for PV and wind turbine setups

Quantity	Values		Units
	PV	Wind turbine	
Rated capacity	35.1	13.2	kW
Mean output	6.81	3.1	kW
Maximum output	36.4	18.2	kW
Penetration	98.9	45	%
Hours of operation	4387	7522	hrs/yr
Levelized cost of energy	0.0259	0.0627	$/kWh

Table 16 shows that the maximum PV output is 36.4kW and the mean PV output is 6.81kW during maximum and mean solar radiations, whereas the greatest wind output is 18.2kW and the mean wind output is 3.1kW during maximum and mean wind speeds. PV's levelized cost of energy is

0.0259 $/kWh cheaper than wind turbines' levelized cost of electricity, which is 0.0627 $/kWh. The PV system has a capacity factor of 19.4%, while the wind turbine system has a capacitor factor of 45.0%. The most optimum scenario has a total renewable penetration of 87.3%.

Figure 59 depicts the yearly electricity generation of electricity by individual power components of the HBMG system and the electricity consumption by the AC load and grid sales. PV array power generation accounts for 54.6% of total electricity generated by the HBMG system (59,651 kWh/year), wind turbine power generation accounts for only 24.9 percent (27,174 kWh/year), and grid purchases account for 20.5 percent (22,411 kWh/year). The AC load consumes 60.6% (60,330kWh/yr.) and 39.4% (39,158kWh/yr.) of the solar PV and wind production is sold to the grid.

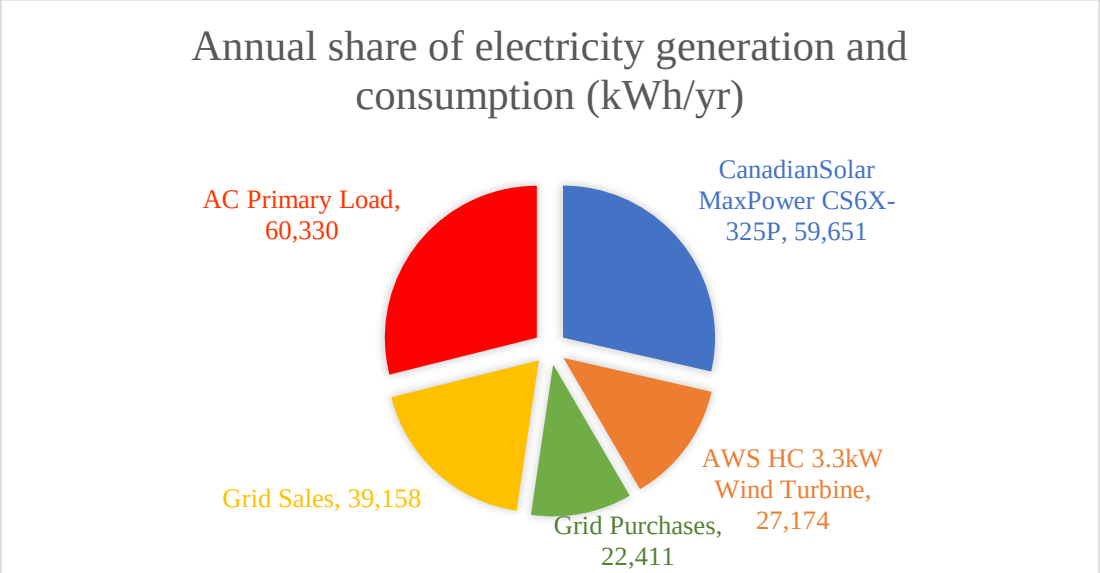

Figure 59. Annual share of electricity generation and consumption from the optimum system a 77.5% RF

Figure 60 depicts a seasonal generation and a year consumption time series plot. The months of January, February, and December have increased electricity consumption; hence production form the distributed generation and grid is higher in those months compared to the rest of the year.

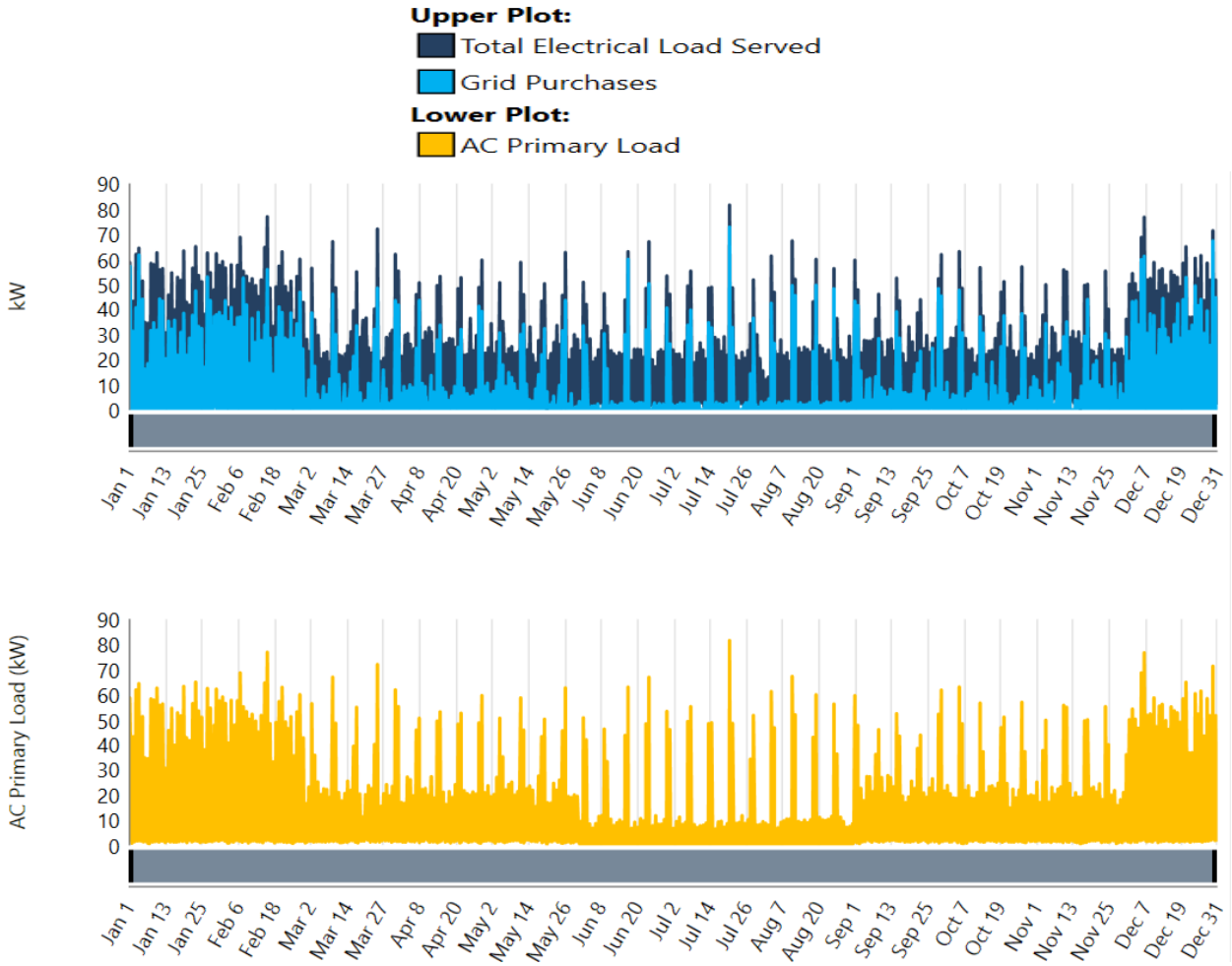

Figure 60. Time series plot of electrical generation and consumption

4.4.3 **Converter optimization results of the optimal system**

The inverter runs for 4,387 hours each year, and the surplus electricity generated by the PV system and wind system is routed into the main grid via the inverter.

Table 17. Inverter and rectifier optimization results of the optimal system

Quantity	Inverter	Rectifier	Units
Capacity	18.6	18.6	kW
Mean output	5.7	0	kW
Maximum output	18.6	0	kW
Capacity factor	30.6	0	%
Hours of Operation	4,387	0	hrs/yr
Energy Out	49,903	0	kWh/yr
Energy In	51,713	0	kWh/yr
Losses	1,810	0	kWh/yr

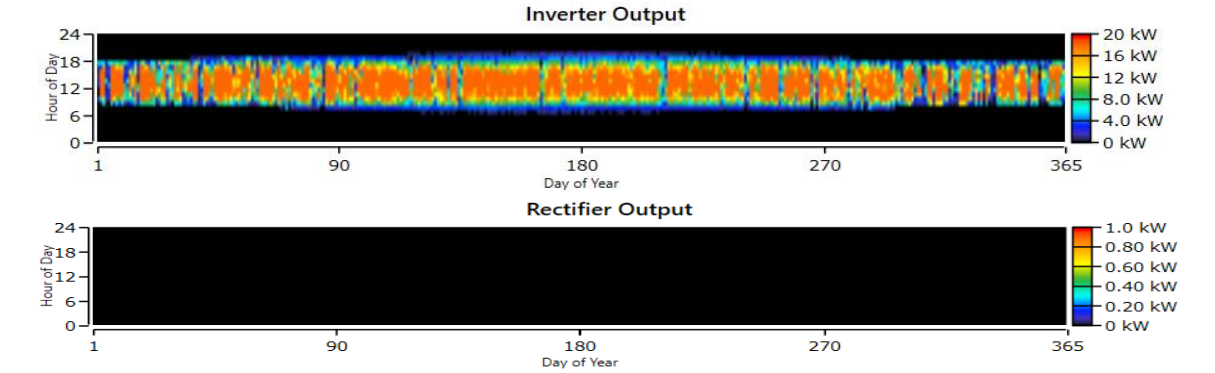

Figure 61. Inverter output (top) and rectifier output (bottom)

4.4.4 Grid

As depicted in table 18 and in figure 61, energy purchased from the grid is higher during the winter months (January, February, and December), implying that less energy is sold. However, solar supplies more energy than the wind from March to November, implying that more energy is sold to the grid because solar's generation capacity percentage share of the system is higher. The majority of the peak load of 50kW or more occurs throughout the winter and summer months, as loads like the CIS and A/C are set on in winter and summer respectively. The annual peak demand is 73 kW.

Table 18. Monthly grid purchases, sales, peak load, and energy charge

Month	Energy Purchased (kWh)	Energy Sold (kWh)	Net Energy Purchased (kWh)	Peak load (kW)	Energy Charge $	Demand charge $
January	4,579	1,980	2,599	62	$358.89	$0
February	3,752	2,115	1,637	56	$269.44	$0
March	1,184	3,324	-2,140	48	($47.77)	$0
April	1,042	3,577	-2,535	44	($74.65)	$0
May	1,031	3,244	-2,213	44	($59.06)	$0
June	704	4,841	-4,137	60	($171.68)	$0
July	757	4,977	-4,220	73	($173.12)	$0
August	807	4,585	-3,778	50	($148.53)	$0
September	1,403	2,632	-1,229	48	$8.72	$0
October	1,264	2,720	-1,457	48	($9.65)	$0
November	1,364	2,975	-1,611	44	($12.34)	$0
December	4,524	2,189	2,336	67	$343.00	$0
Annual	**22,411**	**39,158**	**-16,747**	**73**	**$283.24**	**$0**

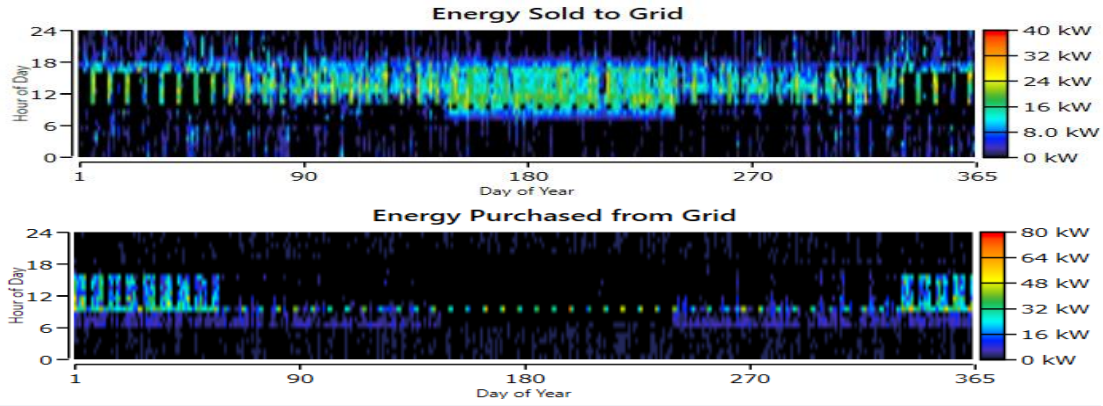

Figure 62. Energy purchased from the grid (top) and energy sold to the grid (bottom)

4.3.3 Emissions

The gases emitted into the atmosphere during the project's life cycle of 25 years come from the conventional sources of the grid. As shown in table 19 and table 20, the only gases emitted are CO_2, sulfur dioxide, and nitrogen oxides.

Table 19. Emissions from the selected optimal system

EMITTED GASES	QUANTITY EMITTED (KG/YR)
Carbon dioxide	14,164
Carbon monoxide	0
Unburned hydrocarbons	0
Particulate matter	0
Sulfur dioxide	61.4
Nitrogen oxides	30
TOTAL	**14,255**

Table 20. Emissions from only the grid

EMITTED GASES	QUANTITY EMITTED (KG/YR.)
Carbon dioxide	38,129
Carbon monoxide	0
Unburned hydrocarbons	0
Particulate matter	0
Sulfur dioxide	165
Nitrogen oxides	80.8
TOTAL	**38,375**

The optimum solution minimizes overall emissions by more than 60% when compared to the grid. The adoption of renewable technologies such as solar and wind in the power generation process has resulted in the mitigation in emissions.

4.4.5 Sensitivity Analysis

The sensitivity variables of solar radiations and wind speed-sensitive variables were proposed in the methodology of this study because solar radiations and wind speed vary from winter to summer to spring and autumn season in this study's project site. Figure 63 depicts the system configuration variation as a result of varied solar and wind resource values, resulting in three types of best optimum configurations and a total of nine different configurations for the optimal system types Graph, with solar radiation ranging from 3.0 to 7.0 kWh/m^2/day on the X-axis and wind speeds ranging from 4.2 to 6.0 m/s on the Y-axis.

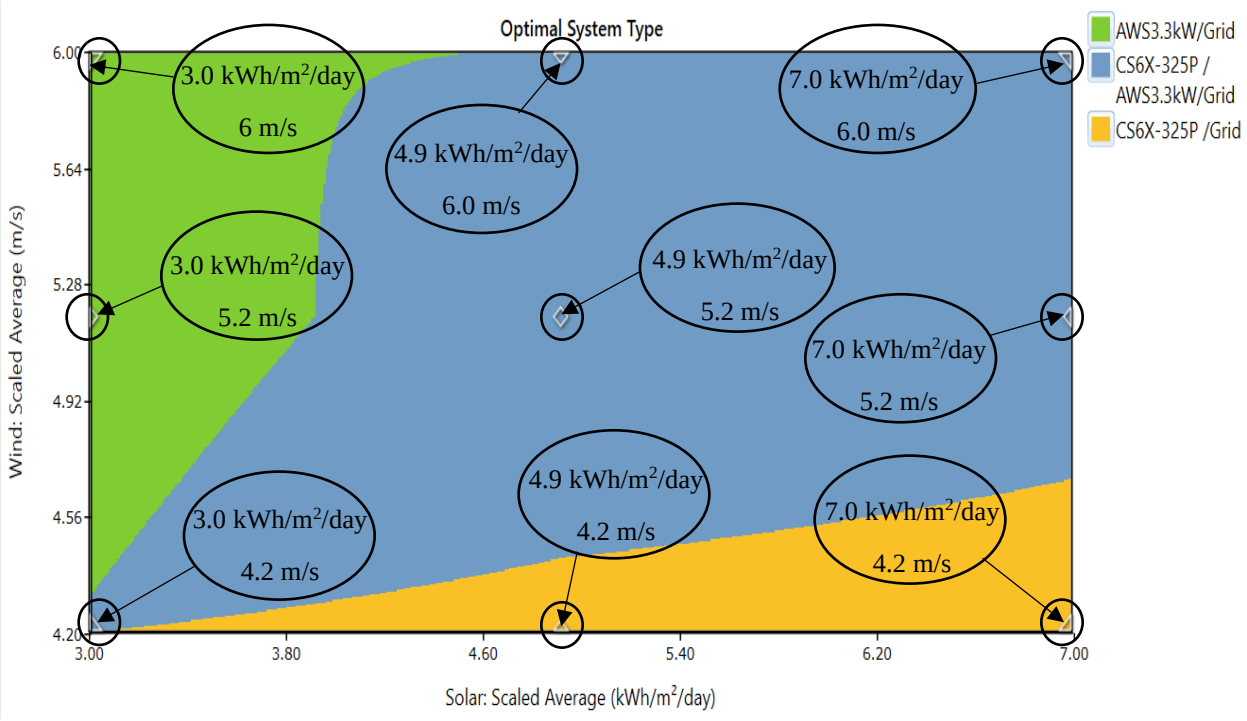

Figure 63. Optimal system types and configurations for different levels of solar radiation and wind speed

As indicated in figure 63, wind/grid system, Solar PV/wind turbine/Grid system, and Solar PV/Grid system are the three types of best optimum configurations obtained. The various configurations presented in this paper may be applicable in places with similar climatic resources.

The surface plot in figure 64. shows that as the solar and wind resource values increases, the system approaches the best optimal setup. When the solar radiation and wind speed values are 7 kWh/m^2/day and 6 m/s, respectively, the NPC for the HBMG drops significantly, but these values are only available for a short period of the year. Therefore its NPC is not picked.

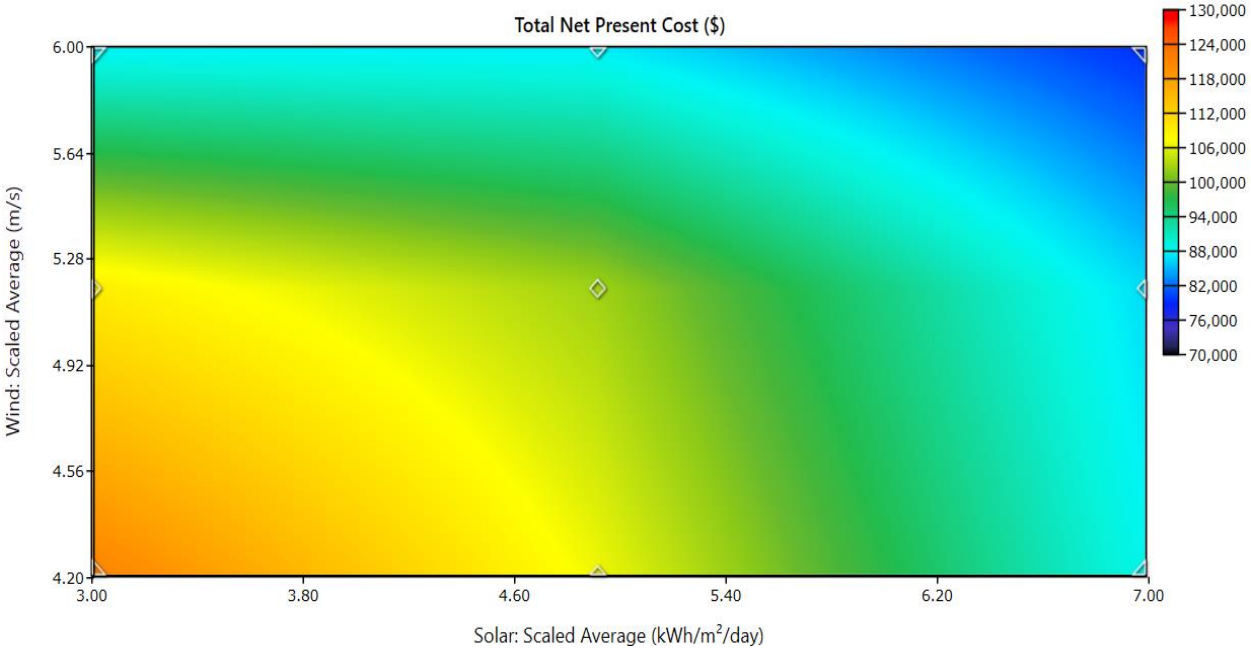

Figure 64. Optimization surface plot for different levels of solar radiation and wind speed with NPC

CHAPTER FIVE

5 Conclusion and Recommendations and Future Suggestions

This section wraps up the research by summarizing the findings, making recommendations, and giving future suggestions.

5.1 Conclusions and Recommendations

In this research, three optimization scenarios were analyzed using the HOMER tool. The scenarios were developed using sustainable energy sources such as solar and wind and a varying number of backup solutions in each scenario. Scenario 1 was considered a stand-alone mode is generating a zero return on investment. In contrast, scenarios 2 and 3 were evaluated in grid-connected modes, except that scenario 2 was analyzed without batteries and scenario 3 was considered with batteries. Scenario 2, with a generated ROI of 2.4%, has a 14-year simple payback and a 17-year discounted payback, whereas scenario 3, with a generated ROI of 2.1%, has a 17-year simple payback and a 24-year discounted payback period. The component size was optimized by HOMER tool depending on the location's solar and wind resources and load demand.

An anticipated rise in faculty load demand in the future can be predicted, necessitating the expansion of renewable energy sources, which will raise costs.

Even though the selected simulated HBMG system's LCOE of 0.0505 is higher than the current cost of electricity per kWh from the traditional grid, which currently supplies the faculty with power, the stimulated HBMG system has several advantages over the traditional grid, including long-term economic benefits, environmental benefits, and reliability advantages. This study matched in with the Algerian government's goals and plans to develop power output from renewable energy resources. As a result, it is recommended that the HBMG system be implemented for the faculty.

Accelerating the government of Algeria's efforts and plans toward sustainable energy projects can help combat emissions from natural gas flaring, which is the country's primary source of electricity generation. Recommendation of carbon sequestration techniques such as growing more forests and storing carbon in the soil, ares type of carbon capture technologies that can help lower carbon levels in the atmosphere. Renewable energy technologies offer long-term socio-economic benefits for a country's development, as fossil fuels will be depleted in the future.

5.2 Future suggestions

- Evaluating the HBMG optimization for the site using the same renewable energy resources but employing a different optimization tool.
- Evaluating the standalone simulated system in this study with the inclusion of a biomass system.
- Conducting an independent assessment or research of the site's resources can help obtain most recent solar and wind data.
- To further enhance the techno-economic and optimal sizing features, a combination of multiple optimization tools should be used.

6 References

[1] M. M. C. Akrofi and S. H. Antwi, “COVID-19 energy sector responses in Africa: A review of preliminary government interventions,” *Energy Res. Soc. Sci.*, vol. 68, no. June, 2020, doi: 10.1016/j.erss.2020.101681.

[2] Ü. Ağbulut, “Turkey’s electricity generation problem and nuclear energy policy,” *Energy Sources, Part A Recover. Util. Environ. Eff.*, vol. 41, no. 18, pp. 2281–2298, 2019, doi: 10.1080/15567036.2019.1587107.

[3] N. Chowdhury, “Is Nuclear Energy Renewable Energy?,” Mar. 22, 2012. http://large.stanford.edu/courses/2012/ph241/chowdhury2/ (accessed Nov. 26, 2021).

[4] T. Castillo-Calzadilla, A. M. Macarulla, O. Kamara-Esteban, and C. E. Borges, “A case study comparison between photovoltaic and fossil generation based on direct current hybrid microgrids to power a service building,” *J. Clean. Prod.*, vol. 244, 2020, doi: 10.1016/j.jclepro.2019.118870.

[5] T. Khatib, A. Mohamed, and K. Sopian, “Optimization of a PV/wind micro-grid for rural housing electrification using a hybrid iterative/genetic algorithm: Case study of Kuala Terengganu, Malaysia,” *Energy Build.*, vol. 47, pp. 321–331, 2012, doi: 10.1016/j.enbuild.2011.12.006.

[6] S. Mohseni, A. C. Brent, and D. Burmester, “Community resilience-oriented optimal micro-grid capacity expansion planning: The case of totarabank eco-village, New Zealand,” *Energies*, vol. 13, no. 15, 2020, doi: 10.3390/en13153970.

[7] P. Tiwari *et al.*, “A Review on Microgrid Based on Hybrid Renewable Energy Sources in South-Asian Perspective,” *Technol. Econ. Smart Grids Sustain. Energy*, vol. 2, no. 1, 2017, doi: 10.1007/s40866-017-0026-5.

[8] Y. E. G. Vera, R. Dufo-López, and J. L. Bernal-Agustín, “Energy management in microgrids with renewable energy sources: A literature review,” *Appl. Sci.*, vol. 9, no. 18, 2019, doi: 10.3390/app9183854.

[9] H. Brahim and A. Liazid, “Topic : Energy policy & planning Electricity planning in Algeria,” no. June, pp. 1–24, 2016, [Online]. Available:

https://www.researchgate.net/publication/304248449_Electricity_planning_in_Algeria/link/5772d2b208aeeec3895414e2/download.

[10] M. Bouznit, M. del P. Pablo-Romero, and A. Sánchez-Braza, "Measures to promote renewable energy for electricity generation in Algeria," *Sustain.*, vol. 12, no. 4, pp. 1–17, 2020, doi: 10.3390/su12041468.

[11] S. Haddoum, H. Bennour, and T. Ahmed Zaïd, "Algerian Energy Policy: Perspectives, Barriers, and Missed Opportunities," *Glob. Challenges*, vol. 2, no. 8, p. 1700134, 2018, doi: 10.1002/gch2.201700134.

[12] N. Bailek and K. Bouchouicha, "Updated status of Renewable and Sustainable Energy Projects in Algeria," *Econ. Var. Renew. Sources Electr. Power Prod.*, no. November, pp. 519–528, 2017, doi: 10.6084/m9.figshare.6169505.

[13] T. Sterner, R. T. Carson, M. Hafstead, P. Howard, and A. Schmitt, "Carbon Pricing in Switzerland : Carbon Pricing," vol. 18, 2020.

[14] B. M. Khenfri Khaider, Grinat Mohammed, "Renewable Energy in Algeria Reality and Perspective," *J. Inf. Syst. Technol. Manag.*, vol. 3, no. 10, pp. 1–19, 2018.

[15] GSI REPORT, "Achieving a Recovery," no. May, 2021.

[16] E. Hossain, J. Hossain, and F. Un-Noor, "Utility grid: Present challenges and their potential solutions," *IEEE Access*, vol. 6, no. October, pp. 60294–60317, 2018, doi: 10.1109/ACCESS.2018.2873615.

[17] D. Restrepo, B. Restrepo-Cuestas, and A. Trejos, "Microgrid analysis using HOMER: A case study," *DYNA*, vol. 85, no. 207, pp. 129–134, 2018, doi: 10.15446/dyna.v85n207.69375.

[18] F. Iqbal and A. S. Siddiqui, "Optimal configuration analysis for a campus microgrid—a case study," *Prot. Control Mod. Power Syst.*, vol. 2, no. 1, 2017, doi: 10.1186/s41601-017-0055-z.

[19] A. K. Sahoo, K. P. Abhitharan, A. Kalaivani, and T. J. Karthik, "Feasibility Study of Microgrid Installation in an Educational Institution with Grid Uncertainty," *Procedia*

Comput. Sci., vol. 70, pp. 550–557, 2015, doi: 10.1016/j.procs.2015.10.099.

[20] Y. V. P. Pavan Kumar and R. Bhimasingu, "Optimal sizing of microgrid for an urban community building in south India using HOMER," *2014 IEEE Int. Conf. Power Electron. Drives Energy Syst. PEDES 2014*, 2014, doi: 10.1109/PEDES.2014.7042059.

[21] S. Salisu, M. W. Mustafa, L. Olatomiwa, and O. O. Mohammed, "Assessment of technical and economic feasibility for a hybrid PV-wind-diesel-battery energy system in a remote community of north central Nigeria," *Alexandria Eng. J.*, vol. 58, no. 4, pp. 1103–1118, 2019, doi: 10.1016/j.aej.2019.09.013.

[22] Q. H. Alsafasfeh, "Performance and feasibility analysis of a grid interactive large scale wind/PV hybrid system based on smart grid methodology case study south part – Jordan," *Int. J. Renew. Energy Dev.*, vol. 4, no. 1, pp. 39–47, 2015, doi: 10.14710/ijred.4.1.39-47.

[23] D. Saheb-Koussa, M. Haddadi, and M. Belhamel, "Economic and technical study of a hybrid system (wind-photovoltaic-diesel) for rural electrification in Algeria," *Appl. Energy*, vol. 86, no. 7–8, pp. 1024–1030, 2009, doi: 10.1016/j.apenergy.2008.10.015.

[24] L. Uwineza, H. G. Kim, and C. K. Kim, "Feasibilty study of integrating the renewable energy system in Popova Island using the Monte Carlo model and HOMER," *Energy Strateg. Rev.*, vol. 33, p. 100607, 2021, doi: 10.1016/j.esr.2020.100607.

[25] A. M. Abdilahi, A. H. Mohd Yatim, M. W. Mustafa, O. T. Khalaf, A. F. Shumran, and F. Mohamed Nor, "Feasibility study of renewable energy-based microgrid system in Somaliland's urban centers," *Renew. Sustain. Energy Rev.*, vol. 40, pp. 1048–1059, 2014, doi: 10.1016/j.rser.2014.07.150.

[26] A. Hirsch, Y. Parag, and J. Guerrero, "Microgrids: A review of technologies, key drivers, and outstanding issues," *Renew. Sustain. Energy Rev.*, vol. 90, no. March, pp. 402–411, 2018, doi: 10.1016/j.rser.2018.03.040.

[27] W. Liu *et al.*, "Smart Micro-grid System with Wind/PV/Battery," *Energy Procedia*, vol. 152, pp. 1212–1217, 2018, doi: 10.1016/j.egypro.2018.09.171.

[28] N. Shirzadi, F. Nasiri, and U. Eicker, "Optimal configuration and sizing of an integrated renewable energy system for isolated and grid-connected microgrids: The case of an urban

university campus," *Energies*, vol. 13, no. 14, pp. 1–18, 2020, doi: 10.3390/en13143527.

[29] B. E. Türkay and A. Y. Telli, "Economic analysis of standalone and grid connected hybrid energy systems," *Renew. Energy*, vol. 36, no. 7, pp. 1931–1943, 2011, doi: 10.1016/j.renene.2010.12.007.

[30] K. B. Thapa, A. Maharjan, K. Kaphle, K. Joshi, and T. Aryal, "Paper Modeling of Wind-Solar Hybrid Power System for Off-Grid in Nepal and a Case Study," *J. Inst. Eng.*, vol. 15, no. 3, pp. 360–367, 2020, doi: 10.3126/jie.v15i3.32223.

[31] N. K. Roy, E. Hossain, and H. R. Pota, "Size Optimization and Sensitivity Analysis of Hybrid Wind / PV Micro-Grids- A Case Study for Bangladesh," *IEEE Access*, vol. 7, no. November, pp. 150120–150140, 2019, doi: 10.1109/ACCESS.2019.2945937.

[32] K. Sutton, S. Zaimeche, A. K. Chanderli, and L. C. Brown, "Algeria | Flag, Capital, Population, Map, & Language | Britannica," *Britannica*, Aug. 26, 2021. https://www.britannica.com/place/Algeria (accessed Nov. 26, 2021).

[33] M. Saleh, "• Algeria: forecast of the population 2020-2040 | Statista," *Statista*, Nov. 10, 2021. https://www.statista.com/statistics/1209759/forecast-of-the-population-in-algeria/ (accessed Nov. 27, 2021).

[34] Michael Hochberg, "Algeria charts a path for renewable energy sector development," 2020. https://www.mei.edu/publications/algeria-charts-path-renewable-energy-sector-development.

[35] Y. Zahraoui, M. R. Basir Khan, I. AlHamrouni, S. Mekhilef, and M. Ahmed, "Current Status, Scenario, and Prospective of Renewable Energy in Algeria: A Review," *Energies*, vol. 14, no. 9, p. 2354, 2021, doi: 10.3390/en14092354.

[36] E. Menichetti, "Support schemes in the South and East Mediterranean countries," in *Fiscal Reforms for Low Carbon Growth in the Mediterranean*, 2018, no. October, [Online]. Available: https://www.cmimarseille.org/center.

[37] E. Diamantis, P. Ferroud, and J. Barba, "Renewables In Algeria – Has The Time Come For IPPs? - Energy and Natural Resources - Algeria," *Mondaq*, 2015. https://www.mondaq.com/renewables/364170/renewables-in-algeria-has-the-time-come-

for-ipps (accessed Sep. 10, 2021).

[38] K. Abdeladim *et al.*, “Renewable Energies in Algeria : Current Situation and Perspectives,” *29th Eur. Photovolt. Sol. Energy Conf. Exhib. Renew.*, no. September, p. 2014, 2014, doi: 10.13140/2.1.1600.4808.

[39] A. B. Stambouli, “An overview of different energy sources in Algeria,” no. February, pp. 1–14, 2011.

[40] World Bank Group, “Global Solar Atlas,” *GLOBAL SOLAR ATLAS*, Oct. 2019. https://globalsolaratlas.info/download/algeria (accessed Nov. 27, 2021).

[41] L. Hammar, “Wind and Solar Energy Resources in Tanzania and Mozambique,” 2011.

[42] L. Hadji, “How is 100 % Renewable Energy Possible for Algeria by 2030 ? Table of Contents,” no. 619, 2016.

[43] A. Boudghene Stambouli, “Algerian renewable energy assessment: The challenge of sustainability,” *Energy Policy*, vol. 39, no. 8, pp. 4507–4519, 2011, doi: 10.1016/j.enpol.2010.10.005.

[44] Y. Zahraoui, M. R. Basir Khan, I. Alhamrouni, S. Mekhilef, and M. Ahmed, “Current status, scenario, and prospective of renewable energy in algeria: A review,” *Energies*, vol. 14, no. 9, 2021, doi: 10.3390/en14092354.

[45] H. Saibi, “Geothermal resources in Algeria,” *Renew. Sustain. Energy Rev.*, vol. 13, no. 9, pp. 2544–2552, 2015, doi: 10.1016/j.rser.2009.06.019.

[46] Y. J. Ma, M. Yu, and X. S. Zhou, “The research on the current situation of Micro-grid,” *Adv. Mater. Res.*, vol. 940, pp. 329–332, 2014, doi: 10.4028/www.scientific.net/AMR.940.329.

[47] D. T. Ton and M. A. Smith, “The U.S. Department of Energy’s Microgrid Initiative,” *Electr. J.*, vol. 25, no. 8, pp. 84–94, 2012, doi: 10.1016/j.tej.2012.09.013.

[48] D. J. Becker and D. A. Kwasinski, “WHAT IS A MICRO-GRID ?,” 2014, [Online]. Available: https://www.psma.com/sites/default/files/uploads/tech-forums-energy-efficiency/presentations/is201-what-micro-grid.pdf.

[49] L. Fusheng, L. Ruisheng, and Z. Fengquan, *Microgrid technology and engineering application*. 2015.

[50] A. N. Akpolat and E. Dursun, "From Microgrid to Smart Grid: A Review of Campus Project," *Int. Eng. Sci. Educ. Conf.*, no. December, pp. 379–386, 2016.

[51] Q. LI, Z. XU, and L. YANG, "Recent advancements on the development of microgrids," *J. Mod. Power Syst. Clean Energy*, vol. 2, no. 3, pp. 206–211, 2014, doi: 10.1007/s40565-014-0069-8.

[52] A. Ali, W. Li, R. Hussain, X. He, B. W. Williams, and A. H. Memon, "Overview of current microgrid policies, incentives and barriers in the European Union, United States and China," *Sustain.*, vol. 9, no. 7, 2017, doi: 10.3390/su9071146.

[53] J. Delony, "5 Prospects for Renewable Microgrid Technology Innovation - Renewable Energy World," *Renewable Energy World*, 2017. https://www.renewableenergyworld.com/storage/5-prospects-for-renewable-microgrid-technology-innovation/#gref (accessed Oct. 04, 2021).

[54] Advanced Energy Centre, "Future of Microgrids & Smart Energy Networks," *Carlet. Sustain. Energy Res. Cent. CSERC*, no. December, pp. 1–7, 2015.

[55] M. Grimley and J. Farrell, "Mighty Microgrids," *ILSR's Energy Democr. Initiat.*, no. March, p. 38, 2016, [Online]. Available: https://ilsr.org/wp-content/uploads/downloads/2016/03/Report-Mighty-Microgrids-PDF-3_3_16.pdf.

[56] M. Carpintero-Rentería, D. Santos-Martín, and J. M. Guerrero, "Microgrids literature review through a layers structure," *Energies*, vol. 12, no. 22, pp. 1–22, 2019, doi: 10.3390/en12224381.

[57] T. Considine, W. Cox, and E. G. Cazalet, "Understanding Microgrids as the Essential Architecture of Smart Energy," *Autom. Diagnostics Anal. Build.*, pp. 345–357, 2021, doi: 10.1201/9781003151906-32.

[58] L. Mariam, M. Basu, and M. F. Conlon, "A Review of Existing Microgrid Architectures," *J. Eng. (United Kingdom)*, vol. 2013, 2013, doi: 10.1155/2013/937614.

[59] H. Laaksonen and K. Kauhaniemi, “Microgrid – Network Concept of the Future,” no. July 2008, 2008.

[60] F. Sioshansi, “Microgrids: from niche to $100 billion market,” *Energy Post*, Feb. 05, 2018. https://energypost.eu/microgrids-from-niche-to-mainstream/ (accessed Nov. 29, 2021).

[61] T. H. E. Environmentaleconomical, B. Of, and T. H. E. Microgrid, “IEEE may/june 2008,” no. june, pp. 54–65, 2008.

[62] G. Mohy-ud-din, K. Muttaqi, and D. Sutanto, *Variability, Scalability and Stability of Microgrids*, no. July. 2019.

[63] Asian Development Bank, *Handbook on Microgrids for Power Quality and Connectivity*, no. July. 2020.

[64] A. A. Irizarry, J. A. Colucci, and E. O’Neill, “Chapter 5 Solar Photovoltaics,” *Achievable Renew. Energy Targets*, pp. 1–96, 2014, [Online]. Available: https://www.uprm.edu/aret/docs/Ch_5_PV_systems.pdf.

[65] V. C. Thomas, “Photovoltaic (PV) Tutorial - MIT,” *PDF4PRO*, 2017. https://pdf4pro.com/view/photovoltaic-pv-tutorial-mit-5ca8a9.html (accessed Nov. 29, 2021).

[66] S. Muhammad Lawan and W. Azlan Wan Zainal Abidin, “A Review of Hybrid Renewable Energy Systems Based on Wind and Solar Energy: Modeling, Design and Optimization,” *Wind Sol. Hybrid Renew. Energy Syst.*, 2020, doi: 10.5772/intechopen.85838.

[67] M. Bin Murtaza, “Solar Electric Photovoltaic Modules | Single Axis Solar Tracking System For Low Power Application,” Feb. 27, 2012. https://singledualaxis.blogspot.com/2012/02/solar-electric-photovoltaic-modules.html (accessed Nov. 29, 2021).

[68] B. Afework, J. Hanania, K. Stenhouse, B. Yyelland, and J. Donev, “Types of photovoltaic cells - Energy Education,” *Energy Education*, 2018. https://energyeducation.ca/encyclopedia/Types_of_photovoltaic_cells (accessed Oct. 04,

2021).

[69] A. Mohammad Bagher, “Types of Solar Cells and Application,” *Am. J. Opt. Photonics*, vol. 3, no. 5, p. 94, 2015, doi: 10.11648/j.ajop.20150305.17.

[70] F. Sohrabi, A. Nikniazi, and H. Movla, “Optimization of Third Generation Nanostructured Silicon- Based Solar Cells,” *Sol. Cells - Res. Appl. Perspect.*, Mar. 2013, doi: 10.5772/51616.

[71] S. Padmanaban, K. Nithiyananthan, S. P. Karthikeyan, and J. B. Holm-Nielsen, *MICROGRIDS*, First edit. CRC Press, 2021.

[72] B. L. Oliva-Chatelain and A. R. Barron, “An Introduction to Solar Cell Technology,” 2011. https://cnx.org/contents/3QU3ovtd@1/An-Introduction-to-Solar-Cell-Technology (accessed Nov. 29, 2021).

[73] A. Han, “Efficiency Of Solar PV, Then, Now And Future,” *Lafayette College site*, 2014. https://sites.lafayette.edu/egrs352-sp14-pv/technology/history-of-pv-technology/ (accessed Aug. 13, 2021).

[74] M. Boxwell, *Solar Electricity Handbook – 2019 Edition: A simple, practical guide to solar energy – designing and installing solar photovoltaic systems.*, 2019 Editi. Greenstream Publishing, 2019.

[75] D. Sinha, A. B. Das, D. K. Dhak, and P. K. Sadhu, “Equivalent circuit configuration for solar PV cell,” *Proc. 2014 1st Int. Conf. Non Conv. Energy Search Clean Safe Energy, ICONCE 2014*, no. April 2018, pp. 58–60, 2014, doi: 10.1109/ICONCE.2014.6808682.

[76] M. H. El-Ahmar, A. H. M. El-Sayed, and A. M. Hemeida, “Mathematical modeling of Photovoltaic module and evalute the effect of varoius paramenters on its performance,” *2016 18th Int. Middle-East Power Syst. Conf. MEPCON 2016 - Proc.*, no. January 2018, pp. 741–746, 2017, doi: 10.1109/MEPCON.2016.7836976.

[77] S. T. Bahta, “Design and Analyzing of an Off-Grid Hybrid Renewable Energy System to Supply Electricity for Rural Areas,” 2013.

[78] M. R. Patel and O. Beik, *Wind and Solar Power Systems: Design, Analysis, and*

Operation, Third edit. CRC Press, 2021.

[79] D. K. Sharma and G. Purohit, “Analysis of the Effect of Fill Factor on the Efficiency of Solar Pv System for Improved Design of Mppt,” no. November, pp. 1281–1282, 2014.

[80] S. Sheik Mohammed and D. Devaraj, “Fuzzy based maximum power point tracking controller for stand alone photovoltaic system using MATLAB/Simulink,” *Int. J. Appl. Eng. Res.*, vol. 10, no. 55, pp. 3101–3106, 2015.

[81] M. S.Sheik and D. Devaraj, “System with Boost Converter using,” *IEE Int. Conf. Circuit, Power Comput. Technol.*, no. August, pp. 814–821, 2014.

[82] A. K. Daud and M. S. Ismail, “Design of isolated hybrid systems minimizing costs and pollutant emissions,” *Renew. Energy*, vol. 44, pp. 215–224, 2012, doi: 10.1016/j.renene.2012.01.011.

[83] Stephen A. Roosa, *Fundamentals of Microgrids Development and Implementation*. 2021.

[84] WES - Wind Energy Solutions, “How many blades are best for wind energy production? - WES, Wind Energy Solutions,” *WES - Wind Energy Solutions*, May 29, 2019. https://windenergysolutions.nl/news/how-many-blades/ (accessed Nov. 29, 2021).

[85] F. Oral, I. S. Ekmekçi, and N. Onat, “Weibull distribution for determination of wind analysis and energy production,” *World J. Eng.*, vol. 12, no. 3, pp. 215–220, 2015, doi: 10.1260/1708-5284.12.3.215.

[86] S. Diaf *et al.*, “A methodology for optimal sizing of autonomous hybrid PV / wind system To cite this version,” *Energy Policy*, vol. 35, pp. 5708–5718, 2007.

[87] J. F. Manwell, J. G. McGowan, and A. L. Rogers, *Wind Energy Explained: Theory, Design and Application*, Second edi. John Wiley & Sons Ltd, 2010.

[88] J. S. pdfu. Libii Njock, “Comparing the calculated coefficients of performance of a class of wind turbines that produce power between 330 kw and 7,500 kw,” *World Trans. Eng. Technol. Educ.*, vol. 11, no. 1, pp. 36–40, 2013.

[89] A. Kaabeche, M. Belhamel, and R. Ibtiouen, “Optimal sizing method for stand-alone hybrid PV / wind power generation system,” *Rev. des Energies Renouvelables SMEE’10*

Bou Ismail Tipaza, no. January 2010, pp. 205–213, 2010, [Online]. Available: http://www.cder.dz/download/smee2010_22.pdf.

[90] F. Ahmad and M. S. Alam, "Optimal Sizing and Analysis of Solar PV, Wind, and Energy Storage Hybrid System for Campus Microgrid," *Smart Sci.*, vol. 6, no. 2, pp. 150–157, 2018, doi: 10.1080/23080477.2017.1417005.

[91] H. Nazaripouya, Y.-W. Chung, and A. Akhil, "Energy Storage in Microgrids: Challenges, Applications and Research Need," *Int. J. Energy Smart Grid*, vol. 3, no. 2, pp. 60–70, 2019, doi: 10.23884/ijesg.2018.3.2.02.

[92] B. Dunn, H. Kamath, and J. M. Tarascon, "Electrical energy storage for the grid: A battery of choices," *Science (80-.).*, vol. 334, no. 6058, pp. 928–935, 2011, doi: 10.1126/science.1212741.

[93] A. Jain and R. Mishra, "Changes & challenges in smart grid towards smarter grid," *Int. Conf. Electr. Power Energy Syst. ICEPES 2016*, no. December 2016, pp. 62–67, 2017, doi: 10.1109/ICEPES.2016.7915907.

[94] B. Bossoufi, M. Lamnadi, M. Trihi, and A. Boulezhar, "Optimal design of stand-alone hybrid power system using wind and solar energy sources," *Int. J. Energy Technol. Policy*, vol. 15, no. 2/3, p. 280, 2019, doi: 10.1504/ijetp.2019.10019646.

[95] X. Zhou, T. Guo, and Y. Ma, "An overview on microgrid technology," *2015 IEEE Int. Conf. Mechatronics Autom. ICMA 2015*, no. 5, pp. 76–81, 2015, doi: 10.1109/ICMA.2015.7237460.

[96] A. Kwasinski, "EE394J10 DG Grid Interconnection | PDF," *Scribd*, 2012. https://www.scribd.com/doc/218984487/EE394J10-DG-Grid-Interconnection (accessed Nov. 29, 2021).

[97] Canyon Hydro *et al.*, "We are IntechOpen , the world ' s leading publisher of Open Access books Built by scientists , for scientists TOP 1 %," *Intech*, vol. 32, no. July, pp. 137–144, 2013, [Online]. Available: http://www.intechopen.com/books/trends-in-telecommunications-technologies/gps-total-electron-content-tec- prediction-at-ionosphere-layer-over-the-equatorial-region%0AInTec%0Ahttp://www.asociatiamhc.ro/wp-

content/uploads/2013/11/Guide-to-Hydropower.pdf.

[98] H. S. H. Chung, H. Wang, F. Blaabjerg, and M. Pecht, "Reliability of power electronic converter systems," *Reliab. Power Electron. Convert. Syst.*, no. December, pp. 1–490, 2016, doi: 10.1049/PBPO080E.

[99] D. Guilbert, B. Yodwong, W. Kaewmanee, and M. Phattanasak, "Power converters for hybrid renewable energy systems with hydrogen buffer storage: A short review," *6th IEEE Int. Conf. Smart Grid, icSmartGrids 2018*, pp. 28–33, 2019, doi: 10.1109/ISGWCP.2018.8634562.

[100] H. Bevrani, B. Francois, and T. Ise, *Microgrid Dynamics and Control*. 2017.

[101] C. Spiegel, "Power Electronics for Renewable Energy Systems," May 22, 2018. https://www.fuelcellstore.com/blog-section/power-electronics-for-renewable-energy-systems (accessed Nov. 29, 2021).

[102] A. Baghbany Oskouei, M. R. Banaei, and M. Sabahi, "Hybrid PV/wind system with quinary asymmetric inverter without increasing DC-link number," *Ain Shams Eng. J.*, vol. 7, no. 2, pp. 579–592, 2016, doi: 10.1016/j.asej.2015.06.008.

[103] P. A. Ashiq, P. H. Anand, A. Suvarnan, L. Krishna, and R. T. Paul, "Hybrid Inverter With Solar Battery Charging," no. May, pp. 1–7, 2020.

[104] M. Nurunnabi, N. K. Roy, and H. R. Pota, "Optimal sizing of grid-tied hybrid renewable energy systems considering inverter to PV ratio - A case study," *J. Renew. Sustain. Energy*, vol. 11, no. 1, 2019, doi: 10.1063/1.5052492.

[105] B. Sivaiah, "Single-Stage Three-Level Isolated AC / DC PFC Converter For High DC-Link Applications," no. 4, pp. 4906–4910, 2016.

[106] S Dr. T. Devaraju, "Lecture Notes on Power Electronics," *Writing*, pp. 1–23, 2003.

[107] S. Rakesh, "Power Electronics Digital Notes," vol. 2, 2015.

[108] Sofia Verigou, "Optimal Sizing of a Microgrid Including Renewable Energy Sources Copyright © 2018 By Sofia Verigou Optimal Sizing of a Microgrid," 2018.

[109] Litos Strategic Communication, "The smart grid: An introduction," *Smart Grid Electr.*

Power Transm., pp. 1–45, 2011, doi: 10.1002/9781119521129.ch15.

[110] M.-C. ALVAREZ, R. CAIRE, and B. RAISON, *SmartGrids*. ISTE Ltd and John Wiley & Sons, Inc, 2012.

[111] C. W. Gellings, "What is the Smart Grid?," *Smart Grid Plan. Implement.*, no. February, pp. 1–33, 2021, doi: 10.1201/9781003151968-1.

[112] M. Krishna Paramathma, D. Devaraj, and R. Malaikannan, "Development of real time monitoring system under smart grid environment," *ARPN J. Eng. Appl. Sci.*, vol. 10, no. 5, pp. 2177–2181, 2015.

[113] C. Hu, S. Luo, Z. Li, X. Wang, and L. Sun, "Energy coordinative optimization of wind-storage-load microgrids based on short-term prediction," *Energies*, vol. 8, no. 2, pp. 1505–1528, 2015, doi: 10.3390/en8021505.

[114] Y. Li *et al.*, "Optimal operation of multimicrogrids via cooperative energy and reserve scheduling," *IEEE Trans. Ind. Informatics*, vol. 14, no. 8, pp. 3459–3468, 2018, doi: 10.1109/TII.2018.2792441.

[115] G. Li, D. Wu, J. Hu, Y. Li, M. S. Hossain, and A. Ghoneim, "HELOS: Heterogeneous load scheduling for electric vehicle-integrated microgrids," *IEEE Trans. Veh. Technol.*, vol. 66, no. 7, pp. 5785–5796, 2017, doi: 10.1109/TVT.2016.2636874.

[116] J. Wang, L. M. Costa, and B. M. Cisse, "From distribution feeder to microgrid: An insight on opportunities and challenges," *2016 IEEE Int. Conf. Power Syst. Technol. POWERCON 2016*, 2016, doi: 10.1109/POWERCON.2016.7753897.

[117] S. Guo, H. Zhao, and H. Zhao, "The most economical mode of power supply for remote and less developed areas in China: Power grid extension or micro-grid?," *Sustain.*, vol. 9, no. 6, 2017, doi: 10.3390/su9060910.

[118] V. Motjoadi, P. N. Bokoro, and M. O. Onibonoje, "A review of microgrid-based approach to rural electrification in South Africa: Architecture and policy framework," *Energies*, vol. 13, no. 9, pp. 1–22, 2020, doi: 10.3390/en13092193.

[119] Q. Fu, A. Nasiri, A. Solanki, A. Bani-Ahmed, L. Weber, and V. Bhavaraju, "Microgrids:

Architectures, Controls, Protection, and Demonstration," *Electr. Power Components Syst.*, vol. 43, no. 12, pp. 1453–1465, 2015, doi: 10.1080/15325008.2015.1039098.

[120] D. Semenov, G. Mirzaeva, C. D. Townsend, and G. C. Goodwin, "Recent development in AC microgrid control-A survey," *2017 Australas. Univ. Power Eng. Conf. AUPEC 2017*, vol. 2017-Novem, no. November, pp. 1–6, 2018, doi: 10.1109/AUPEC.2017.8282457.

[121] M. Saad, B. Arif, and M. A. Hasan, *2 - Microgrid architecture, control, and operation*. Elsevier Ltd, 2018.

[122] H. Shayeghi and A. Younesi, *Microgrid Architectures, Control and Protection Methods*, no. January. 2020.

[123] H. Pan, M. Ding, A. Chen, R. Bi, L. Sun, and S. Shi, "Research on distributed power capacity and site optimization planning of AC/DC hybrid micrograms considering line factors," *Energies*, vol. 11, no. 8, pp. 1–18, 2018, doi: 10.3390/en11081930.

[124] S. Save, "Optimization of Hybrid Micro-Grids," CALIFORNIA STATE UNIVERSITY NORTHRIDGE, 2018.

[125] P. Kumar, R. Pukale, N. Kumabhar, and U. Patil, "Optimal Design Configuration Using HOMER," *Procedia Technol.*, vol. 24, pp. 499–504, 2016, doi: 10.1016/j.protcy.2016.05.085.

[126] R. Fu *et al.*, "HOMER (Hybrid Optimization of Multiple Electric Renewables). Core capabilities," no. November, pp. 1–5, 2018.

[127] P. Lilienthal, "Rural Electrification Models and Costs - Homer Energy," *SlideShare*, 2015. https://www.slideshare.net/sustenergy/rural-electrification-models-and-costs (accessed Sep. 03, 2021).

[128] A. Levchenko, "Seasons in Algeria: Weather and Climate," *Seasons of the Year*, 2021. https://seasonsyear.com/Algeria (accessed Sep. 11, 2021).

[129] M. Morad, M. Nayel, A. A. Elbaset, and A. I. A. Galal, "Sizing and Analysis of Grid-Connected Microgrid System for Assiut University Using HOMER Software," *2018 20th Int. Middle East Power Syst. Conf. MEPCON 2018 - Proc.*, no. 1, pp. 694–699, 2019, doi:

10.1109/MEPCON.2018.8635166.

[130] O. Hafez and K. Bhattacharya, “Optimal planning and design of a renewable energy based supply system for microgrids,” *Renew. Energy*, vol. 45, pp. 7–15, 2012, doi: 10.1016/j.renene.2012.01.087.

[131] H. Rezk, M. A. Abdelkareem, and C. Ghenai, “Performance evaluation and optimal design of stand-alone solar PV-battery system for irrigation in isolated regions: A case study in Al Minya (Egypt),” *Sustain. Energy Technol. Assessments*, vol. 36, no. May, p. 100556, 2019, doi: 10.1016/j.seta.2019.100556.

7 Appendix

7.1 Appendix A

A.1: Summary of electrical appliances used to estimate the Faculty of Technology's daily electric load for the months of the winter season

1. Department lecture rooms loads

Winter months							
Category	**Load**	**Number of load**	**Rated Capacity (w)**	**Operation duration (Hrs/day)**	**Operation Hours (Hrs)**	**AC Load KWh/day**	**Electrical power demand (kW)**
Departments							
Dept. of ArchEng	CIR	120	132	9:00-16:00	7	110.88	15.84
	CFL	160	13	8:00-17:00	9	18.72	2.08
	Projector	8	10	9:00-16:00	7	0.56	0.08
Dept. of EEE	CIR	44	132	9:00-16:00	7	40.656	5.808
	CFL	44	13	8:00-17:00	9	5.148	0.572
	Projector	6	10	9:00-16:00	7	0.42	0.06
Dept. of BMedEng	CIR	120	132	9:00-16:00	7	110.88	15.84
	CFL	144	13	8:00-17:00	9	16.848	1.872
	Projector	6	10	9:00-16:00	7	0.42	0.06
Dept. of TelcomEng	CIR	72	132	9:00-16:00	7	66.528	9.504
	CFL	96	13	8:00-17:00	9	11.232	1.248
	Projector	7	10	9:00-16:00	7	0.49	0.07
	Lab computers	200	120	9:00-12:00	3	72	24
Dept. of CivEng	CIR	96	132	9:00-16:00	7	88.704	12.672
	CFL	128	13	8:00-17:00	9	14.976	1.664
	Projector	6	10	9:00-16:00	7	0.42	0.06
Dept. of Hydraulics	CIR	54	132	9:00-16:00	7	49.896	7.128
	CFL	54	13	8:00-17:00	9	6.318	0.702
	Projector	5	10	9:00-16:00	7	0.35	0.05
Dept. of MechEng	CIR	60	132	9:00-16:00	7	55.44	7.92
	CFL	60	13	8:00-17:00	9	7.02	0.78
	Projector	5	10	9:00-16:00	7	0.35	0.05

2. Office loads

Winter months							
Category	**Load**	**Number of load**	**Rated Capacity (w)**	**Operation duration (Hrs/day)**	**Operation Hours (Hrs)**	**AC Load KWh/day**	**Electrical power demand (kW)**
Offices							
Dean's office including including offices for Vice dean incharge of Pedagogy and student issues, and vice dean incharge of post graduation, research and external relations (3 offices)	CIR	6	132	9:00-16:00	7	5.544	0.792
	2 lamp FL	9	32	8:00-17:00	9	2.592	0.288
	Desktop Computer	6	120	14:00-16:00	2	1.44	0.72
	Printer	5	50	12:00-13:00	1	0.25	0.25
Assistance vice dean office in charge of pedagogy and student issues including offices for Head of education department, Head of teaching department & evaluation, and Head of statistics & student internships (4 offices)	CIR	8	132	9:00-16:00	7	7.392	1.056
	2 lamp FL	8	32	8:00-17:00	9	2.304	0.256
	Desktop Computer	8	120	14:00-16:00	2	1.92	0.96
	Printer	5	50	12:00-13:00	1	0.25	0.25
Assistance vice dean office in charge of research and external relations and offices for Head of cooperations & foreign relations, Research activities department and Training follow up service for post graduation, Training follow up service for post graduation (4).	CIR	8	132	9:00-16:00	7	7.392	1.056
	2 lamp FL	8	32	8:00-17:00	9	2.304	0.256
	Desktop Computer	8	120	14:00-16:00	2	1.92	0.96
	Printer	5	50	12:00-13:00	1	0.25	0.25
Genaral Secretary office including offices for Personnel department, Budget & accounting, Animation service: Scientific, cultural & sporting, Service of maintenance, and Internal security service (6)	CIR	12	132	9:00-16:00	7	11.088	1.584
	2 lamp FL	12	32	8:00-17:00	9	3.456	0.384
	Desktop Computer	7	120	14:00-16:00	2	1.68	0.84
	Printer	6	50	12:00-13:00	1	0.3	0.3
Head of Arch. Dept. office including offices for Deputy head of Arch. Dept., Chairman of Scientific Committee Arch. Dept, Arch.Dept License Manager, and Arch.Dept Masters Manager (5)	CIR	10	132	9:00-16:00	7	9.24	1.32
	2 lamp FL	10	32	8:00-17:00	9	2.88	0.32
	Desktop Computer	5	120	14:00-16:00	2	1.2	0.6
	Printer	5	50	12:00-13:00	1	0.25	0.25
Head of Bmed. Dept. office including Deputy head of Bmed. Dept., Chairman of Scientific Committee BMed. Dept., BMed.Dept License Managers - 2 managers, and BMed.Dept Masters Managers - 3managers (8)	CIR	16	132	9:00-16:00	7	14.784	2.112
	2 lamp FL	16	32	8:00-17:00	9	4.608	0.512
	Desktop Computer	8	120	14:00-16:00	2	1.92	0.96
	Printer	8	50	12:00-13:00	1	0.4	0.4
Head of Civ.Dept. office including Deputy Head of Civ.Dept., Chairman of Scientific Committee Civ.Dept., Civ.Dept License Manager, and Civ.Dept Masters Managers - 5 mangers (9)	CIR	18	132	9:00-16:00	7	16.632	2.376
	2 lamp FL	18	32	8:00-17:00	9	5.184	0.576
	Desktop Computer	9	120	14:00-16:00	2	2.16	1.08
	Printer	9	50	12:00-13:00	1	0.45	0.45
Head of EEE Dept. office including offices for Deputy Head of EEE.Dept., Chairman of Scientific Committee EEE.Dept., EEE.Dept License Managers - 4 managers, and EEE.Dept Masters Managers - 6 managers (13)	CIR	26	132	9:00-16:00	7	24.024	3.432
	2 lamp FL	26	32	8:00-17:00	9	7.488	0.832
	Desktop Computer	13	120	14:00-16:00	2	3.12	1.56
	Printer	13	50	12:00-13:00	1	0.65	0.65
Head of Telcom.Dept. office including offices for Deputy Head of Telcom.Dept., Chairman of Scientific Committee Telcom.Dept., Telcom.Dept License Manager, and Telcom.Dept Masters Managers - 2 managers (6)	CIR	12	132	9:00-16:00	7	11.088	1.584
	2 lamp FL	12	32	8:00-17:00	9	3.456	0.384
	Desktop Computer or PCs	6	120	14:00-16:00	2	1.44	0.72
	Printer	6	50	12:00-13:00	1	0.3	0.3
Head of Hydraulics.Dept. office including offices Deputy Head of Hydraulic.Dept., Chairman of Scientific Committee Hydraulics.Dept., Hydraulics.Dept License Manager, and Hydraulics.Dept Managers Managers - 2 managers (6)	CIR	12	132	9:00-16:00	7	11.088	1.584
	2 lampFL	12	32	8:00-17:00	9	3.456	0.384
	Desktop Computer	6	120	14:00-16:00	2	1.44	0.72
	Printer	6	50	12:00-13:00	1	0.3	0.3
Head of Mech.Dept. office including offices for Deputy Head of Mech.Dept., Chairman of Scientific Committee Mech.Dept., Mech.Dept License Managers - 4 managers, Mech.Dept Masters Manager - 2 mangers (9).	CIR	18	132	9:00-16:00	7	16.632	2.376
	2 lamp FL	18	32	8:00-17:00	9	5.184	0.576
	Desktop Computer	9	120	14:00-16:00	2	2.16	1.08
	Printer	9	50	12:00-13:00	1	0.45	0.45

3. Library, outdoor lighting, PAUWES, kitchen, and personal gadgets loads

Winter months							
Category	**Load**	**Number of load**	**Rated Capacity (w)**	**Operation duration (Hrs/day)**	**Operation Hours (Hrs)**	**AC Load KWh/day**	**Electrical power demand (kW)**
Library, outdoor lighting, PAUWES, kitchen, and personal gadgets loads							
	CIR	20	132	9:00-16:00	7	18.48	2.64
	CFL	30	13	8:00-17:00	9	3.51	0.39
	LED lamps	15	9	8:00-17:00	9	1.215	0.135
	T6 lamp FL	12	86	8:00-17:00	9	9.288	1.032
	Printer	4	50	12:00-13:00	1	0.2	0.2
Library load	Desktop computer	12	120	14:00-16:00	2	2.88	1.44
	Three headed outdoor street lamps	20	100	19:00-7:00	12	24	2
	Polycarbonate outdoor post latern with frosted acrylic glass, black	25	100	19:00-7:00	12	30	2.5
	LED round gate light	30	7	19:00-7:00	12	2.52	0.21
	LED road lamps	40	20	19:00-7:00	12	9.6	0.8
Outdoor lighting	LED outdoor street lights	45	60	19:00-7:00	12	32.4	2.7
	CIR	22	132	9:00-16:00	7	20.328	2.904
	CFL	66	13	8:00-17:00	9	7.722	0.858
	Projectors	5	10	9:00-16:00	7	0.35	0.05
	2 lamp FL	20	32	8:00-17:00	9	5.76	0.64
	Desktop Computer or PC	10	120	14:00-16:00	2	2.4	1.2
	Printer	3	50	12:00-13:00	1	0.15	0.15
	Electric stove	1	1800	10:00-12:00	2	3.6	1.8
	Oven	1	1250	12:00-14:00	2	2.5	1.25
	Coffee maker	1	900	9:00-10:00	1	0.9	0.9
	Dish washer	1	900	9:00-10:00	1	0.9	0.9
	Blender	1	600	11:00-12:00	1	0.6	0.6
	Food processor	1	600	11:00-12:00	1	0.6	0.6
	Multicooker	1	500	11:00-12:00	1	0.5	0.5
PAUWES building load	Water boiler	1	1500	9:00-10:00	1	1.5	1.5
	Electric stove	1	9000	7:00-10:00	3	27	9
	Dish washer	2	1000	7:00-8:00	1	2	2
	Bread Baking oven machines	1	15000	6:00-8:00	2	30	15
	Electric fryer	2	5000	8:00-9:00	1	10	10
	Steam oven	4	1000	8:00-11:00	3	12	4
	Freezers	10	500	6:00-12:00	6	30	5
The kitchen appliances	CFL	20	13	6:00-12:00	6	1.56	0.26
	Phones	200	4	9:00-19:00	10	8	0.8
Estimated personal gadgets	Laptops	200	50	9:00-19:00	10	100	10

A.2: Summary of electrical appliances used to estimate the Faculty of Technology's daily electricity load for the months of spring and autumn seasons

1. Department lecture rooms loads

Spring and Autumn months							
Category	**Load**	**Number of load**	**Rated Capacity (w)**	**Operation duration (Hrs/day)**	**Operation Hours (Hrs)**	**AC Load KWh/day**	**Electrical power demand (kW)**
Departments							
	CFL	160	13	8:00-17:00	9	18.72	2.08
Dept. of ArchEng	Projector	8	10	9:00-16:00	7	0.56	0.08
	CFL	44	13	8:00-17:00	9	5.148	0.572
Dept. of EEE	Projector	6	10	9:00-16:00	7	0.42	0.06
	CFL	144	13	8:00-17:00	9	16.848	1.872
Dept. of BMedEng	Projector	6	10	9:00-16:00	7	0.42	0.06
	CFL	96	13	8:00-17:00	9	11.232	1.248
	Projector	7	10	9:00-16:00	7	0.49	0.07
Dept. of TelcomEng	Computer lab	200	120	9:00-12:00	3	72	24
	CFL	128	13	8:00-17:00	9	14.976	1.664
Dept. if CivEng	Projector	6	10	9:00-16:00	7	0.42	0.06
	CFL	54	13	8:00-17:00	9	6.318	0.702
Dept. of Hydraulics	Projector	5	10	9:00-16:00	7	0.35	0.05
	CFL	60	13	8:00-17:00	9	7.02	0.78
Dept. of MechEng	Projector	5	10	9:00-16:00	7	0.35	0.05

2. Office loads

Spring and Autumn months							
Category	**Load**	**Number of load**	**Rated Capacity (w)**	**Operation duration (Hrs/day)**	**Operation Hours (Hrs)**	**AC Load KWh/day**	**Electrical power demand (kW)**
Offices							
Dean's office including including offices for Vice dean incharge of Pedagogy and student issues, and vice dean incharge of post graduation, research and external relations (3 offices)	2 lamp FL	9	32	8:00-17:00	9	2.592	0.288
	Desktop Computer	6	120	14:00-16:00	2	1.44	0.72
	Printer	5	50	12:00-13:00	1	0.25	0.25
Assistance vice dean office in charge of pedagogy and student issues including offices for Head of education department, Head of teaching department & evaluation, and Head of statistics & student internships (4 offices)	2 lamp FL	8	32	8:00-17:00	9	2.304	0.256
	Desktop Computer	8	120	14:00-16:00	2	1.92	0.96
	Printer	5	50	12:00-13:00	1	0.25	0.25
Assistance vice dean office in charge of research and external relations and offices for Head of cooperations & foreign relations, Research activities department and Training follow up service for post graduation, Training follow up service for post graduation (4).	2 lamp FL	8	32	8:00-17:00	9	2.304	0.256
	Desktop Computer	8	120	14:00-16:00	2	1.92	0.96
	Printer	5	50	12:00-13:00	1	0.25	0.25
Genaral Secretary office including offices for Personnel department, Budget & accounting, Animation service: Scientific, cultural & sporting, Service of maintenance, and Internal security service (6)	2 lamp FL	12	32	8:00-17:00	9	3.456	0.384
	Desktop Computer	7	120	14:00-16:00	2	1.68	0.84
	Printer	6	50	12:00-13:00	1	0.3	0.3
Head of Arch. Dept. office including offices for Deputy head of Arch. Dept., Chairman of Scientific Committee Arch. Dept, Arch.Dept License Manager, and Arch.Dept Masters Manager (5)	2 lamp FL	10	32	8:00-17:00	9	2.88	0.32
	Desktop Computer	5	120	14:00-16:00	2	1.2	0.6
	Printer	5	50	12:00-13:00	1	0.25	0.25
Head of Bmed. Dept. office including Deputy head of Bmed. Dept., Chairman of Scientific Committee BMed. Dept., BMed.Dept License Managers - 2 managers, and BMed.Dept Masters Managers - 3managers (8)	2 lamp FL	16	32	8:00-17:00	9	4.608	0.512
	Desktop Computer	8	120	14:00-16:00	2	1.92	0.96
	Printer	8	50	12:00-13:00	1	0.4	0.4
Head of Civ.Dept. office including Deputy Head of Civ.Dept., Chairman of Scientific Committee Civ.Dept., Civ.Dept License Manager, and Civ.Dept Masters Managers - 5 mangers (9)	2 lamp FL	18	32	8:00-17:00	9	5.184	0.576
	Desktop Computer	9	120	14:00-16:00	2	2.16	1.08
	Printer	9	50	12:00-13:00	1	0.45	0.45
Head of EEE Dept. office including offices for Deputy Head of EEE.Dept., Chairman of Scientific Committee EEE.Dept., EEE.Dept License Managers - 4 managers, and EEE.Dept Masters Managers - 6 managers (13)	2 lamp FL	26	32	8:00-17:00	9	7.488	0.832
	Desktop Computer	13	120	14:00-16:00	2	3.12	1.56
	Printer	13	50	12:00-13:00	1	0.65	0.65
Head of Telcom.Dept. office including offices for Deputy Head of Telcom.Dept., Chairman of Scientific Committee Telcom.Dept., Telcom.Dept License Manager, and Telcom.Dept Masters Managers - 2	2 lamp FL	12	32	8:00-17:00	9	3.456	0.384
	Desktop Computer or PCs	6	120	14:00-16:00	2	1.44	0.72
	Printer	6	50	12:00-13:00	1	0.3	0.3
Head of Hydraulics.Dept. office including offices Deputy Head of Hydraulic.Dept., Chairman of Scientific Committee Hydraulics.Dept., Hydraulics.Dept License Manager, and Hydraulics.Dept Managers	2 lampFL	12	32	8:00-17:00	9	3.456	0.384
	Desktop Computer	6	120	14:00-16:00	2	1.44	0.72
	Printer	6	50	12:00-13:00	1	0.3	0.3
Mech.Dept., Chairman of Scientific Committee Mech.Dept., Mech.Dept License Managers - 4 managers, Mech.Dept Masters Manager - 2 mangers (9).	2 lamp FL	18	32	8:00-17:00	9	5.184	0.576
	Desktop Computer	9	120	14:00-16:00	2	2.16	1.08
	Printer	9	50	12:00-13:00	1	0.45	0.45

3. Library, outdoor lighting, PAUWES, kitchen, and personal gadgets loads

Spring and Autumn months							
Category	**Load**	**Number of load**	**Rated Capacity (w)**	**Operation duration (Hrs/day)**	**Operation Hours (Hrs)**	**AC Load KWh/day**	**Electrical power demand (kW)**
Library, outdoor lighting, PAUWES, kitchen, and personal gadgets loads							
	CFL	30	13	8:00-17:00	9	3.51	0.39
	LED lamps	15	9	8:00-17:00	9	1.215	0.135
	T6 lamp FL	12	86	8:00-17:00	9	9.288	1.032
	Printer	4	50	12:00-13:00	1	0.2	0.2
Library	Desktop computer	12	120	14:00-16:00	2	2.88	1.44
	Three headed outdoor street lamps	20	100	19:00-7:00	12	24	2
	Polycarbonate outdoor post latern with frosted acrylic glass, black	25	100	19:00-7:00	12	30	2.5
	LED round gate light	30	7	19:00-7:00	12	2.52	0.21
	LED road lamps	40	20	19:00-7:00	12	9.6	0.8
Outdoor lighting	LED outdoor street lights	45	60	19:00-7:00	12	32.4	2.7
	CFL	66	13	8:00-17:00	9	7.722	0.858
	Projectors	5	10	9:00-16:00	7	0.35	0.05
	2 lamp FL	20	32	8:00-17:00	9	5.76	0.64
	Desktop Computer or PC	10	120	14:00-16:00	2	2.4	1.2
	Printer	3	50	12:00-13:00	1	0.15	0.15
	Electric stove	1	1800	10:00-12:00	2	3.6	1.8
	Oven	1	1250	12:00-2:00	2	2.5	1.25
	Coffee maker	1	900	9:00-10:00	1	0.9	0.9
	Dish washer	1	900	9:00-9:30	0.5	0.45	0.9
	Blender	1	600	11:00-11:30	0.5	0.3	0.6
	Food processor	1	600	11:00-12:00	1	0.6	0.6
	Multicooker	1	500	11:00-12:00	1	0.5	0.5
PAUWES building load	Water boiler	1	1500	9:00-10:00	1	1.5	1.5
	Electric stove	1	9000	7:00-10:00	3	27	9
	Dish washer	2	1000	7:00-8:00	1	2	2
	Bread Baking oven machines	1	15000	6:00-8:00	2	30	15
	Electric fryer	2	5000	8:00-9:00	1	10	10
	Steam oven	4	1000	8:00-11:00	3	12	4
	Freezers	10	500	6:00-12:00	6	30	5
The kitchen appliances	CFL	20	13	6:00-12:00	6	1.56	0.26
	Phones	200	4	9:00-16:00	7	5.6	0.8
Estimated personal gadgets	Laptops	200	50	9:00-16:00	7	70	10

A.3: Summary of electrical appliances used to estimate the Faculty of Technology's daily electricity load for the months of summer season

1. Offices, outdoor lighting, and PAUWES loads

Summer months							
Category	**Load**	**Number of load**	**Rated Capacity (w)**	**Operation duration (Hrs/day)**	**Operation Hours (Hrs)**	**AC Load KWh/day**	**Electrical power demand (kW)**
Offices, outdoor lighting, and PAUWES							
Dean's office including including offices for Vice dean incharge of Pedagogy and student issues, and vice dean incharge of post graduation, research and external relations (3 offices)	A/C	2	1550	12:00-16:00	4	12.4	3.1
	2 lamp FL	4	32	8:00-17:00	9	1.152	0.128
	Desktop Computer	2	120	14:00-16:00	2	0.48	0.24
	Printer	2	50	12:00-13:00	1	0.1	0.1
Assistance vice dean office in charge of pedagogy and student issues including offices for Head of education department, Head of teaching department & evaluation, and Head of statistics & student internships (4 offices)	A/C	1	1550	12:00-16:00	4	6.2	1.55
	2 lamp FL	3	32	8:00-17:00	9	0.864	0.096
	Desktop Computer	3	120	14:00-16:00	2	0.72	0.36
	Printer	1	50	12:00-13:00	1	0.05	0.05
Assistance vice dean office in charge of research and external relations and offices for Head of cooperations & foreign relations, Research activities department and Training follow up service for post graduation, Training follow up service for post graduation (4).	A/C	1	1550	12:00-16:00	4	6.2	1.55
	2 lamp FL	3	32	8:00-17:00	9	0.864	0.096
	Desktop Computer	8	120	14:00-16:00	2	1.92	0.96
	Printer	1	50	12:00-13:00	1	0.05	0.05
Genaral Secretary office including offices for Personnel department, Budget & accounting, Animation service: Scientific, cultural & sporting, Service of maintenance, and Internal security service (6)	A/C	1	1550	12:00-16:00	4	6.2	1.55
	2 lamp FL	4	32	8:00-17:00	9	1.152	0.128
	Desktop Computer	2	120	14:00-16:00	2	0.48	0.24
	Printer	1	50	12:00-13:00	1	0.05	0.05
Head of Arch. Dept. office including offices for Deputy head of Arch. Dept., Chairman of Scientific Committee Arch. Dept, Arch.Dept License Manager, and Arch.Dept Masters Manager (5)	A/C	1	1550	12:00-16:00	4	6.2	1.55
	2 lamp FL	2	32	8:00-17:00	9	0.576	0.064
	Desktop Computer	1	120	14:00-16:00	2	0.24	0.12
	Printer	1	50	12:00-13:00	1	0.05	0.05
Head of Bmed. Dept. office including Deputy head of Bmed. Dept., Chairman of Scientific Committee BMed. Dept., BMed.Dept License Managers - 2 managers, and BMed.Dept Masters Managers - 3managers (8)	A/C	1	1550	12:00-16:00	4	6.2	1.55
	2 lamp FL	3	32	8:00-17:00	9	0.864	0.096
	Desktop Computer	1	120	14:00-16:00	2	0.24	0.12
	Printer	1	50	12:00-13:00	1	0.05	0.05
Head of Civ.Dept. office including Deputy Head of Civ.Dept., Chairman of Scientific Committee Civ.Dept., Civ.Dept License Manager, and Civ.Dept Masters Managers - 5 mangers (9)	A/C	1	1550	12:00-16:00	4	6.2	1.55
	2 lamp FL	2	32	8:00-17:00	9	0.576	0.064
	Desktop Computer	1	120	14:00-16:00	2	0.24	0.12
	Printer	1	50	12:00-13:00	1	0.05	0.05
Head of EEE Dept. office including offices for Deputy Head of EEE.Dept., Chairman of Scientific Committee EEE.Dept., EEE.Dept License Managers - 4 managers, and EEE.Dept Masters Managers - 6 managers (13)	A/C	1	1550	12:00-16:00	4	6.2	1.55
	2 lamp FL	3	32	8:00-17:00	9	0.864	0.096
	Desktop Computer	1	120	14:00-16:00	2	0.24	0.12
	Printer	1	50	12:00-13:00	1	0.05	0.05
Head of Telcom.Dept. office including offices for Deputy Head of Telcom.Dept., Chairman of Scientific Committee Telcom.Dept., Telcom.Dept License Manager, and Telcom.Dept Masters Managers - 2 managers (6)	A/C	1	1550	12:00-16:00	4	6.2	1.55
	2 lamp FL	1	32	8:00-17:00	9	0.288	0.032
	Desktop Computer or PCs	1	120	14:00-16:00	2	0.24	0.12
	Printer	1	50	12:00-13:00	1	0.05	0.05
Head of Hydraulics.Dept. office including offices Deputy Head of Hydraulic.Dept., Chairman of Scientific Committee Hydraulics.Dept., Hydraulics.Dept License Manager, and Hydraulics.Dept Managers Managers - 2 managers (6)	A/C	1	1550	12:00-16:00	4	6.2	1.55
	2 lampFL	2	32	8:00-17:00	9	0.576	0.064
	Desktop Computer	1	120	14:00-16:00	2	0.24	0.12
	Printer	1	50	12:00-13:00	1	0.05	0.05
Head of Mech.Dept. office including offices for Deputy Head of Mech.Dept., Chairman of Scientific Committee Mech.Dept., Mech.Dept License Managers - 4 managers, Mech.Dept Masters Manager - 2 mangers (9).	A/C	1	1550	12:00-16:00	4	6.2	1.55
	2 lamp FL	3	32	8:00-17:00	9	0.864	0.096
	Desktop Computer	1	120	14:00-16:00	2	0.24	0.12
	Printer	1	50	12:00-13:00	1	0.05	0.05
Library	CFL	15	13	8:00-17:00	9	1.755	0.195
	LED lamps	8	9	8:00-17:00	9	0.648	0.072
	T6 lamp FL	2	86	8:00-17:00	9	1.548	0.172
	Printer	2	50	12:00-13:00	1	0.1	0.1
	Desktop computer	2	120	14:00-16:00	2	0.48	0.24
Outdoor lighting	Three headed outdoor street lamps	20	100	19:00-7:00	12	24	2
	Polycarbonate outdoor post latern with frosted acrylic glass, black	25	100	19:00-7:00	12	30	2.5
	LED round gate light	30	7	19:00-7:00	12	2.52	0.21
	LED road lamps	40	20	19:00-7:00	12	9.6	0.8
	LED outdoor street lights	45	60	19:00-7:00	12	32.4	2.7
PAUWES building load	CFL	20	13	8:00-17:00	9	2.34	0.26
	A/C	3	1550	12:00-16:00	4	18.6	4.65
	2 lamp FL	10	32	8:00-17:00	9	2.88	0.32
	Desktop Computer or PC	3	120	14:00-16:00	2	0.72	0.36
	Printer	1	50	12:00-13:00	1	0.05	0.05

7.2 Appendix B

B.1: Solar PV Module specifications

Item	Specification
Manufacturer	Canadian Solar
Country	Canada
Maximum Power (Pmax)	325 W
PV Module Technology	Poly-crystalline, 6 inch
No. of Cells	72 (6 x 12)
Module Efficiency STC	16.94%
Operating Temperature	-40°C ~ +85°C
Open circuit voltage (Voc)	45.5 V
Maximum Power Voltage (Vmp)	37.0 V
Short-circuit Current (Isc)	9.34 A
Maximum Power Current (Imp)	8.78 A
Power Tolerance	0 ~ + 5 W
Maximum system voltage	1000 V (IEC) or 1000 V (UL)
Temperature coefficients of Pmax	-0.41 % / °C
Temperature coefficients of Voc	-0.31 % / °C
Temperature coefficients of Isc	0.053 % / °C
Nominal operating cell temperature (NOCT)	45±2 °C
Dimensions	1954 x 982 x 40 mm (76.9 x 38.7 x 1.57 in)
Weight	22 kg (48.5 lbs)

B.2: Wind turbine specifications

Item	Specification
Manufacturer	Australian Wind and Solar (ASW)
Country	Australia
Type	AWS HCM 3.3kW
Rated power	3300W
Peak Output	3650W
Number of blades	3 standard (6 for extra charge)
Rotor diameter	4.65m / 15ft
Cut-in wind speed	2.7m/s, 6mph
Rated Wind Speed	10.5m/s, 24mph
Hub height	12m
Tip Speed Ratio	8.5
Yaw control	Passive by Tail Vane
Poles	16
RPM—50Hz/60Hz	375 / 450
Over Speed Limit	525RPM / 70Hz
Swept Area	6.4 sq.m / 175 sq.feet
Survival Wind Speed	55 m/s
Suggested Routine Maintenance	Annual Inspection